NTNU – Trondheim
Norwegian University of
Science and Technology

Uncertainties In Predicted Extreme Wave Induced Platform Response

Tianzuo Yao

Marine Technology
Submission date: June 2014
Supervisor: Sverre Kristian Haver, IMT

Norwegian University of Science and Technology
Department of Marine Technology

NTNU

UNCERTAINTIES IN PREDICTED EXTREME WAVE INDUCED PLATFORM RESPONSE

MASTER THESIS
BY
TIANZUO YAO

Submission date: June 2014
Supervisor: Prof. II Sverre Haver, IMT
Department of Marine Technology
Norwegian University of Science and Technology

Acknowledgment

This Master Thesis has been written during the spring 2014 at the Department of Marine Technology, Norwegian University of Science and Technology, Trondheim, Norway. The thesis has been submitted to partially fulfill the requirement for completing the degree of Master of Science.

I would like to take this opportunity to express my great thanks to my supervisor Prof. Sverre K. Haver, who has guided me so much on theory study and report writing. He has been extremely patient to answer all my questions and help me solve the problems. In addition to assisting me through the work of this thesis, he has also lectured the course TMR4195 Design of Offshore Structure, which I have attended in the spring semester 2013. This course helps me to learn the basic theory with respect to the extreme value prediction and raise my interest to continue on the study.

I would also like to thank all my friends here in Department of Marine Technology. They provide selfless assistance to me on software learning, and help me get through the hard time. I am truly grateful for their contributions.

Tianzuo Yao

M.Sc. Thesis 2014

for

Stud.techn.

Tianzuo Yao

Uncertainties in predicted extreme wave induced platform response

(Usikkerheter i estimert ekstrem blgeindusert plattformrespons.)

In connection with design of offshore structures two limit states, ULS and ALS, have to be controlled to ensure a sufficient robustness against overload failure. The characteristic environmental response involved in these limit states are defined in terms of its annual probability of being exceeded, q. For ULS $q = 10^{-2}$, while for the accidental limit state, ALS, $q = 10^{-4}$. In order to obtain consistent estimates for such rare extremes, some sort of a long term analysis, accounting properly for all sources of inherent randomness, should be carried out.

In the following the investigation shall be limited to wave induced response. The basic response variable is the 3-hour extreme value, X_{3h}. It may furthermore be assumed that all weather approach from the same direction, i.e. a stationary short term sea state is characterized by the significant wave height, H_s, and the spectral peak period, Tp. Denoting the conditional distribution of X_{3h} given the sea state characteristics, H_s and T_p, by $F_{X_{3h}|H_sT_p}(x|h,t)$, a possible estimate for the long term distribution of X_{3h} reads:

$$F_{X_{3h}}(x) = \int_h \int_t F_{X_{3h}|H_sT_p}(x|h,t) f_{H_sT_p}(h,t) dtdh \tag{1}$$

Where $f_{H_sT_p}(h,t)dtdh$ is the joint probability density function for simultaneously occurring H_s and T_p.

For a general response problem, the challenge is to establish the short term distribution of the 3-hour extreme value for all possible combinations of sea state characteristics. In order to investigate uncertainties as functions of the nature of the underlying response problem, a generic response problem is introduced. The short term distribution of X_{3h} is assumed to follow a Gumbel distribution:

$$F_{X_{3h}|H_sT_p}(x|h,t) \to exp\{-exp\{-\frac{x-\alpha(h,t)}{\beta(h,t)}\}\} \tag{2}$$

The parameters can be expressed in terms of the lower moments, expected value and standard deviation of X_{3h}:

$$\beta = 0.7797\sigma_{X_{3h}} \tag{3}$$

$$\alpha = \mu_{X_{3h}} - 0.5772\beta \tag{4}$$

The generic problem is defined by assuming that the conditional mean is given on the form:

$$\mu_{X_{3h}}(h,t) = c_1 h^{c_2}[1 + \cos^{c_3}(\frac{2\pi(t-c_4)}{c_5})] \tag{5}$$

$$\sigma_{X_{3h}}(h,t) = c_2 c_6 \mu_{X_{3h}}(h,t) \tag{6}$$

By properly varying the coefficients, a variety of response problems can be approximated.

Above the long term distribution is obtained using the all sea states approach. Another possibly better approach is to select the storm maximum response, X_s, as the basic variable and merely include storms exceeding a certain threshold for the significant wave height. This approach will be referred to as the peak-over-threshold approach. Finally, for very complex response problems, an approximate long term analysis must be done. One possible approach is the environmental contour method.

The purpose of this thesis is to investigate the adequacy of the 3 methods referred for estimating q-probability response for various generic response systems. Uncertainties associated with various approaches shall be discussed.

The candidate may follow his own approach for addressing the problem described. But a possible division into sub-tasks are given below:

1. As an extended introduction, the candidate should familiarize himself the notation generic response system. One should select parameters for the mean and standard deviation for some few response cases. A linear (in h_s) response problem should be considered, a quadratic response problem should be included and for both these one could select a couple of period sensitivity cases.

2. The wave data is given by the NORA10 database. A file giving a full set of weather characteristics every 3 hours from 1957 to 2011 will be made available. A joint probability distribution function for total Hs and associated spectral peak period shall be prepared.

3. Using the all sea state approach, q-probability extremes shall be estimated for the the selected response cases. For one of the cases one should aim for quantifying the uncertainties associated with the predicted extreme value. The latter study should be introduced by discussing sources of uncertainties.

4. For the POT approach one shall first of all demonstrate how one can establish the conditional distribution function for the storm maximum response given the most probable largest storm response. Check to which extent the conditional storm maximum response given the most probable largest response can be approximated by a Gumbel distribution. Investigate if distribution function for the variable $X_s/\tilde{x}_s$, where $\tilde{x}_s$ denotes the most probable largest storm response, is independent of the actual storm. Investigate how the Gumbel parameters for $X_s/\tilde{x}_s$ vary from response case to response case.

5. Calculate the most probable largest storm response for all storms and all response cases. Fit a distribution function for each response case. Estimate the long term distribution function for X_s for all response cases. Thereafter estimate q-probability extremes. For the same response cases as considered in point 3,

assess the uncertainties associated with estimates for the q-probability responses.

6. Compare results for the two approaches and discuss possible differences.

7. Determine the environmental contour lines from the fitted joint distribution of Hs. Calculate approximate estimates for q-probability values for the various response cases using standard recommendations found in Norsok N-003. Investigate the adequacy of the standard recommendations by using the results from the long term analysis to determine the correct percentile. Summarize the work by pointing out the major findings of the work.

The work may show to be more extensive than anticipated. Some topics may therefore be left out after discussion with the supervisor without any negative influence on the grading.

The candidate should in his report give a personal contribution to the solution of the problem formulated in this text. All assumptions and conclusions must be supported by mathematical models and/or references to physical effects in a logical manner. The candidate should apply all available sources to find relevant literature and information on the actual problem.

The report should be well organised and give a clear presentation of the work and all conclusions. It is important that the text is well written and that tables and figures are used to support the verbal presentation. The report should be complete, but still as short as possible.

The final report must contain this text, an acknowledgement, summary, main body, conclusions, suggestions for further work, symbol list, references and appendices. All figures, tables and equations must be identified by numbers. References should be given by author and year in the text, and presented alphabetically in the reference list. The report must be submitted in two copies unless otherwise has been agreed with the supervisor.

The supervisor may require that the candidate should give a written plan that describes the progress of the work after having received this text. The plan may contain a table of content for the report and also assumed use of computer resources.

From the report it should be possible to identify the work carried out by the candidate and what has been found in the available literature. It is important to give references to the original source for theories and experimental results.

The report must be signed by the candidate, include this text, appear as a paperback, and - if needed - have a separate enclosure (binder, diskette or CD-ROM) with additional material.

Supervisor: Prof. II Sverre Haver, Statoil ASA.

Abstract

Before the long term response prediction is performed, a generic response function is firstly introduced. The generic response function is given as a function of weather characteristics in terms of h_s and t_p, and the shape of response function is decided by several parameters. By studying the effect of the parameters on response, one can get the response cases with different sensitivity to wave period and non-linearity to significant wave height. With a set of properly selected parameters, one can get the response function closest to the real response case. This is very convenient for long term response prediction, since it can avoid the time domain analysis.

There are two major approaches to decide long term response in this thesis. In the all sea state approach, distribution function for h_s and t_p are determined based on the entire hindcast data. Then the probability scatter for occurrence of different combinations of h_s and t_p is calculated. Then the long term response distribution is decided by combining the generic response function.

POT method focuses only on storms with significant wave height larger than a minimum threshold. The distribution of the largest most probable response for each storm, and the conditional distribution of the largest realization given the most probable response can be found from the storm sample. Then the long term distribution of response can be decided by intergrating over the largest most probable response.

Environmental contour line method is also performed in the thesis. It is used to determine the worst sea states and the target percentile. Environmental contour line method is an approximate method, but it provides a good verification to the result from the all sea state approach. Meanwhile, the author will discuss all the uncertainties involved when estimating long term extremes by different approaches.

Besides comparing results between the all sea state approach and the POT approach, further verification is performed. There are majorly two alternatives: firstly, wave crest height is studied instead of response value; secondly, weather characteristics are extracted directly from hindcast data instead of the modeled function. These modifications can provide good verifications for the all sea state approach and the POT approach.

Contents

List of Figures

List of Tables

Nomenclature

α	Location Parameter of Gumbel distribution or most probable response for each step in storm
β	Scale parameter of Gumbel distribution or radius of contour in u-space
Γ	Gamma function
γ	Parameter of Weibull distribution
μ	Mean value of sample
ω	Angular frequency
$\overline{v^+}$	Zero-crossing period
Φ	Standard normal distribution
σ	Standard deviation of sample
σ^2	Variance of sample
θ	Parameter of Weibull distribution
a_n	Parameters in function of mean $ln(t_p)$ against h_s
b_n	Parameters in function of variance $ln(t_p)$ against h_s, particularly, b_1 is the width paramter
c	Damping coefficient
c_n	Parameters in the response function
$F_V(v)$	Cumulative probability function for ratio v
$F_{\tilde{Y}}(\tilde{y})$	Cumulative probability function for the largest most probable response
$f_{\tilde{Y}}(\tilde{y})$	Density probability function for the largest most probable response
$F_{C_{3h}}(c)$	Cumulative probability function for wave crest
$f_{H_sT_p}(h,t)$	Joint probability density function for simutaneously occuring H_s and T_p
$F_{H_S}(h_s)$	Cumulative probability distribution function of significant wave height H_s

$F_{X_{3h}}(x)$	Cumulative probability distribution function of stochastic variable x
H_s	Significant wave height
h_{th}	Threshold value for selecting storms
k	Parameter of Weibull distribution or stiffness
m	Mass
$m(h,t)$	Number of wave crests for a given 3-hour sea state
N	Number of 3-hour steps per year
n_1	Expected storms per year
p_e	Exceedance probability
$P_{i,j}$	Relative probability of each sea states exceedance probability
q	Annual exceedance probability
$Q_{X_{Exc}}(x)$	Exceedance probability of certain response for all sea state
$Q_{X_{Nonexc}}$	Exceedance probability of certain response under given sea state
R_0	External force
T_p	Spectral peak period
t_z	Zero-crossing period
u	Random numbers from 0 to 1 in Monte Carlo method
u_0	Response amplitude
u_1, u_1	Axis of u-space in environmental contour line method
v	Ratio between the largest realization and the most probable largest response for each storm
v^+	Zero-crossing frequency
X_{3h}	3-hour extreme value

Chapter 1

Introduction

1.1 Background

In the design of offshore structures, a characteristic load is firstly required. Then the response can be calculated by multiplying the characteristic load by a partial safety factor. If the response is larger than the maximum capacity of the structure, the structure would fail. In Norwegian rules and regulations, this value is calculated by a specified annual exceedance probabilities, q.

When $q = 10^{-2}$, the control is defined as the ultimate limit state control, ULS. The ultimate limit state is important for structural safety and usually applied on components.

When $q = 10^{-4}$, the control is defined as the accidental limit control, ALS. The purpose of ALS control is to ensure that the structure will not be completely damaged in an abnormal event.

In order to obtain consistent estimates for such rare extremes, some sort of a long term analysis, accounting properly for all sources of inherent randomness, should be carried out.

1.2 Objective

The purpose of this thesis is to investigate the adequacy of the three methods for estimating q-probability response for various generic response systems. Uncertainties associated with the various approaches shall be discussed.

One should firstly get good control over the generic response system, study the non-linearity to significant wave height and sensitivity to spectral peak period.

For the all sea state approach, a joint probability distribution function for significant wave height and associated spectral peak period should be built based on NORA10 database. Q-annual probability extremes should be estimated using all sea state approach.

For the POT approach, the distribution of the largest most probable response for each storm, and the conditional distribution of the largest realization given the

most probable response should be established. The distribution function for long term response and the q-annual probability extremes should be determined.

By comparing the differences between the two approaches, the resources of uncertainties should be studied. The environmental contour line from the fitted joint distribution needs to be decided. The target percentile should be calculated based on the results from long term analysis and adequacy of the percentiles from the recommendations in Norsok N-003 should be investigated.

Major findings of the thesis and suggestions to further work should be given at the end of the thesis.

Chapter 2

Generic Response System

In this chapter, the generic response problem is studied. It includes three basic sections. Firstly, the method for calculating the long term response distribution from generic response problem. Secondly, basic theory regarding the short term response distribution. Thirdly, the generic response function and the effect of its parameters on the short term distribution of response.

All the following chapters on the long term distribution of response are based on the theory mentioned in this chapter. Throughout the thesis, the investigation will be limited to wave induced response.

2.1 Long Term Distribution of 3-hour Extreme Response

Denoting the basic response variable, 3-hour extreme value X_{3h}. The long term distribution of X_{3h}, $F_{X_{3h}}(x)$ reads:

$$F_{X_{3h}}(x) = \int_h \int_t F_{X_{3h}|H_s T_p}(x|h,t) f_{H_s T_p}(h,t) dt dh \tag{2.1}$$

This method is quite convenient for linear response systems where the response problem is characterized by a transfer function. All that needed is a procedure for selecting a proper wave spectrum for the various combinations of the sea state characteristics and a joint probabilistic model for H_S and T_P, according to Haver(1998).

2.2 Short Term Distribution of 3-hour Extreme Response

It is believed that the short term distribution of X_{3h} can be reasonably well modelled by a Gumbel distribution. This is proved in the following sections.

2.2.1 Linear Response Case

The sea surface elevation is assumed to be Gaussian process. Due to the assumption of linear response system, the response process can also be modelled as a Gaussian process. Then the global response maxima X_{3h}, is therefore reasonably well modelled by a Raleigh distribution.

$$F_{X_{3h,single}|H_sT_p}(x|h,t) = 1 - exp[-\frac{1}{2}(\frac{x}{\sigma(h,t)})^2] \tag{2.2}$$

For a given 3-hour duration of sea state, assuming that all global response maxima during the sea state are statistically independent and identically distributed, the distribution of 3-hour maxima reads:

$$F_{X_{3h}|H_sT_p}(x|h,t) = \{F_{X_{3h,single}|H_sT_p}(x|h,t)\}^{m(h,t)} = \{1 - exp[-\frac{1}{2}(\frac{x}{\sigma(h,t)})^2]\}^{m(h,t)} \tag{2.3}$$

where m(h, t) is the number of wave crests in 3-hour:

$$m(h,t) = \frac{3 \cdot 3600}{0.77 \cdot t_p} \tag{2.4}$$

m(h, t) is a rather large number. While for Eq. (2.3), when $m \to \infty$:

$$F_{X_{3h}|H_sT_p}(x|h,t) \to exp\{-exp\{-\frac{x - \alpha(h,t)}{\beta(h,t)}\}\} \tag{2.5}$$

with

$$\alpha(h,t) = \sigma(h,t)\sqrt{2ln(m(h,t))} \tag{2.6}$$

$$\beta(h,t) = \frac{\sigma(h,t)}{\sqrt{2ln(m(h,t))}} \tag{2.7}$$

Thus for linear case, the short term distribution of response can be modelled by a Gumbel distribution.

2.2.2 Non-linear Response Case

In this case, the global response maxima X_{3h} can be modelled by a 2-paramter Weibull distribution function given the sea state characteristics:

$$F_{X_{3h,single}|H_sT_p}(x|h,t) = 1 - exp\{-(\frac{x}{\lambda})^\theta\} \tag{2.8}$$

The probability density function for each response:

$$f_{X_{3h,single}|H_sT_p}(x|h,t) = \frac{\theta}{\lambda}(\frac{x}{\lambda})^{\theta-1}exp\{-(\frac{x}{\lambda})^{\theta}\} \tag{2.9}$$

For a given 3-hour duration of sea state, assuming that all global response maximas during the sea state are statistically independent and identically distributed, the distribution of this variable reads:

$$F_{X_{3h,single}|H_sT_p} = \{1 - exp[-(\frac{x}{\lambda})^{\theta}]\}^{m} \tag{2.10}$$

It can be seen that the probability density function is proportional to $exp[-(\frac{x}{\lambda})^{\theta}]$ with a scale factor $\frac{\theta}{\lambda}(\frac{x}{\lambda})^{\theta-1}$. Under this condition, with $m \to \infty$:

$$F_{X_{3h}|H_sT_p}(x|h,t) \to exp\{-exp\{-\frac{x-\alpha(h,t)}{\beta(h,t)}\}\} \tag{2.11}$$

Thus for non-linear case, the short term distribution of response can also be modeled by a Gumbel distribution. Provided that the Weibull distribution as known, the Gumbel parameters read:

$$\alpha = \theta(lnm)^{\frac{1}{\lambda}} \tag{2.12}$$

$$\beta = \frac{\theta}{\lambda}(lnm)^{\frac{1-\lambda}{\lambda}} \tag{2.13}$$

These estimations are approximate results, but they are rather accurate as far as $\lambda \geq 1$. Under this condition the convergence towards the asymptotic forms rather fast. If $\lambda < 1$, the convergence is rather slow and the asymptotic form is non-conservative as compared to the exact model. One should therefore be careful of using the asymptotic distribution if $\lambda < 1$. For $\lambda = 1$, the asymptotic model would be exact for all values of m, while for $\lambda > 1$ the asymptotic model would be on conservative side. More explanations can be found in Haver(2011).

2.2.3 Summary of Generic Response Case

From the demonstration above, the short term distribution of X_{3h} is assumed to be well modelled by Gumbel distribution, according to Haver and Bergsvik(2012).

$$F_{X_{3h}|H_sT_p}(x|h,t) = exp\{-exp\{-\frac{x-\alpha(h,t)}{\beta(h,t)}\}\} \tag{2.14}$$

In practical problem, it is a challenge to determine $\alpha(h,t)$ and $\beta(h,t)$. But in this part, one only focuses on a generic response problem, then $\alpha(h,t)$ and $\beta(h,t)$ are studied for illustrative purposes:

$$\beta = 0.7797\sigma_{X_{3h}} \tag{2.15}$$

$$\alpha = \mu_{X_{3h}} - 0.5772\beta \tag{2.16}$$

$\alpha(h,t)$ is the location parameter in the Gumbel distribution, which is majorly determined by the conditional mean of response. $\beta(h,t)$ is the scale parameter, which is obtained by the standard deviation of the response value. In the following study, instead of actual response value, $\alpha(h,t)$ and $\beta(h,t)$ are investigated, for effect of c_1 to c_6.

2.3 Study of Parameters

The generic problem is defined by assuming that the conditional mean and standard deviation are given on the form:

$$\mu_{X_{3h}}(h,t) = c_1 h^{c_2}[1 + \cos^{c_3}(\frac{2\pi(t-c_4)}{c_5})] \tag{2.17}$$

$$\sigma_{X_{3h}}(h,t) = c_2 c_6 \mu_{X_{3h}}(h,t) \tag{2.18}$$

The effects of different parameters are summarized according to their different positions.

2.3.1 Effect of c_1 and c_2

It can be easily seen from the term $c_1 h^{c_2}$ that c_1 works as a scale parameter. By multiplying c_1, $\mu_{X_{3h}}(h,t)$ and $\sigma_{X_{3h}}(h,t)$ can be scaled to the correct magnitude. Since one does not focuse on a practical problem in this thesis, c_1 is set to be an arbitrary positive number.

c_2 is the parameter that decides whether it is a linear response problem or a quadratic response problem to significant wave height. The effect of c_2 on $\alpha(h,t)$ is shown in Fig. (2.1):

It can be seen from Fig. (2.1) that, $\alpha(h,t)$ varies linearly with $c_2 = 1$, while quadratically with $c_2 = 2$. It suggests that c_2 is the parameter that decides whether it is a linear response problem or non-linear response problem.

2.3.2 Effect of c_4

The effect of c_4 on $\alpha(h,t)$ is shown in Fig. (2.2).

As can be seen from Fig. (2.2), c_4 is the parameter that decides the peak value of the response curve, i.e. the natural period of the response system.

But it is important to note that, a simple cosine curve cannot give an accurate description for all response problems under various situations. For example, the natural period of heave of catenary moored semi-submersible is 23-26s, when c_4 is taken as 10s, the cosine function may give a good description of the non-resonance

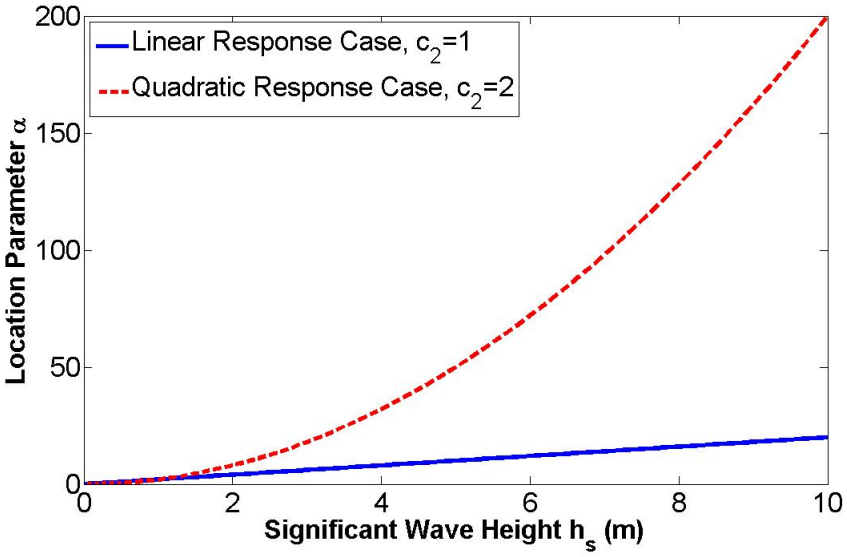

Figure 2.1: Effect of c_2 on Location Parameter α

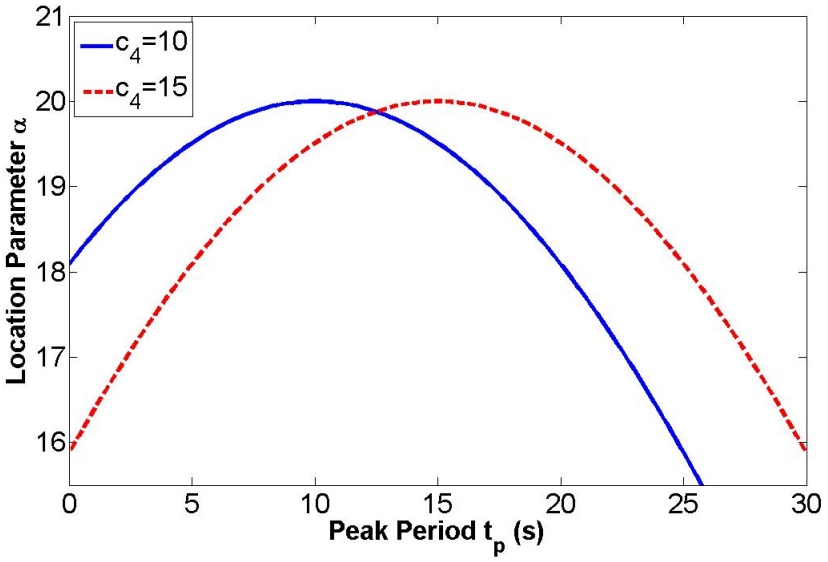

Figure 2.2: Effect of c_4 on Location Parameter α

response region, but the resonance region is not well covered in the cosine curve. Similarly, if c_4 is taken as 23-26s, the cosine curve will give a good description of the resonance behavior, but the non-resonance region is not covered. This can be fixed by introducing a more complex response curve. It is suggested for further study.

2.3.3 Effect of c_3 and c_5

c_3 and c_5 are used to obtain the period sensitivity to spectral wave period. The term including c_3 and c_5 is $1 + \cos^{c_3}(\frac{2\pi(t-c_4)}{c_5})$. Different combinations of c_3 and c_5 will give different response results. Take quadratic response case as an example:

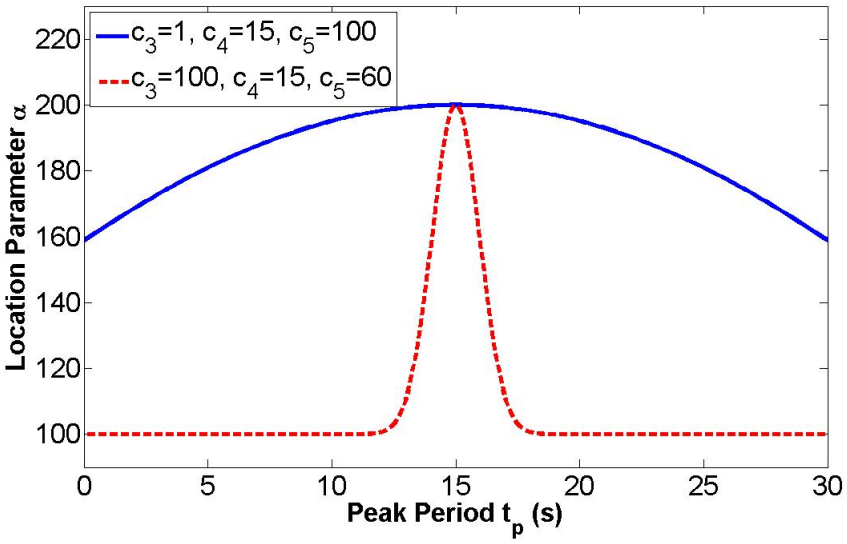

Figure 2.3: Effect of c_3 and c_5 on Location Parameter α

It can be seen from Fig. (2.3) that the combination of $c_3 = 1, c_4 = 15, c_5 = 100$ stands for the non-period sensitive case. By selecting $c_5 \gg c_4 \gg c_3$, the response problem does not have a big variation over t_p.

The combination of $c_3 = 100, c_4 = 15, c_5 = 60$ stands for the period-sensitive case. In this case, the response has an obvious variation near natural period c_4.

2.3.4 Effect of c_6

c_6 is a measure of the variability around the mean value of 3-hour maximum X_{3h}.

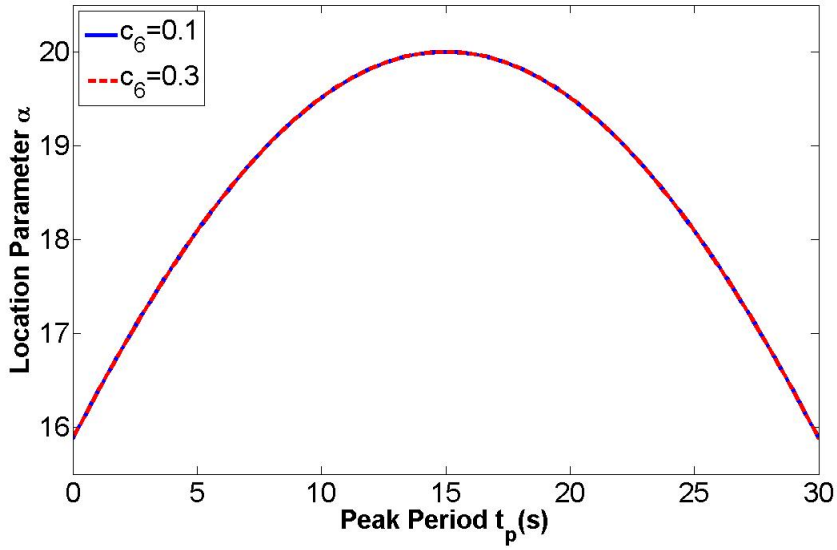

Figure 2.4: Effect of c_6 on Location Parameter α

As can be seen from Fig. (2.4), curves for $c_6 = 0.1$ and $c_6 = 0.3$ overlaps, thus c_6 has very small effect on the location parameter α. And as can be seen from

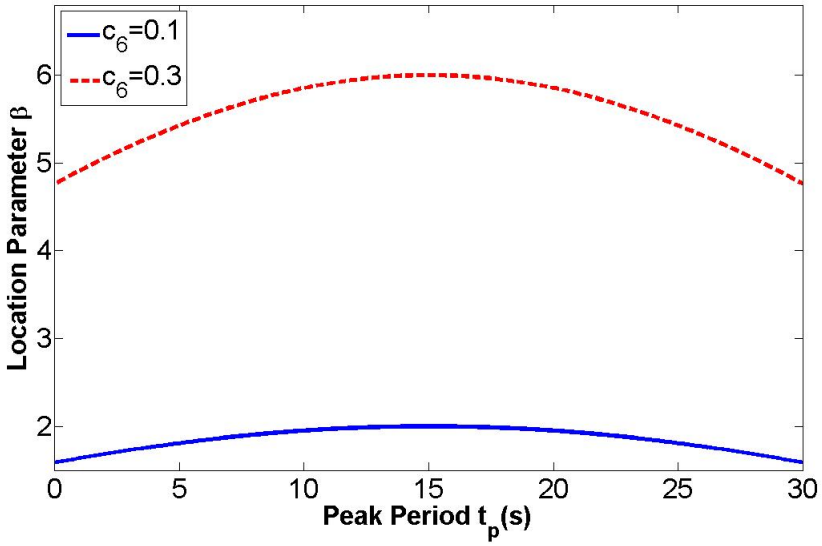

Figure 2.5: Effect of c_6 on Scale Parameter β

Fig. (2.5), c_6 has effect on scale parameter $\sigma_{X_{3h}}(h,t)$. It symbolizes the variability around the mean value of 3-hour maximum X_{3h}.

2.3.5 Summary of Effects of c_1-c_6:

c_1 is the scale parameter. c_2 decides the non-linearity to significant wave height of the response problem. Combination of c_3 and c_5 decides the sensitivity to spectral wave priod. c_4 is the natural period of a response system. c_6 is a measure of the variability around the mean 3-hour maximum X_{3h}.

However, it is important to notice that the response function in this chapter is a generic response function, it can only give a general description of the response problem. For a real structure, the shape of the response function is much more complicated. Thus a more detailed response function should be studied in the future.

In the following chapters, if it is not specified, the default value of c_1 is 1, c_4 is 15, and c_6 is 0.1. c_2, c_3 and c_5 are much more related to the response problem, so it will be specified in different cases.

Chapter 3

All Sea State Long Term Analysis

In this chapter, all sea state long term analysis of response is discussed. It is made up of three sections: firstly, the method to establish joint probability model for H_s and T_p; secondly, long term response analysis based on the joint probabilistic model; thirdly, study the effect of the response function on final response.

3.1 Joint Probabilistic Model for H_s and T_p

Hindcast data is obtained from the Norwegian Reanalysis Archive (NORA10). It is available from Sep. 1957 to Jun. 2013. Information about speed and direction of wind, significant wave height H_s, spectral peak period T_p and major direction of wave are given in the hindcast data. In this project, only the wave in the main direction is taken into consideration.

3.1.1 Distribution for H_s

A 3-parameter Weibull distribution model is used to produce distribution function for H_s. The cumulative function of the three-parameter Weibull distribution reads:

$$F_{H_S}(h_s) = 1 - exp\{-(\frac{h_s - \theta}{\lambda})^k\} \tag{3.1}$$

where θ is the location parameter, λ is the scale parameter and k is the shape parameter.

There are two methods to decide θ, λ and k. one is linear fitting on a Weibull probability paper, another one is method of moment. Method of linear fitting in probability paper for Weibull distribution is utilized here.

By doing a transformation of Eq. (3.1), it can be shown:

$$ln(-ln(1 - F_{H_s}(h_s))) = kln(x - \theta) - k \ln \lambda \tag{3.2}$$

$ln(-ln(1-F_{H_s}(h_s)))$ and $ln(x-\theta)$ are two axis on the Weibull probability paper.

By doing a least square fitting, θ, λ and k can be decided. Details can be found in Yao(2014). For the best fitting, the parameters are decided as:

$$\theta = 0.4; \tag{3.3}$$

$$\lambda = 2.25; \tag{3.4}$$

$$k = 1.29; \tag{3.5}$$

The distribution function $F_{H_s}(h_s)$ is plotted on Weibull probability paper in Fig. (3.1).

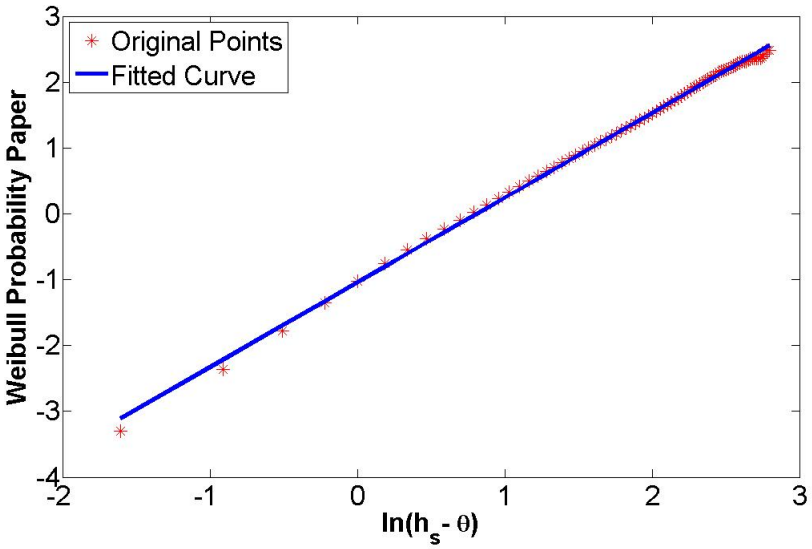

Figure 3.1: Linear Fitting of h_s on 3-Parameter Weibull Probability Paper

Fig. (3.1) suggests that the 3-parameter Weibull distribution gives a good description of significant wave height. Thus the expression for 3-parameter Weibull distribution function is denoted as:

$$F_{H_S}(h_s) = 1 - exp\{-(\frac{h_s - 0.4}{2.25})^{1.29}\} \tag{3.6}$$

The fitted cumulative model is plotted with the original data in Fig. (3.2) to show the fitting result.

3.1.2 Distribution for T_p given H_s

Log-normal distribution is used to model T_p for a given H_s:

$$f_{T_P|H_S}(t_p|\mu,\sigma) = \frac{1}{\sqrt{2\pi}\sigma t_p} exp\{-\frac{(ln(t_p) - \mu)^2}{2\sigma^2}\} \tag{3.7}$$

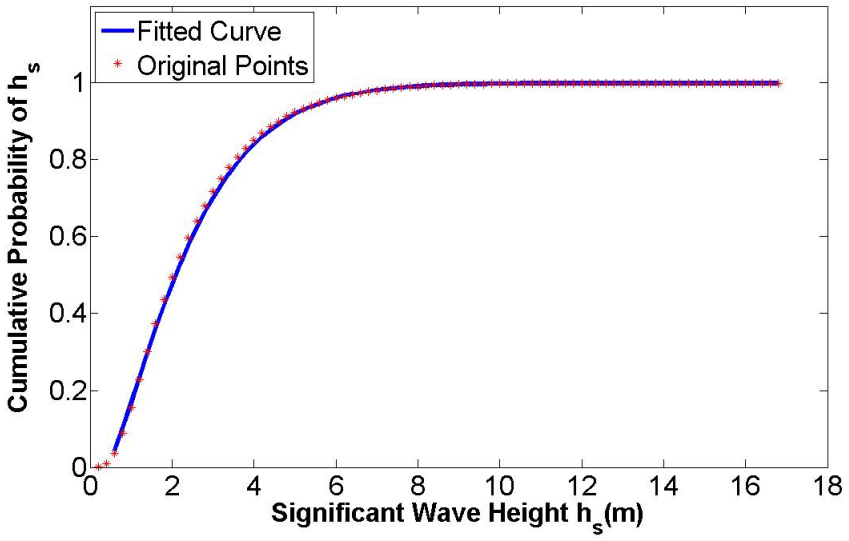

Figure 3.2: Cumulative Probability of Significant Wave Height

$$F_{T_P|H_S}(t_p|\mu,\sigma) = \Phi(\frac{ln(t_p)-\mu}{\sigma}) \tag{3.8}$$

where

$$\mu = a_1 + a_2 \cdot h_s^{a_3} \tag{3.9}$$

$$\sigma^2 = b_1 + b_2 \cdot exp(-h_s \cdot b_3) \tag{3.10}$$

It is important to notice that μ and σ^2 are the mean and variance of the sample $ln(t_p)$. There are two methods to decide μ and σ^2. One is linear fitting in Log-normal probability paper; the other is the method of moment.

a. Least square method

Eq. (3.8) can be transformed into:

$$\Phi^{-1}(F_{T_P|H_S}(t_p|\mu,\sigma)) = \frac{ln(t_p)}{\sigma} - \frac{\mu}{\sigma} \tag{3.11}$$

For a given h_s, a linear relationship between $\Phi^{-1}(F_{T_P|H_S}(t_p|\mu,\sigma))$ and $ln(t_p)$ can be found. Thus by doing linear fitting for each class of h_s, can μ and σ be decided.

b. Method of moment

For a given class of H_s, the mean and variance of T_P is calculated as μ_{t_p} and $\sigma^2_{t_p}$. From Bernt(2010), the relationship between μ_{t_p}, $\sigma^2_{t_p}$ and μ, σ^2 reads:

$$\mu_{t_p} = e^{\mu+\frac{\sigma^2}{2}} \tag{3.12}$$

$$\sigma^2_{t_p} = (e^{\sigma^2}-1)e^{2\mu+\sigma^2} \tag{3.13}$$

By solving Eq. (3.12) and Eq. (3.13), the value of μ and σ^2 is decided as:

$$\mu = \frac{1}{2} ln(\frac{\mu_{t_p}^4}{\mu_{t_p}^2 + \sigma_{t_p}^2}) \tag{3.14}$$

$$\sigma^2 = ln(\frac{\sigma_{t_p}^2}{\mu_{t_p}^2} + 1) \tag{3.15}$$

Thus for each class of H_s, a set of μ and σ can be decided.

The comparison between two methods is shown as below.

For $H_s = 1.9m$ (representing class [1.85m, 1.95m]):

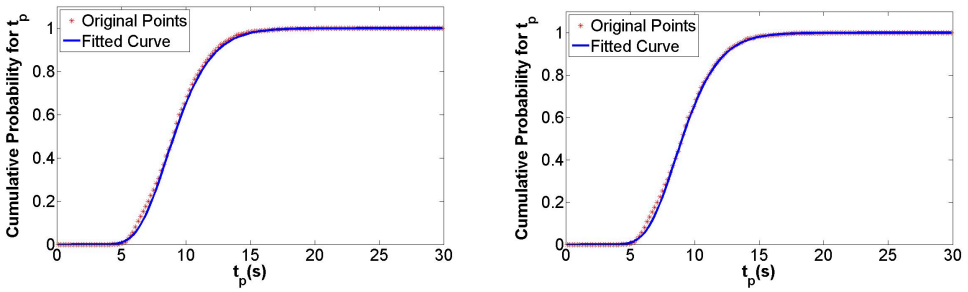

(a) Method of Moment (b) Method of Linear Fitting

Figure 3.3: For $H_s = 1.9m$ (representing class [1.85m, 1.95m])

Comparisons for $h_s = 3.9m, 5.9m, 7.9m, 9.9m$ are shown in Appendix, Figs. (A.1 to A.4).

The results in Figs. (3.3 to A.4) suggest that the method of moment gives better result. Thus the method of moment is used to calculate μ and σ in this thesis work.

Then the relationship between μ, σ and h_s can be decided by using non-linear fitting tool in Matlab. It is decided as:

$$\mu = 1.09 + 1.019 h_s^0.2 \tag{3.16}$$

$$\sigma^2 = 0.009 + 0.1022 \cdot exp(-0.36 \cdot h_s) \tag{3.17}$$

Fitting for μ, σ of t_p against h_s is shown in Fig. (3.4).

Then the relationship between μ, σ and h_s can be decided by using non-linear fitting tool in Matlab.

Fitting for μ, σ of t_p against h_s is shown in Fig. (3.4)

As shown in Fig. (3.4), by extrapolating the fitted curve to all actual values of h_s, the value of h_s for 0.63, 10^{-1}, 10^{-2} and 10^{-4} annual probability, and the conditional mean and the 90% range of t_p for each h_s can be calculated. The results are presented in Tab. (3.1).

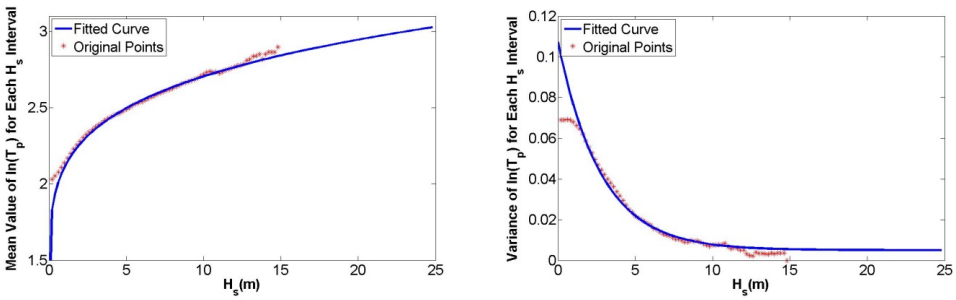

(a) Non-linear Fitting for μ (b) Non-linear Fitting for σ^2

Figure 3.4: Non-linear Fitting for μ and σ^2

Table 3.1: Extreme Values of h_s and t_p from Long Term Analysis

Annual Probability	h_s(m)	Mean t_p(s)	5%(s)	95%(s)
0.63	12.2	15.96	14.30	17.81
10^{-1}	14.19	16.78	15.18	18.73
10^{-2}	16.54	17.81	16.12	19.49
10^{-3}	20.97	19.30	17.64	21.12

However, it can be read from Fig. (3.4) that, the extrapolated curve gives a good description for the middle part of the curve, but poor description for the tail region. And since the tail region corresponds to the extreme values, it is important to study the uncertainties corresponding to this region. Further discussion is referred to Section 4.2 in Chapter 4.

3.1.3 Verification of Joint Probabilistic Model

It is important to check that the cumulative probability for $f_{H_s}(h_s)$ and $f_{T_p|H_s}(t_p|h_s)$ from 0 to the estimated maximum is equal to exact 1. For the ULS case, the exceedance probability p_e is:

$$p_e = \frac{q}{N} = \frac{10^{-2}}{2920} = 3.4 \cdot e^{-6} \tag{3.18}$$

For the ALS case, the exceedance probability p_e is:

$$p_e = \frac{q}{N} = \frac{10^{-4}}{2920} = 3.4 \cdot e^{-8} \tag{3.19}$$

It can be seen that the extreme value corresponds to p_e with very small magnitude. Thus the joint probability model has to be very accurate in order to give a reasonable estimation for the extreme sea state.

In order to do this, the cumulative probability is scaled to exact 1 by mathematical method. The probability for each interval of H_s is calculated by:

$$\Delta F_{H_s}(h_{s_i}) = F_{H_s}(h_{s_{i+1}}) - F_{H_s}(h_{s_i}) \tag{3.20}$$

The upper level for h_s is chosen to be 25m.

$$F_{H_{s,sum}}(h_s) = \Sigma[\Delta F_{H_s}(h_{s_i})] \tag{3.21}$$

According to the result, $F_{H_{s,sum}}(h_s)$ is not exact 1. This is due to the fact that though a high value 25m is, there is still a probability that the h_s exceeds 25m in reality. The scaled probability for each interval is calculated by dividing $\Delta F_{H_s}(h_{s_i})$ by $F_{H_{s,sum}}(h_s)$. Then the cumulative probability is equal to 1 exactly.

Similar procedures are done for T_P. The upper level of T_p is chosen to be 30s.

3.1.4 Scatter Diagram for Environmental Characteristics

Since cumulative probability model for H_s, and T_p for given H_s is established, a probability scatter diagram for environmental characteristics can be established. The probability scatter diagram gives information about the occurrence probability of a specific environmental characteristic situation, i.e. a specific combination of H_s and T_p. The scatter diagram is calculated as:

$$\begin{aligned} P_{i,j} &= \delta F_{H_s}(h_{s_i}) \cdot \delta F_{T_p|H_s}(t_{p_i}|h_{s_i}) \\ &= [F_{H_s}(h_{s_{i+1}}) - F_{H_s}(h_{s_i})] \cdot [F_{T_p|H_s}(t_{p_{i+1}}|h_{s_i}) - F_{T_p|H_s}(t_{p_i}|h_{s_i})] \end{aligned} \tag{3.22}$$

It is to be noticed that since distribution of $F_{H_s}(h_s)$ and $F_{T_p|H_s}(t_p|h_s)$ have been scaled up to exact 1, the sum of the probability scatter diagram will also be exact 1. This is very important for long term analysis of response.

3.2 Long Term Response Study

In the first chapter, the author has already introduced the generic response function. By choosing different combinations of c_1 to c_6, a response shape which is sensitive or non-sensitive to t_p, linear or non-linear to h_s can be established.

3.2.1 Linear and Non-period Sensitive Case

In this case, the values for c_1 to c_6 are presented in Table(3.2).

Table 3.2: Parameters for Linear and Non-period Sensitive Case

c_1	c_2	c_3	c_4	c_5	c_6
1	1	1	15	100	0.1

According to the results at the end of this section, the 10000-year response is 48.18. In order to give an accurate estimation for the extreme value with 10000-year return period, the upper limit for long term value is set to be 54, which corresponds to $q = 10e^{-5}$ annual exceedance probability. The upper limit for response is calculated based on this principle for the following cases.

Then cumulative probability for increasing response can be calculated. By presenting the cumulative probability against response value on a Gumbel probability paper, it is rather easy to indicate level of 10^{-2} and 10^{-4} annual probability response.

Since the upper tail points have good linear behavior, an extrapolated straight line is fitted to the interested points on the probability paper in Fig. (3.5). However, it is important to notice that, there is no theory support for fitting a straight line to upper tail region, and accurate result should be read directly from the original data.

In this case, only points with y value in range [10, 19.49] are selected for linear fitting. The reason is that for the lower limit of range: it can be seen from Fig. (3.5) that, the points do not show linear characteristic perfectly in the range $y \in (0, 10)$, but behave much better in $y > 10$. So $y = 10$, i.e. $-ln(-ln(F(x)) = 10$ is chosen to be the lower limit.

For the upper limit of range: it is not necessary to go into too small probability. For the 10^5 year as return period, the corresponding exceedance per 3-hour sea state is $\frac{10^{-5}}{2920}$. The corresponding non-exceedance probability is $1 - \frac{10^{-5}}{2920}$, then $-ln(-ln(1 - \frac{10^{-5}}{2920})) = 19.49$. A return priod of 10^5-year is enough for estimating response for 10^2 and 10^4 year as return period, so 19.49 is chosen to be the upper limit. Similar steps have been done for both linear and quadratic, period sensitive and non-sensitive cases.

The fitted straight lines against original data are plotted in Fig. (3.5):

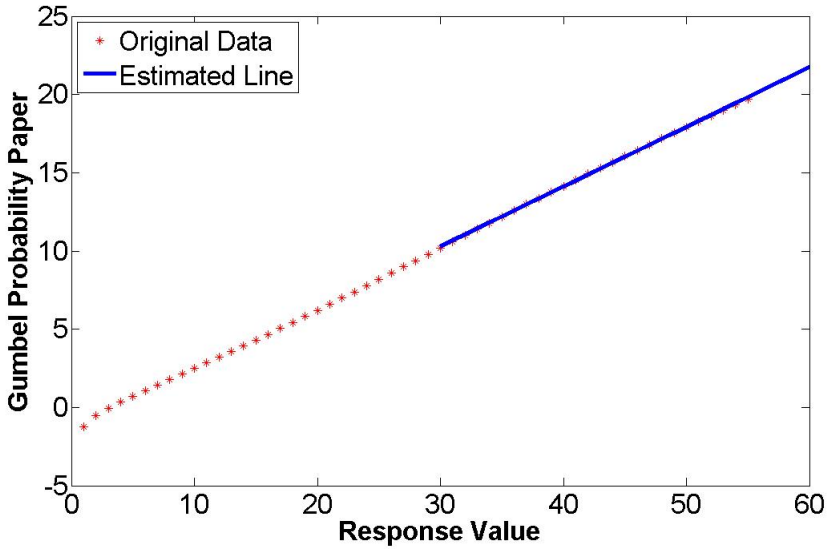

Figure 3.5: Cumulative Probability plotted on Gumbel Probability Paper for Non-Period Sensitive and Linear Case

For the 100-year return period case, the non-exceedance probability reads:

$$F_{X_{3h,100}} = 1 - \frac{1}{292000} \tag{3.23}$$

$$-ln(-ln(F_{X_{3h,100}})) = -ln(-ln(1 - \frac{1}{292000})) = 12.58 \tag{3.24}$$

The 100-year response value is

$$X_{3h,100} = 36.0 \tag{3.25}$$

For the 10000-year return period case, the non-exceedance probability reads:

$$F_{X_{3h,100}} = 1 - \frac{1}{29200000} \tag{3.26}$$

$$-ln(-ln(F_{X_{3h,100}})) = -ln(-ln(1 - \frac{1}{292000})) = 17.18 \tag{3.27}$$

The 100-year response value is

$$X_{3h,100} = 48.1 \tag{3.28}$$

3.2.2 Quadratic and Non-period Sensitive Case

In this case, the values for c_1 to c_6 be denoted in Tab. (3.3):

Table 3.3: Parameters for Quadratic and Non-period Sensitive Case

c_1	c_2	c_3	c_4	c_5	c_6
1	2	1	15	100	0.1

The upper limit for long term value is set to be 1320 to ensure enough accuracy. And similarly as for the linear case, the fitted straight line against original points is plotted in Fig. (3.6).

It can be seen from Fig. (3.6) that the extrapolated straight line does not give a good description of the original data. Thus the original data, instead of the extrapolated line is used to estimate the extreme response value. Corresponding response values are:

$$X_{3h,100} = 625.2 \tag{3.29}$$

$$X_{3h,10000} = 1073.6 \tag{3.30}$$

3.2.3 Linear and Period Sensitive Case

In this case, the values for c_1 to c_6 are shown in Tab. (3.4).

The upper limit for long term value is set to be 53 to ensure enough accuracy. The fitted straight line against original points is plotted in Fig. (3.7).

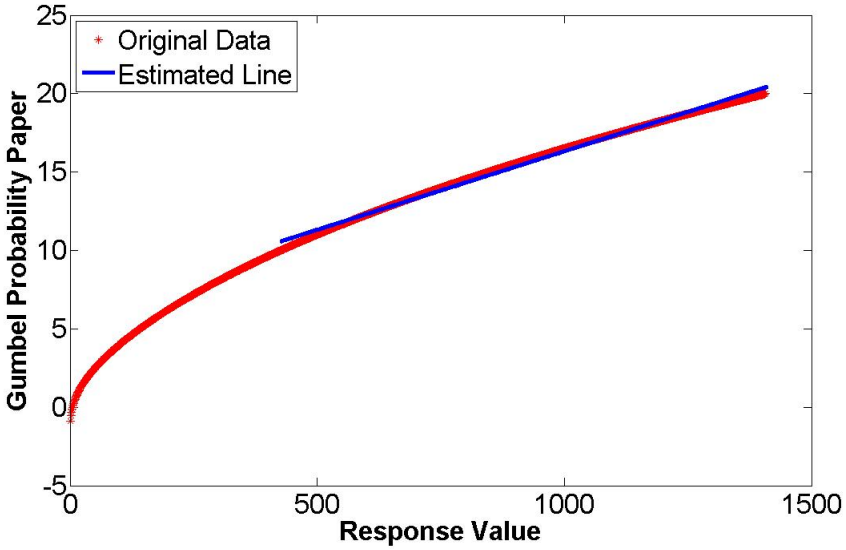

Figure 3.6: Cumulative Probability plotted on Gumbel Probability Paper for Non-Period Sensitive and Quadratic Case

Table 3.4: Parameters for Linear and Period Sensitive Case

c_1	c_2	c_3	c_4	c_5	c_6
1	1	100	15	60	0.1

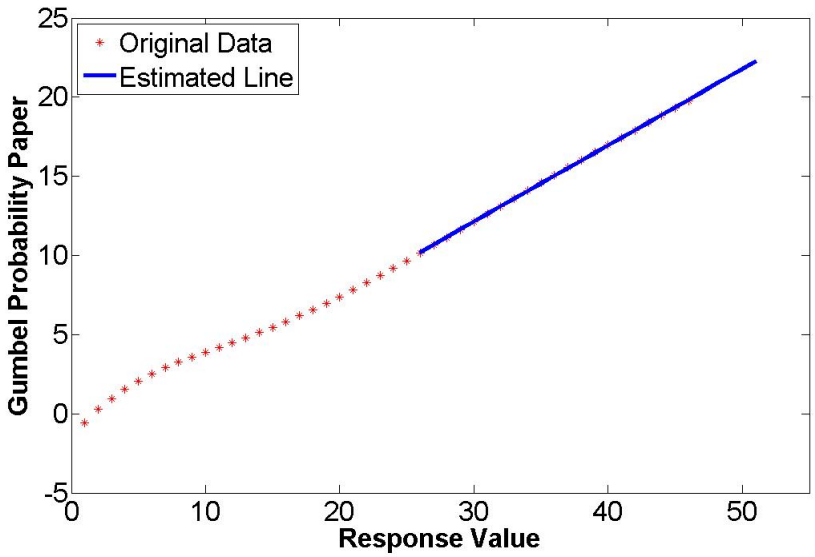

Figure 3.7: Cumulative Probability plotted on Gumbel Probability Paper for Period Sensitive and Linear Case

The extrapolated straight line gives fairly good description of the points in the upper range, thus the estimated extreme response can be easily calculated:

$$X_{3h,100} = 30.9 \tag{3.31}$$

$$X_{3h,10000} = 40.5 \tag{3.32}$$

3.2.4 Quadratic and Period Sensitive Case

In this case, the values for c_1 to c_6 are shown in Tab. (3.5).

Table 3.5: Parameters for Quadratic and Period Sensitive Case

c_1	c_2	c_3	c_4	c_5	c_6
1	2	100	15	60	0.1

The upper limit for long term response value is set to be 711 to ensure enough accuracy. The fitted straight line against original points is plotted in Fig. (3.8)

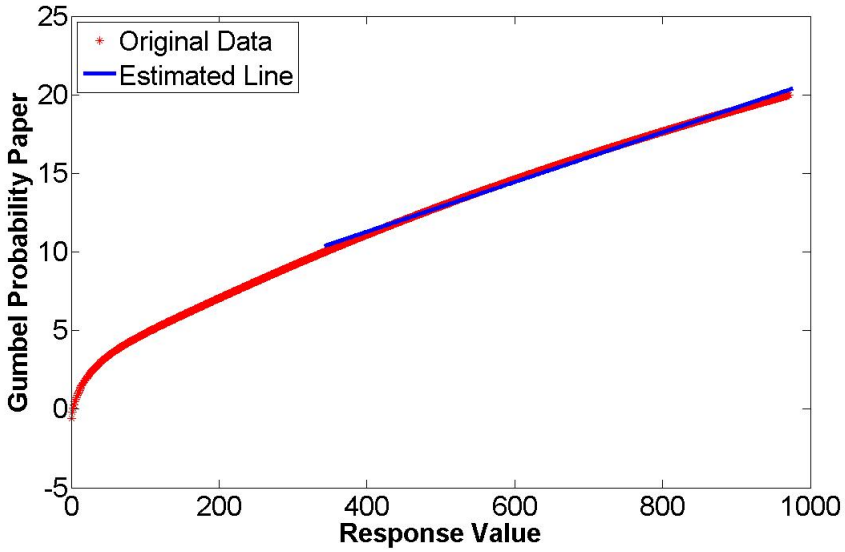

Figure 3.8: Cumulative Probability plotted on Gumbel Probability Paper for Period Sensitive and Quadratic Case

It can be seen from Fig. (3.8) that the extrapolated straight line is not satisfactory, so original data is used to estimate the extreme response value. Corresponding response values are:

$$X_{3h,100} = 480.8 \tag{3.33}$$

$$X_{3h,10000} = 766.9 \tag{3.34}$$

3.3 Discussion of Effect of Response Function on Final Response

In the following studies, the default value of b_1 is 0.005. $c_2 = 1$ is denoted as linear response case, $c_2 = 2$ is denoted as quadratic response case. The combination of $c_3 = 1$, $c_5 = 100$ is denoted as non-period sensitive response case, or NPS. The combination of $c_3 = 100$, $c_5 = 60$ is denoted as period sensitive response case, or PS.

3.3.1 Study of the Ratio between 10000-year and 100-year Response

The response values from full long term analysis are summarized in Tab. (3.6). The ratio between $X_{3h,10000}$ and $X_{3h,100}$ is calculated.

Table 3.6: Extreme Responses from Long Term Analysis for Different Period Sensitivity and Non-Linearity Cases

	$X_{3h,100}$	$X_{3h,10000}$	Ratio
Linear and Non-Period Sensitive	36.0	48.1	1.3
Quadratic and Non-Period Sensitive	625.2	1073.6	1.7
Linear and Period Sensitive	30.9	40.5	1.3
Quadratic and Period Sensitive	480.8	766.9	1.6

The ratio corresponds to the safety factor used in design of offshore structures. The ALS extreme loads can be roughly estimated by multiplying ULS extreme value by the safety factor. It can be seen that for different response problems, the ratio is very different from each other. Thus one should pay extra attention when choosing safety factor to estimate ALS extreme response.

It can also be found that for the non-period sensitive case, the square of ratio for linear case is 1.8, which is close to the ratio for the quadratic case 1.7. While for the period sensitive case, the square of ratio for linear case is 1.7, which is close to the ratio for the quadratic case 1.6. This result can, to some extent, prove that the estimated response value is of right amplitude.

3.3.2 Important Weather Characteristic Region for Extreme Response

By studying important region for response exceedance, one can see directly which combinations of sea states have major contribution to the most probable long term response. The method to find important region for long term response exceedance is shown as below.

Based on previous study, one has already known the distribution function for non-exceedance probability of response under a given sea state, i.e. $F_{X_{Nonexc}|H_sT_p}(x|h_st_p)$. Thus the exceedance probability under given sea state is:

$$Q_{X_{Nonexc}|H_sT_p}(x|h_st_p) = 1 - F_{X_{Exc}|H_sT_p}(x|h_st_p) \tag{3.35}$$

The exceedance probability of response can be calculated by:

$$Q_{X_{Exc,i,j}}(x) = Q_{X_{Exc}|H_sT_p}(x|h_s, t_p) \cdot \delta F_{H_sT_p}(h_s, t_p) \tag{3.36}$$

By summing all $F_{X_{Exc}}(x)$, the exceedance probability for all sea states reads:

$$Q_{X_{Exc}}(x) = \sum_{i=1}^{I}\sum_{j=1}^{J} Q_{X_{Exc,i,j}}(x) \tag{3.37}$$

Where capital I denotes the total number of h_s, capital J denotes the total number of t_p. Then the weighting of exceedance probability of each sea state can be calculated by:

$$P_{i,j} = \frac{Q_{X_{Exc,i,j}}(x)}{Q_{X_{Exc}}(x)} \tag{3.38}$$

$P_{i,j} > 0.1\%$ is selected as the important region of exceedance. Here non-period sensitive linear case with $b_1 = 0.005$ is taken for example. The important contribution area is plotted together with the environmental contour line in Fig. (3.9). The environmental contour line is only for illustrative purpose, the method to establish an environmental contour line will be discussed later in thesis.

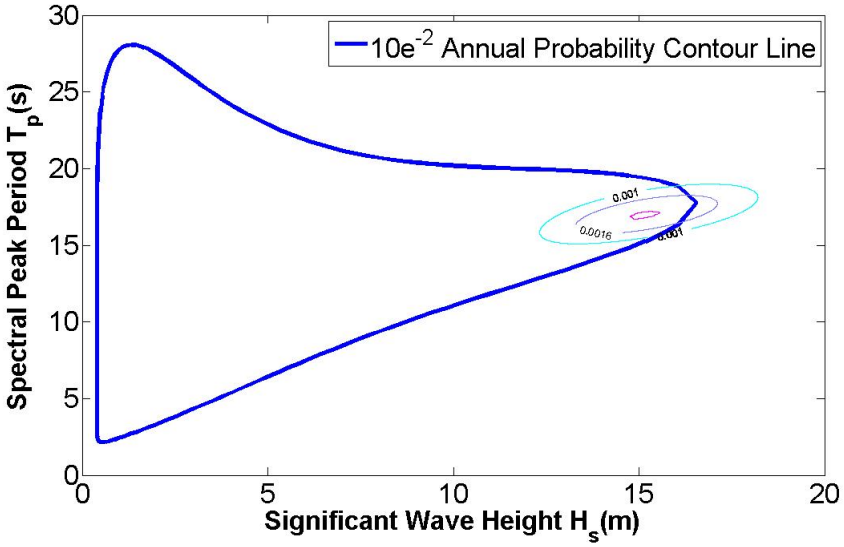

Figure 3.9: Important Contribution Area plotted with Environmental Contour Line

Cases with different period sensitivity, non-linearity and b_1 are presented in Appendix, Figs. (A.5 to A.8).

It is shown that the important region for exceedance appears with different shapes and in different positions for different response cases.

The region for quadratic response case appears to be shorter in h_s range and fatter in t_p range, both for the non-period sensitive and period sensitive case. This is because for the quadratic case, the effect of h_s is larger on final response than for the linear case, thus the important region becomes more concentrated in h_s range.

The region for period sensitive case appears to be in lower h_s and t_p range, both for the linear and quadratic response case. This is because the effect of t_p becomes larger, and a sea state close to the natural period of structure will give the largest response. Thus the important region is concentrated around the natural period of structure, 14s, in this case. The effect of h_s becomes relatively smaller, thus the region does not appear in the highest h_s range.

The region for low t_p variance case, i.e. b_1=0.00073 , appears to be narrower than that for larger t_p variance case, i.e. b_1=0.005, as can be seen in Fig. (A.6). This is due to the upper range of the environmental contour is narrower, thus the important region is compressed. Reason for this will be discussed in Chapter 4.

3.3.3 Effect of Non-linearity

(1) Effect of Non-linearity on Final Response

In order to study the effect of non-linearity, different values of c_2 are used to calculate the response and important area for exceedance of X_{100}. The 100-year extreme response values are presented in Tab. 3.7:

Table 3.7: Extreme Responses for Different Non-linearity Cases

	NPS			PS		
	X_{100}	X_{10000}	Ratio	X_{100}	X_{10000}	Ratio
$c_2 = 0.75$	17.6	21.9	1.244	15.6	19.3	1.237
$c_2 = 1$	36.0	48.1	1.336	30.9	40.5	1.311
$c_2 = 1.5$	151.0	229.4	1.519	122.1	177.3	1.452
$c_2 = 2$	627.8	1087.5	1.732	480.6	773.7	1.610

It can be seen that, for both period-sensitive and non-period sensitive cases, different values of c_2 have a big effect on the response value. The response value has increased obviously with the increasing $X_{3h,100}$. The ratio between X_{10000} and X_{100} is calculated. The reason has been discussed in Chapter 2, regarding the effect of c_2.

(2) Effect of Non-linearity on Important Region

The important area for exceedance of X_{100} is plotted in Fig. (3.10). The outer contour denotes the sea state with contribution equal to 0.1%, the inner ones are with contribution higher than 0.1%.

For the period sensitive case, comparison figures are shown in Appendix, Fig. (A.9).

It can be seen that, either for period sensitive or non-period sensitive case, different values of c_2 do not have a big effect on shape of the important area for exceedance

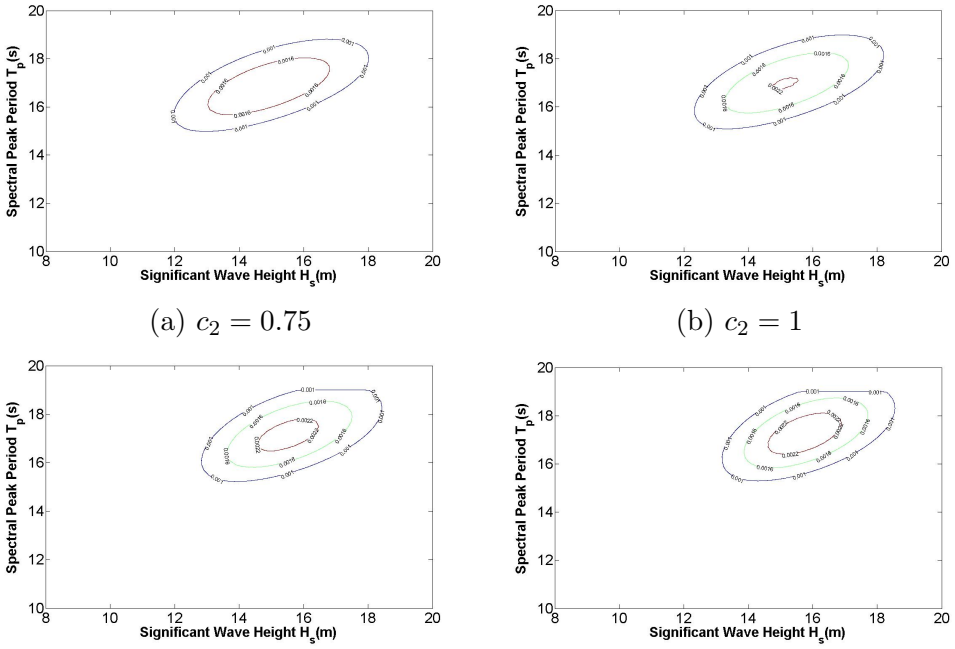

(a) $c_2 = 0.75$ (b) $c_2 = 1$

(c) $c_2 = 1.5$ (d) $c_2 = 2$

Figure 3.10: Comparison between Different c_2 for Non-period Sensitive Case

of X_{100}. It suggests that as long as the period sensitivity of a structure is specified, the effect of non-linearity will not have an obvious effect on response.

3.3.4 Effect of Period Sensitive and Non-period Sensitive on Response Value

(1) Effect of Period Sensitivity on Final Response

From Tab. (3.7), it can be seen that for same non-linearity, response for period sensitive case is smaller than response for non-period sensitive case. This can be explained by theoretical view and physical reason.

a. The theoretical reason

From Eq. (2.17), $\mu_{X_{3h}}(h,t)$ can be written as:

$$\mu_{X_{3h}}(h,t) = G_1(h) \cdot G_2(t) \tag{3.39}$$

with,

$$G_1(h) = c_1 \cdot h^{c_2} \tag{3.40}$$

$$G_2(t) = 1 + \cos^{c_3}\left(\frac{2\pi(t-c_4)}{c_5}\right) \tag{3.41}$$

For non-period sensitive case, c_5 is of a large value, and thus $G_2(t)$ is close to 2, it does not have a big variation over the period, as shown in Fig. (2.3). Therefore the response is majorly decided by $G_1(h)$.

While for the period-sensitive case, $G_2(t)$ has a steep variation over the period, as shown clearly in Fig. (2.3). $G_2(t)$ is smaller than 2 for most part of its period, thus $\mu_{X_{3h}}(h,t)$ for period sensitive case will also be smaller than $\mu_{X_{3h}}(h,t)$ for non-period sensitive case.

Therefore response for period sensitive case is smaller than that for non-period sensitive case.

b. The Physical Reason

Different combinations of parameters mean different response problems. It means that different structures are considered here. In this case, surge motion of a floating platform is taken as an example for the period sensitive response problem, rigid platform is taken as an example for the non-period sensitive structure.

If a structure is period sensitive, large response will only occur when period of the input load is close to natural period of the structure. For example, the surge motion of a floating platform will have the largest response when it is in resonance with the dynamic wind forces. According to Larsen(2012), the dynamic equilibrium between external force and the damping force reads:

$$\omega \cdot u_0 \cdot c = R_0 \tag{3.42}$$

where ω is the angualr frequency, u_0 is the response amplitude, c is the damping coefficient and R_0 is the external force.

Generally speaking, damping effect for period sensitive structures is larger than for non-period sensitive structures. The response for period sensitive case will be much limited by damping effect, thus the value will be smaller.

While if a structure is non-period sensitive, the response value will keep stable over the entire wave period. For example, response for rigid platform is not much affected by the period of wave force. According to Larsen(2012), the dynamic equilibrium for rigid platform reads:

$$u_0 \cdot k = R_0 + \omega^2 u_0 \cdot m \tag{3.43}$$

where m is the mass of structure.

In Eq. (3.42), term $\omega^2 u_0 \cdot m$ will normally be smallest since ω is less than the Eigen frequency. This means that (roughly speaking) there is equilibrium between the external force and the restoring force in the structure, and not affected by damping. It can also be seen that the inertia forces act in the same direction as the external force, and this leads to a higher response than the pure static response.

Therefore it can be concluded that for certain response problems, response for the period sensitive case is smaller than the response for non-period sensitive case.

It can be seen that since the response problem is not specified, there are many uncertainties in the analysis. Therefore the physical reason is only a qualitative analysis.

(2) Effect of Period Sensitivity on Important Region

Similar figures for important area for exceedance of X_{100} are plotted in Fig. (3.11), $c_2 = 0.75$ is taken for an example.

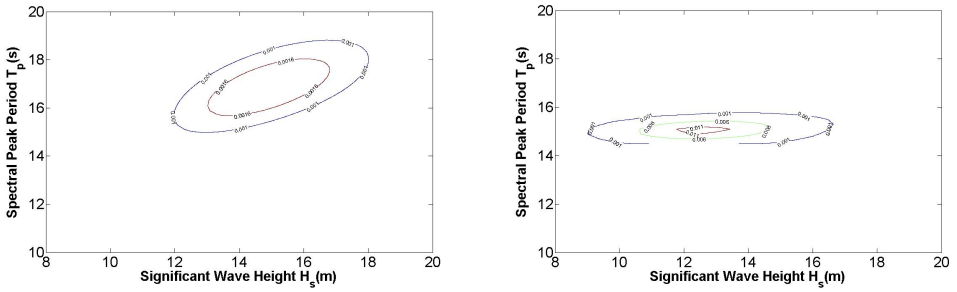

(a) Non-period Sensitive (b) Period Sensitive

Figure 3.11: Comparison between Non-period Sensitive and Period Sensitive Case for $c_2 = 0.75$

More comparisons for $c_2 = 1$, $c_2 = 1.5$, $c_2 = 2$ are shown in Appendix, Figs. (A.10 to A.12).

There are two observations:

a. It can be obviously seen from Fig. (3.11) that the important area for period sensitive case appears shorter but wider than for non-period sensitive case. The reason is that for non-period sensitive case, H_s has more effect on final response, so the important region appears to be more concentrated in H_s range. While for period sensitive case, the importance of H_s becomes smaller, thus the region spreads longer in H_s range. The reason for this behavior has been discussed in Section 3.3, Chapter 3.

b. The corresponding important region appears in smaller H_s and T_p ranges for period sensitive case

Taking TLP for example, the spectral period close to its natural period is more important to the response. While for rigid platform, it is the significant wave height that decides directly the response. So h_s and t_p of important sea state for period sensitive case tends to be in different positions from non-period sensitive case.

3.3.5 Effect of Width Parameter of $ln(T_p)$ Variance

Width parameter of $ln(T_p)$ variance means the value of b_1 in Eq. (3.10). b_1 is the parameter which decides the magnitude of σ^2, especially for large h_s range. Thus b_1 is an important parameter for large response prediction.

(1) Effect of Width Parameter on Final Response

Response values calculated from full long term analysis are summarized in Tab. (3.8).

It can be seen from the table that b_1 does not have a big effect on the final response. The reason is that b_1 is the parameter which decides variance, but it does not affect the expected value.

Table 3.8: Extreme Responses for Different Non-linearity and Period Sensitivity Cases

	$X_{3h,100}$	
	$b_1 = 0.005$	$b_1 = 0.00073$
Linear and Non-Period Sensitive	36.0	36.1
Quadratic and Non-Period Sensitive	625.2	628.4
Linear and Period Sensitive	30.9	30.4
Quadratic and Period Sensitive	480.8	461.8

(2) Effect of Width Parameter on Important Region

Similar figures for important area for exceedance of X_{100} are plotted in Fig. (3.12).

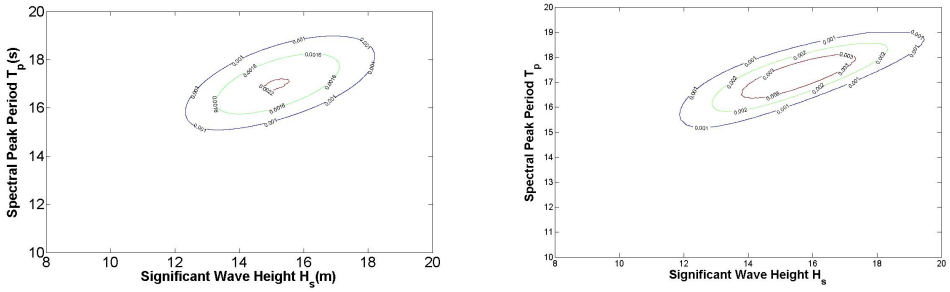

(a) $b_1 = 0.005$ (b) $b_1 = 0.00073$

Figure 3.12: Comparison between Different b_1 for Linear and Non-Period Sensitive case

More comparisons for different non-linearity and period sensitivity are shown in Appendix, Figs. (A.13 to A.15).

It can be seen from Fig. (3.12) that for both period-sensitive and non-period sensitive cases, the important region of $b_1 = 0.00073$ is narrower than for $b_1 = 0.005$. The reason is that b_1 is the main parameter which decides the magnitude of the variance, and the variance is reflected as bandwidth in the figures. Thus the larger is b_1, the wider is the band.

3.4 Summary

In this chapter, firstly the author describes the method to establish joint distribution of h_s and t_p for a given h_s. Then the probability scatter diagram of h_s and t_p is established. Based on this, the long term distribution of response can be calculated.

Then the effect of response function on final response value and important contribution region is studied. It can be included that structure with different non-linearity and period sensitivity will have quite different response behaviors, even under the same sea state.

Regarding the long term response value, one should pay enough attention to the

ratio between $X_{3h_{10000}}$ and $X_{3h_{100}}$, since it corresponds to the safety factor one uses in engineering design. The ratio varies much for different response cases. Thus it is important for an engineer to choose the proper safety factor for a specific structure.

The important contribution region gives important information about the important sea states for ULS design. One should notice that for different response problem, the important region lies in different H_s and T_p range. Thus if one is trying to find the most important sea states, it is important to take the specific structure into consideration, since different response problems correspond to different important sea states.

Chapter 4

Environmental Contour Line Method

4.1 Motivation for Adopting Environmental Contour Line

According to Haver et. al(2012), it will be quite time-consuming to establish the short term distribution of the 3-hour maximum response given the sea state characteristics for very complex response problems. For such cases it would be useful to have a method where one could estimate long term extremes from a carefully selected short term sea state. The environmental contour method may represent a possible approach. In particular, this can be useful for cases where one have to estimate q-probability response extremes directly from model tests.

This is the general purpose of environmental contour line method. In this chapter, the author only focuses on the establishment of environmental contour line and the target percentile estimated from environmental contour line method. Compared to all sea state long term approach, environmental contour line method is only an approximated method. Thus the target percentile estimated can only be used for verification purpose.

4.2 Basic Knowledge about Environmental Contour Line

4.2.1 Establishment of Environmental Contour Line

The contour line of H_s and T_p is defined as a line contour of combination of H_s and T_p, corresponds to exceedance probability of p_e, where $p_e = 10^{-2}$ per year for ULS and $p_e = 10^{-4}$ for ALS. In this project, IFORM technique is used to establish the lines of constant probability of exceedance.

From last chapter, the joint probability distribution model $f_{H_sT_p}(h,t)$ is established. Then the probability of exceedance p_e reads:

$$p_e = \int\int_{A_f} f_{H_s T_p}(h,t) dh_s dt_p \tag{4.1}$$

where A_f is the failure set.

Instead of solving the integral in physical parameter space, it can be transformed to a space defined by 2 independent and standard Gaussian variables, u_1 and u_2. u_1 corresponds to H_s and u_2 corresponds to T_p, assuming that H_s is the most important parameter. Since a priori relation between the physical parameters and standard Gaussian parameters is not known, a proper transformation can be determined by requiring:

$$\Phi(u_1) = F_{H_s}(h_s) \tag{4.2}$$

$$\Phi(u_2) = F_{T_p|H_s}(t_p|h_s) \tag{4.3}$$

then,

$$u_1 = \Phi^{-1}[F_{H_s}(h_s)] \tag{4.4}$$

$$u_2 = \Phi^{-1}[F_{T_p|H_s}(t_p|h_s)] \tag{4.5}$$

The contour lines in the u-space are circles with radius equal to β, the definition of β can be seen in Fig. (4.1).

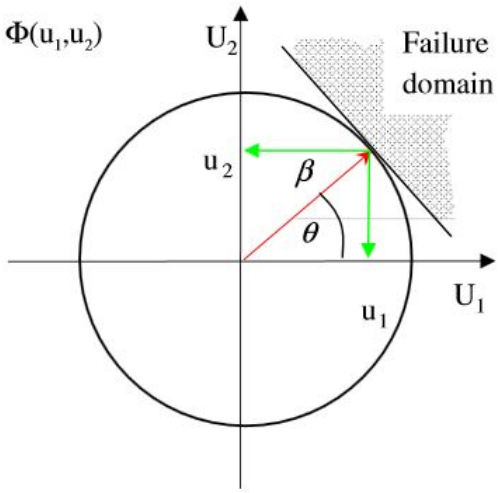

Figure 4.1: Definition of u-space for the ULS case

$$p_e = \frac{q}{N} = \frac{10^{-2}}{2920} \tag{4.6}$$

$$\beta = \Phi^{-1}(p_e) = 4.5 \tag{4.7}$$

For the ALS case,

$$p_e = \frac{q}{N} = \frac{10^{-4}}{2920} \tag{4.8}$$

$$\beta = \Phi^{-1}(p_e) = 5.4 \tag{4.9}$$

Assuming the failure boundary is a tangent to the circle with radius, β, the radius is uniquely related to the target exceedance probability, p_e:

$$\beta = \Phi^{-1}(p_e) \tag{4.10}$$

Then values of u_1, u_2 can be decided as coordinates on the circle with radius β. $u_1$and u_2 have relationship:

$$u_1^2 + u_2^2 = \beta^2 \tag{4.11}$$

Since u_1 and h_s, u_2 and t_p are uniquely connected, values of h_s and t_p can be decided by:

$$h_s = F_{H_s}(h_s)^{-1}\Phi(u_1) \tag{4.12}$$

$$t_p = F_{T_p|H_s}(t_p|h_s)^{-1}\Phi(u_2) \tag{4.13}$$

Thus points on the contour line in the physical space are decided.

This process is shown as:(Baarholm et. al(2010))

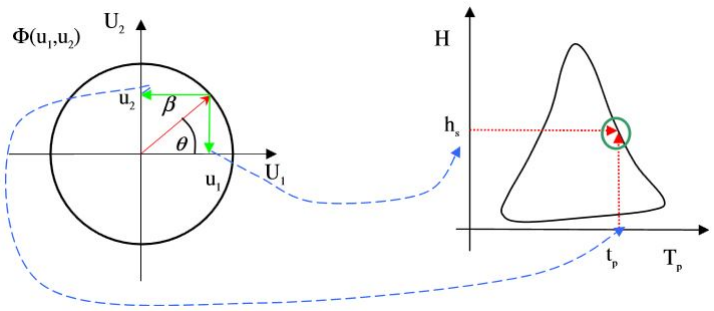

Figure 4.2: Transformation from U-space to Physical-space

The distribution of H_s and T_p have been established in Chapter 3. Following the above procedures, the environmental contour line in physical space and u-space are established as in Fig. (4.3).

4.2.2 Study of Failure Domain on Environmental Contour Line

Failure domain on environmental contour is studied in this section. It is assumed that the worst sea state corresponds to point $A(T_{p,A}, H_{s,A})$, thus the green area is the failure domain. A transformation from the physical space to the u-space is shown in Fig. (4.4).

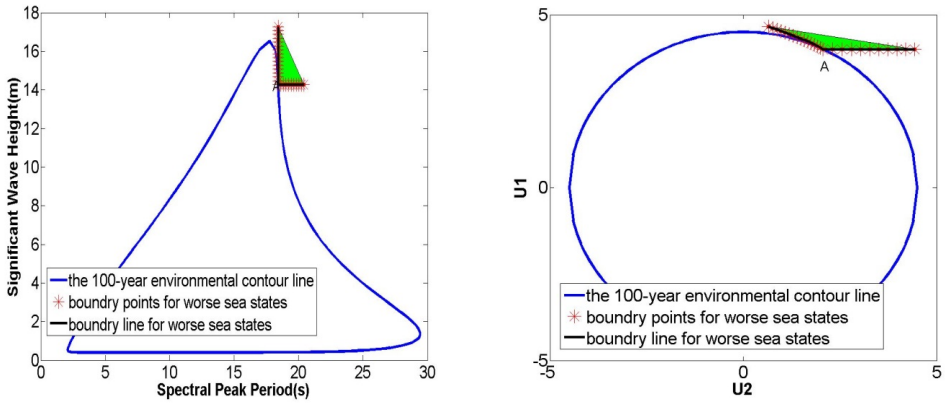

(a) Method of Moment (b) Method of Linear Fitting

Figure 4.3: Failure Domain in Physical-space and U-space

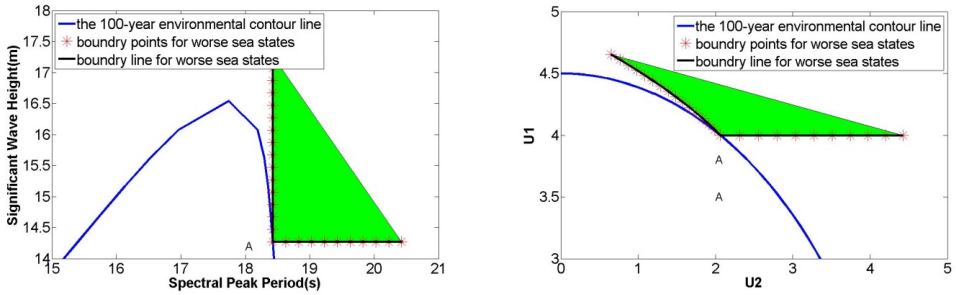

(a) Method of Moment (b) Method of Linear Fitting

Figure 4.4: Failure Domain in physical-space and u-space

It can be seen that the failure boundary in u-space is not the tangent line, but a curved line over point A. However in practical, the failure boundary in u-space is taken as the tangent line over point A. This approximation is well on the safe side for area lower-right to point A, but is a little on the dangerous side for area to the upper-left of point A, since the failure boundary bends towards the cycle. This might be one of the uncertainties involved when calculating target percentiles.

4.3 Uncertainties of Environmental Contour Line

The shape of the environmental contour line is decided directly by the fitted model for h_s and t_p. In the previous study, 3-parameter Weibull distribution model gives a good estimation for the long term significant wave height. Fitting for mean value of $ln(t_p)$ for each h_s interval also gives a good result. But the fitting for variance of $ln(t_p)$ does not give a good description for large h_s, as shown in Fig. (4.5).

The function for variance of $ln(t_p)$ reads:

$$\sigma^2 = b_1 + b_2 \cdot exp(-h_s \cdot b_3) \tag{4.14}$$

It can be seen that for large h_s, the term $b_2 \cdot exp(-h_s \cdot b_3)$ is negligible, thus b_1

is the only parameter which decides the magnitude of σ^2. And b_1 is the major uncertainty of environmental contour line method.

In order to study the effect of b_1, four sets of parameters for fitting for variance of t_p for each h_s interval are shown in Fig. (4.5).

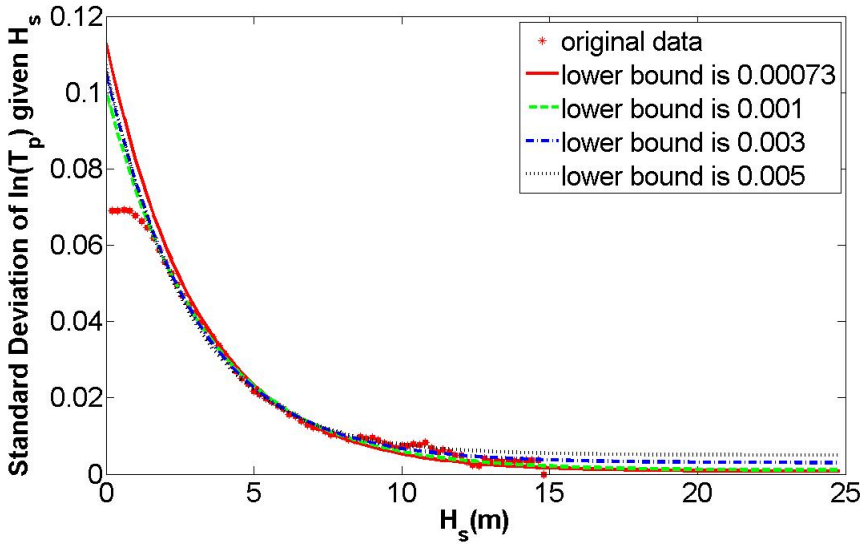

Figure 4.5: Standard Deviation of $ln(T_p)$ given H_s for Various Models

A zoomed-in figure for lower tail of σ^2 shows more information on large h_s. It is plotted in Fig. (4.6).

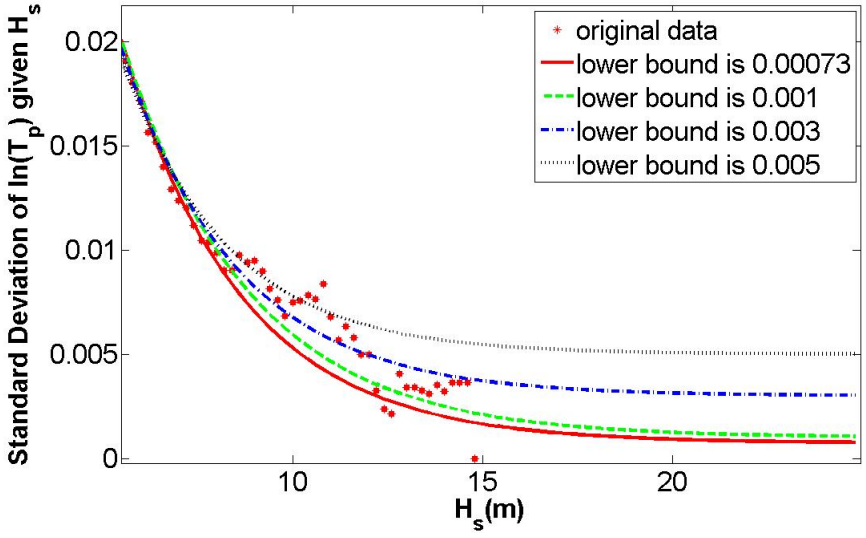

Figure 4.6: Zoomed-in Version of Standard Deviation of $ln(T_p)$ given H_s for Various Models

It can be seen from Fig. (4.6) that $b_1 = 0.00073$ is the lower bound regarding the large significant wave heights. However, the data for the largest significant wave heights are possibly corresponding to merely one or two storm events. Therefore one do hesitate to give full weight to this result. It is indicated that a proper

simulation should be somewhere between the lower bound $b_1 = 0.00073$ and upper bound $b_1 = 0.005$. But in order to ensure enough safety in extreme sea states, $b_1 = 0.005$ is maintained. The default value of b_1 is set to be 0.005 throughout the thesis.

Various environmental contour lines for different b_1 are shown in Fig. (4.7).

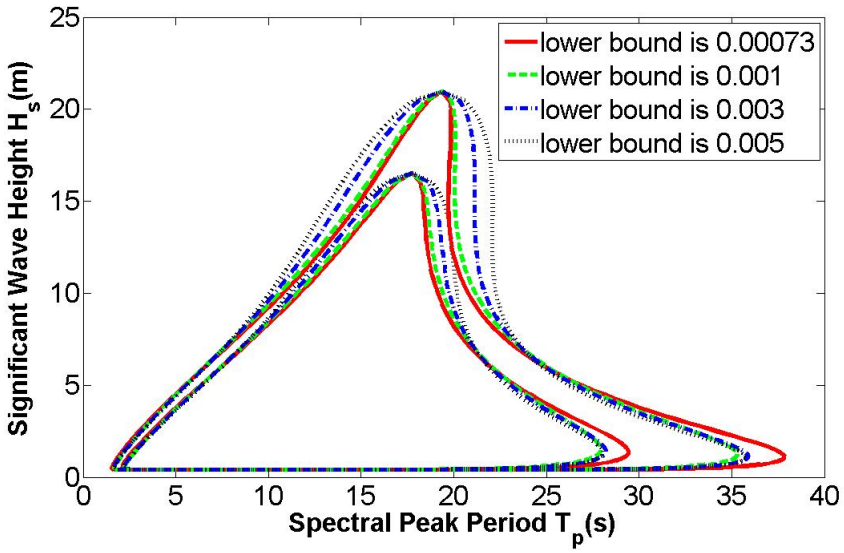

Figure 4.7: Environmental Contours for Various Lower Bounds for the Conditional Variance of $\ln(T_p)$

If the most important sea state along the contour is the peak of the contour, which is the case for most non-period sensitive response problems, the uncertainty of b_1 is not very important. However, for response problems governed by steepest sea state along the contour, b_1 can be a crucial parameter. It can be observed that the steepest part for $b_1 = 0.00073$ on the 10000-year contour line actually coincides with the steepest part for $b_1 = 0.005$ on the 100-year contour line. Further information is referred to Haver et. al(2012).

It can be concluded that b_1 is an important parameter regarding choosing the worst sea. Larger b_1 corresponds to larger h_s and t_p combinations, i.e. worse sea states for design purpose, which is on the safe side. Thus despite its conservatism, b_1 is still set to be 0.005 in practical engineering.

4.4 Target Percentile for Extreme Response Cases

4.4.1 Introduction of Target Percentile

Same as previous, one can transform the integral of response to a space defined by standard Gaussian variable u_3. To determine a proper transformation by requiring:

$$\Phi(u_3) = F_{X_{3h}|T_p,H_s}(x|t_p, h_s) \tag{4.15}$$

then,

$$u_3 = \Phi^{-1}(F_{X_{3h}|T_p,H_s}(x|t_p, h_s)) \tag{4.16}$$

In Fig. (4.7), the various models for different b_1 are shown. If the most important sea state along the contour for a given response quantity are close to the peak of the contour, which will be the case for most practical problems, the value of b_1 is not very important. However, for response problems been governed by steep sea states, this can be a crucial parameter. It can be observed that the steepest part for $b_1 = 0.00073$ on the 10000-year contour line actually coincides with the steepest part for $b_1 = 0.005$ on the 100-year contour line.(Haver et. al(2012))

Therefore when $u_3 = 0$, which corresponds to the red point in Fig. (4.8), $f_{X_{3h}|T_p,H_s}(x|t_p, h_s)$ has the largest probability. In this case, $X_{u_3=0}$ is the most probable value for the given sea state.

According to Haver(2012), the median response in this point is too low, the point on the red contour did not come out as the design point. In order to obtain the design response, a higher percentile must be selected. The larger u_3 is in the design point, the higher must the percentile be.

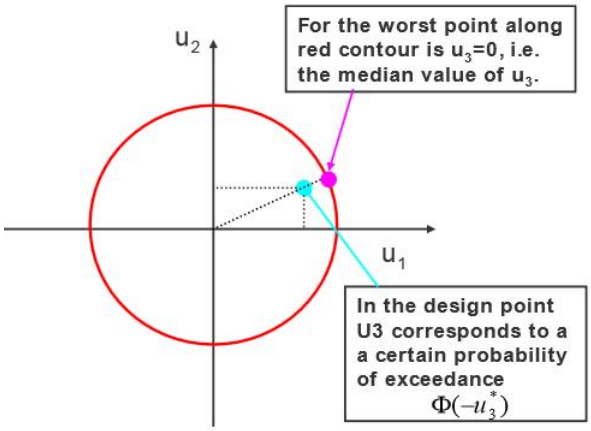

Figure 4.8: Physical Meaning of u_3

It is not easy to give a theoretical argument for what percentile should be selected. Based on experience with problems where the contour method results are compared to results from full long term analysis, a reasonable percentile for $q = 10^{-2}$ is 90%. For $q = 10^{-4}$, there seems to be a tendency of going to a slightly higher percentile and a possibility could be 95%. (Haver et. al(2012))

It is important to notice that the environmental contour line method is an approximate method, while the full long term analysis gives the correct prediction. Thus the percentile here can be regarded as an indication of the correctness of the environmental contour line method. If the percentile does lie in 85% to 90%, it suggests that the environmental contour line method is an accurate method to estimate extreme values. While if the percentile deviates far from the expected value, in this case, smaller than the expected value, it suggests that the environmental contour line method gives an overestimation of the most probable sea state.

4.4.2 Verification Study of the Target Percentile

In this case, a verification study is performed. Response value for $X_{3h,100}$ and $X_{3h,10000}$ have already been decided from the full long term analysis. So the target percentile can be calculated as:

$$F_{X_{3h}} = exp\{exp[-(\frac{x-\alpha(h,t)}{\beta(h,t)})]\} \tag{4.17}$$

where $\alpha(h,t)$ and $\beta(h,t)$ are decided from Eq. (2.6) and Eq. (2.7).

There are two steps to decide the percentile:

(1) Identify the most unfavorable hurricane peak event in view of the response under consideration. For a complex response problem, this is done by doing some time domain simulations or model tests of 3-hour duration for some few sea states along the critical part of the contour.

But in this case, a simplified method is applied. A measure of the 3-hour extreme levels for each hurricane is obtained by:

$$X_3h = \overline{x} + k \cdot s_{X_{3h}} \tag{4.18}$$

According to Haver et. al(2012), $\overline{x}$ and $s_{X_{3h}}$ are the mean and standard deviation of the 3-hour extreme value for the various selected hurricane peak events along the contour respectively. k is a factor used for pointing to a proper extreme value level. It will typically be a value around 1.3-1.5 depending on the coefficient of variation of X_{3h}.

(2) When this point is identified, corresponding parameters for the Gumbel distribution can be decided. The response value from full long term analysis has already been decided in Chapter 2. Then the target percentile can be calculated.

The linear and non-period sensitive case is taken for an example, the results are shown in Tab. (4.1). Cases with different non-linearity and period sensitivity are shown in Appendix, Tabs. (B.1 to B.3).

Table 4.1: Extreme Values and Target Percentile for Linear and Non-period Sensitive Case

	x(response)	α	β	P	$\frac{\alpha}{\beta}$
$q = 0.01$ per year	36.0	31.3677	2.5610	85.10%	0.08
$q = 0.0001$ per year	48.1	39.3529	3.2130	93.67%	0.08

4.4.3 Comments on the Percentile

The expected percentile for response is much higher than 50%, hopefully lies in 85% to 90% (Norsok, N003). However, it is seen from Tab. (4.1) that for some cases, the percentiles are well below expectation.

(1) Effect of b_1, c_2 and Period Sensitivity

In order to study the effect of non-linearity parameter c_1, environmental contour breadth parameter b_1 and period sensitivity, a summary of response and target percentile in different situations are shown in Tab. (4.2).

Table 4.2: Summary of Results for Different Non-linearity, Width Parameter, Period-sensitivity and Return Period Cases

Case: $q = 0.01$		$b_1 = 0.00073$		$b_1 = 0.001$		$b_1 = 0.003$		$b_1 = 0.005$	
		NPS	PS	NPS	PS	NPS	PS	NPS	PS
$c_2 = 0.75$	Val.	17.6	15.4	17.6	15.4	17.6	15.5	17.6	15.6
	Pct.	86.25%	85.36%	86.25%	83.55%	86.25%	76.26%	86.25%	73.17%
$c_2 = 1$	Val.	36.0	30.4	36.0	30.5	36.0	30.8	36.0	30.9
	Pct.	85.10%	85.55%	85.10%	82.81%	85.10%	75.95%	85.10%	71.90%
$c_2 = 1.5$	Val.	151.0	118.4	151.0	119.0	151.0	120.8	151.0	122.0
	Pct.	83.11%	85.07%	83.11%	81.87%	83.11%	75.47%	83.11%	70.43%
$c_2 = 2$	Val.	625.2	461.8	625.2	465.5	625.2	475.6	625.2	482.4
	Pct.	81.25%	84.08%	81.25%	81.81%	81.25%	75.62%	81.25%	69.95%
Case: $q = 0.01$		$b_1 = 0.00073$		$b_1 = 0.001$		$b_1 = 0.003$		$b_1 = 0.005$	
		NPS	PS	NPS	PS	NPS	PS	NPS	PS
$c_2 = 0.75$	Val.	22.0	18.8	22.0	18.9	22.0	19.1	22.0	19.3
	Pct.	95.02%	98.30%	95.02%	98.30%	95.02%	96.04%	95.02%	93.81%
$c_2 = 1$	Val.	48.1	39.0	48.1	39.3	48.1	40.0	48.1	40.5
	Pct.	93.67%	98.58%	93.67%	97.97%	93.67%	95.07%	93.67%	92.67%
$c_2 = 1.5$	Val.	229.4	165.2	229.4	167.1	229.4	172.8	229.4	177.3
	Pct.	91.45%	97.80%	91.45%	97.17%	91.45%	93.34%	91.45%	89.81%
$c_2 = 2$	Val.	1073.6	696.3	1073.6	707.8	1073.6	744.1	1073.6	733.7
	Pct.	89.76%	97.27%	89.76%	96.36%	89.76%	92.14%	89.76%	87.79%

Here are some observations:

a. same width parameter b_1 and period-sensitivity

The response values increase with increasing c_2. The response percentiles decrease with increasing c_2.

This can be easily explained by Eq. (2.14) to Eq. (2.17), for a given long term response value X, the larger c_2 will lead to larger expected value $\mu_{X_{3h}}$, standard deviation $\sigma_{X_{3h}}$ of X_3h, and then larger parameters of the Gumbel distribution α and β, but smaller percentile $F_{X_{3h}|H_sT_p}$.

From practical point of view, if the effect of non-linearity is larger, the response will be larger. For example, the response which is quadratic to h_s will be larger than that which is linear to h_s. For the percentile: if the effect of non-linearity is larger, the expected value of X_{3h}, $\mu_{X_{3h}}$ will be larger, thus the percentile will be smaller. It suggests that with increasing c_2, the environmental contour line method tends to give overestimation of the most probable sea state.

In addition, it can be observed that compared with width parameter b_1 and period sensitivity, the effect of c_2 on percentile is not significant. This suggests that c_2 is not the major parameter which decides the accuracy of the environmental contour line method.

b. For same breadth parameter b_1 and non-linearity parameter c_2

The response values are larger for non-period sensitive case than that for period sensitive case. The percentile, however, does not show an obvious pattern.

Reason of the response has been discussed in Section 3.3, Chapter 3. For the percentile: the percentile is commonly decided by response value x and the worst sea state, thus it does not show an obvious pattern.

In the example given above, the non-period sensitive case and the period sensitive case are chosen to be two extreme cases. The response is either very sensitive or very insensitive to period, as plotted in Fig. (2.3). But in practical, the structure may lie somewhere between the two extreme cases. Thus the non-period sensitive case may give an underestimation of the most probable sea state with too high percentile, and the period sensitive case may give an overestimation of the most probable sea state with a too low percentile.

Further study regarding period sensitivity will be discussed in Part(2) of Section 4.4.3.

c. For same non-linearity parameter c_2 and period-sensitivity

The response value does not vary much for different b_1. Since b_1 only has effect on the variance for t_p, but does not affect the expected mean t_p. b_1 is the parameter which decides the width of environmental contour. But it will not affect the long term prediction of response.

However, the percentiles for different b_1 show different trends for NPS and PS case. For NPS case, the percentiles do not change, while for PS case, the percentiles decrease with increasing b_1.

More details are studied here, the coordinates of the selected worst sea state, h_s and t_p are shown in the following tables. For the non-period sensitive case:

Table 4.3: Coordinates of the Worst Sea State Point in the Physical Space for Non-period Sensitive Case

NPS	$b_1 = 0.00073$	$b_1 = 0.001$	$b_1 = 0.003$	$b_1 = 0.005$
h_s	16.6	16.6	16.6	16.6
t_p	17.8	17.8	17.8	17.8

For the NPS case, the selected worst sea state is the one with largest h_s. It is the top point on the 100-year contour line. It suggests that for the NPS case, b_1 does not have an effect on selection of the worst sea state and target percentile.

Table 4.4: Coordinates of the Worst Sea State Point in the Physical Space for Period Sensitive Case

NPS	$b_1 = 0.00073$	$b_1 = 0.001$	$b_1 = 0.003$	$b_1 = 0.005$
h_s	14.3	14.3	14.7	15.2
t_p	15.4	15.2	15.2	15.3

For the period sensitive case, the selected worst sea states are the red points to the left of the top point on the 100 year contour lines, which is shown in the Fig.

(4.9):

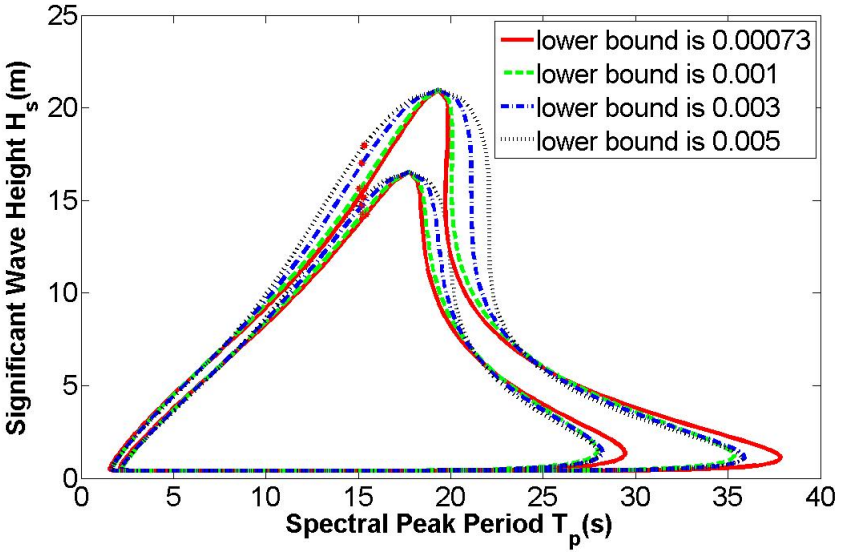

Figure 4.9: Selected Worst Sea State Points along the Environmental Contour Line

It is observed that h_s is not the only important variable to decide the worst sea state. It can be observed that t_p around 15s is an important region for worst sea state, which corresponds to c_4 in Eq. (2.17), c_4 decides the peak of the cosine wave of response. Therefore, it can be concluded that for the period sensitive case, both h_s and t_p are important variables that decide the worst sea state.

The reason for the response percentile decreases with increasing b_1: b_1 is the parameter which decides the variability of $ln(t_p)$ for a given h_s, the larger b_1 is, the larger variability does $ln(t_p)$ have. This is plotted in Fig. (4.9). Larger b_1 results in wider environmental contour line, especially the upper part. The position of the worst sea state is changed, results in an obvious increase of h_s. This may result in an overestimation of the most probable sea state, and then a lower percentile.

However, beyond all the analysis above, there are still some percentiles which are below recommendation from Norsok-003, which is 85% to 95%. The author suggests that further work should be done regarding the correct range of percentile.

(2) Effect of Other Parameters

a. Further Study for Effect of c_3 and c_5:

In the previous study, only two sets of c_3 and c_5 are selected for period sensitive and non-period sensitive case respectively. In order to study the effect of period sensitivity, different sets of parameters for period sensitivity are studied as below.

Firstly, the effect of different combinations of c_3 and c_5 is shown in Fig. (4.11):

Then an example with $b_1 = 0.005$, $c_2 = 2$ and 100-year value is calculated in Tab. (4.5).

It can be seen that the larger c_3 and smaller c_5 is, the smaller the value and percentile will be.

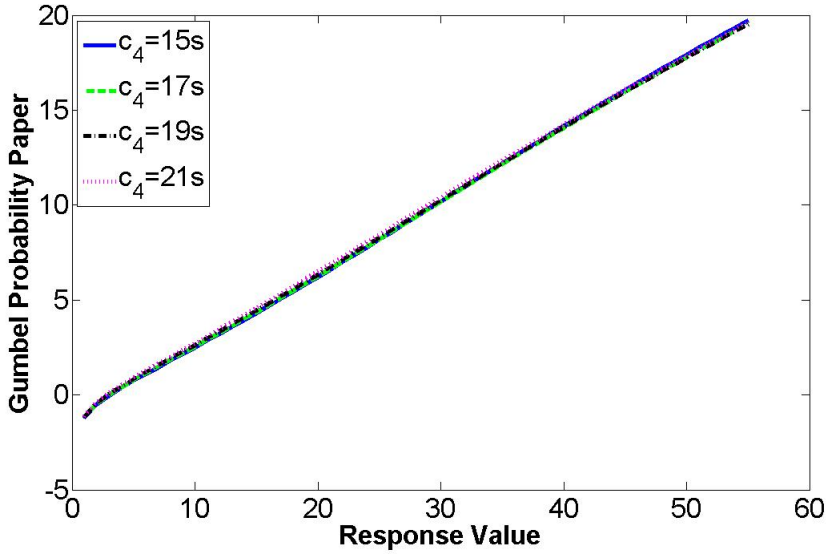

Figure 4.10: Effect of Different Combinations of c_3 and c_5 on Location Parameter α

Table 4.5: Extreme Value and Target Percentile for Different Scale Parameter Cases

	NPS		Case 1		Case 2		Case 3		Case 4		PS	
	c_3	c_5	c_3	c_5	c_3	c_5	c_3	c_5	c_3	c_5	c_3	c_5
	1	100	30	100	70	100	30	60	70	60	100	60
Val.	625.2		562.1		529.8		523.1		493.6		482.4	
Pct.	81.25%		80.86%		78.49%		77.77%		72.79%		69.95%	

c_3 together with c_5 decides the shape of the response curve. A larger c_3 and smaller c_5 will result in a steeper response curve, which mean the response is more sensitive to peak period. This has been discussed in Section 3.3 in Chapter 2.

Another important thing here is to notice here is a smooth trend from NPS case to PS case, decreasing gradually from 81.25%to 69.95%.

b. Effect of c_4:

As mentioned in the first chapter, c_4 decides the position where the largest response occurs. In this section, the effect of c_4 on long term response and percentile are studied. An example with $b_1 = 0.005$ is performed. Response values and percentiles for different cases are presented in Fig. (4.11) and Tab. (4.6).

It can be seen from Fig. (4.11a) , Fig. (4.11b)and Tab. (4.6) that, for non-period sensitive case, c_4 do not have significant effect on final result. This can also be explained in Fig. (4.11a), for non-period sensitive case, the response do not have an obvious variation over peak period.

While for the period sensitive case, it can be clearly seen in Fig. (4.11c) and Fig. (4.11d) that there are a bending for each curve on the Gumbel probability paper. And the bending starts at different places. It is found that the smaller c_4 is, the earlier the bending starts. This behavior suggests the relationship between sea

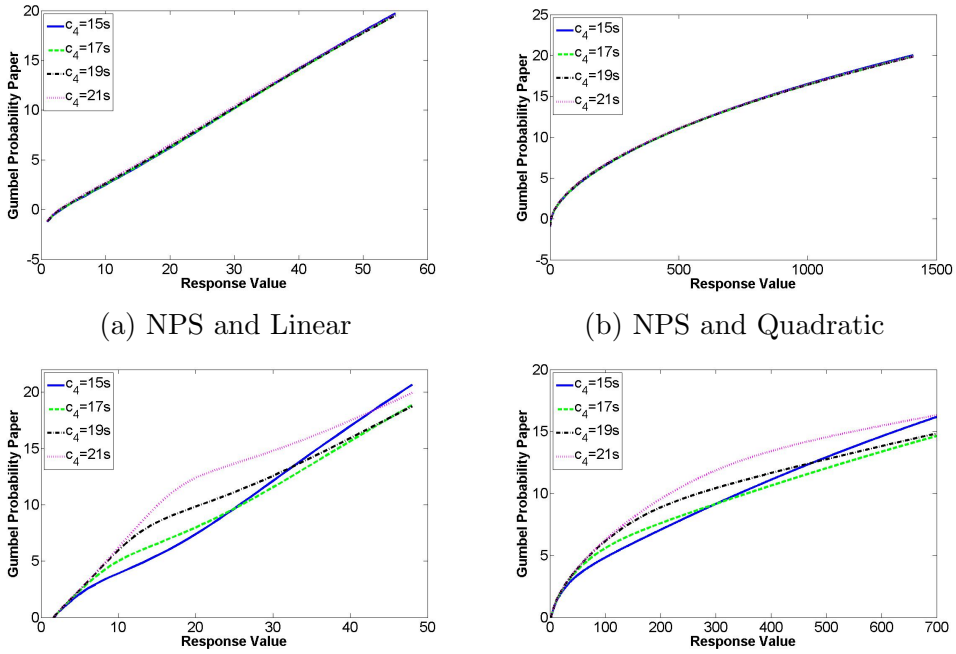

(a) NPS and Linear

(b) NPS and Quadratic

(c) PS and Linear

(d) PS and Quadratic

Figure 4.11: Cumulative Probability for Different c_4 plotted on Gumbel Probability Paper

Table 4.6: Extreme Value and Target Percentile for Different Period Sensitivity Cases

$c_2 = 2$		$c_4 = 15$		$c_4 = 17$		$c_4 = 19$		$c_4 = 21$	
		q=0.01	0.0001	0.01	0.0001	0.01	0.0001	0.01	0.0001
NPS	Val.	34.5	36.0	35.9	34.1	45.7	48.1	48.4	46.5
	Pct.	96.91%	85.10%	83.77%	83.04%	94.96%	93.67%	92.41%	91.36%
PS	Val.	19.5	30.9	25.98	18.1	25.3	40.5	41.89	24.5
	Pct.	86.71%	71.90%	27.17%	84.97%	95.94%	92.67%	87.04%	93.44%
$c_2 = 2$		$c_4 = 15$		$c_4 = 17$		$c_4 = 19$		$c_4 = 21$	
		q=0.01	0.0001	0.01	0.0001	0.01	0.0001	0.01	0.0001
NPS	Val.	599.5	625.2	626.3	594.8	1025.9	1073.6	1089.0	1058.4
	Pct.	82.02%	81.25%	80.66%	80.10%	90.56%	89.76%	89.05%	88.58%
PS	Val.	551.8	482.4	418.5	315.5	316.1	733.7	891.6	554.5
	Pct.	89.43%	69.95%	58.09%	80.96%	81.18%	87.79%	77.62%	89.82%

states and the natural period of response.

It is firstly believed that response of system increases fastest when the wave peak period is near its natural period. In Fig. (4.11c) and Fig. (4.11d), the flattest part of the curve corresponds to the fastest increasing response region, which corresponds to the natural period of response c_4. Thus a smaller c_4 corresponds to an earlier bending of the curve and smaller response value.

c. Effect of c_6:

c_6 is a measure of the variability around the mean 3-hour maximum. The effect

of c_6 on long term response and percentile is studied in this section. An example with $b_1 = 0.005$, $c_2 = 1$ and 100-year values is calculated as in Tab. (4.7).

Table 4.7: Extreme Value and Target Percentile for Different Position Parameter Cases

		$c_6 = 0.05$	$c_6 = 0.1$	$c_6 = 0.11$	$c_6 = 0.12$	$c_6 = 0.15$	$c_6 = 0.2$
NPS	Val.	33.5	36.0	36.8	37.5	40.0	44.7
	Pct.	71.21%	85.10%	86.92%	88.33%	91.62%	94.62%
PS	Val.	28.4	30.9	31.6	32.3	34.6	38.7
	Pct.	16.8%	71.9%	76.49%	80.18%	87.12%	92.24%

It can be seen from Tab. (4.7) that the long term response value has an obvious increase when c_6 increases. The reason is that, the long term response will be larger accounting for the variability, while c_6 does not have a significant effect on $\alpha(h,t)$ and $\beta(h,t)$, so in general the percentile goes up.

From practical point of view, if higher variability is considered, the all sea state approach will give an overestimated result, thus a higher percentile is expected. On the other hand, if the variability is chosen as low as 0.0073, it means that the long term prediction method will probably give an underestimated result, and thus low percentiles are found in NPS and PS cases.

For the NPS case, the percentiles seem to be in a reasonable range. While for the PS cases, low percentiles are found for $c_6 < 0.15$. It suggests that certain amount of variability should be taken into account to ensure an accurate result.

4.5 Summary

This chapter works as a supplementary study for the all sea state long term response method. In this chapter, the author gives a brief introduction of environmental contour line method and target percentile. By studying parameters from response functions effect on final result, one can have better understanding of the response problem.

It can be concluded that for non-period sensitive case, c_2 is the major parameter which has effect on the response. The reason is that, if the structure is not sensitive to wave period, significant wave height will be the only factor which affects final response and target percentile. In the response function, c_2 is the only parameter which is directly related to significant wave height h_s, thus if one is designing a non-period sensitive structure, more focus should be put on the non-linearity of the response problem.

While for period sensitive case, the response problem becomes more complicated. c_2 is not the only parameter which decides the result. Both c_4 and combination of c_3 and c_5 have effect on the final response and target percentile. Generally speaking, period sensitive problem tends to have smaller response value and target percentile than non-period sensitive problem. And if the natural period of a structure is close to the peak period of the worst sea state, it will have larger

response value. But the relationship between c_4 and target percentile remains unclear. Therefore, compared with non-period sensitive case, one should pay extra attention to the natural period and the period sensitivity of the structure. However, uncertainties remain if one is using environmental contour line method to decide the long term extreme response.

The value of c_6 determines the variability taken into consideration. It works as an overall compensation for all the uncertainties regarding the response function. Thus a properly chosen c_6 will result in an accurate response value and target percentile.

In conclusion, the non-linearity, period sensitivity, natural period of the structure, and uncertainties involved when choosing parameters for the response function should be taken into consideration, and then a reliable response function could be built.

Chapter 5

Peak over Threshold Method

5.1 Motivation for the Peak over Threshold Method

Provided the response problem under consideration is independent of the previous history of sea state characteristics, the long term approach as formulated in Chapter 2 is rather convenient for not too complicated response problems. If this is not the case, the long term response analysis has to be carried out in the time domain, i.e. the probabilistic characteristics of the response problem is calculated for each adjacent 3-hour period. This is conveniently handled by adopting the random storm approach.

The random storm approach has been more frequently used abroad than within Norway. Reason for this is that the extreme response is basically governed by the occurrences of some few extreme hurricanes. Between the hurricanes, weather conditions are rather benign and of no effect regarding prediction of response extremes. In for example the Gulf of Mexico, it has not been common to utilize routine wave measurements as the basis for establishing design environmental conditions. One good reason for this could be that hurricanes, which are representing design conditions, are so rare that a very long period of measurements would be required before a reliable joint model of the environmental characteristics could be established based on measurements. For such an area, the hindcast technique is very convenient. Since hurricanes-at most-merely occupy some few days per year at each site, a continuous hindcast is typically not considered interesting and one has rather focused on producing reliable hindcast results for all important historical hurricanes for which the meteorological basis data are available. The random storm approach is originally formulated for estimating wave and response extremes corresponding to given return periods based on the availability of a sufficient amount of storm data.[Haver, 2011]

5.2 Introduction of Peak over Threshold Method

The hindcast data from NORA10 is available from 1957 to 2013. For illustrative purpose, the threshold for storm is firstly set to be 6m. It can be counted from the hindcast data that there are 1299 storms in total, with an average duration

of 6.03 steps, or 18.1 hours for each storm. It can be seen that there is no sufficient amount of data for reliable research, especially when the expected extremes corresponds to an annual exceedance probabilities in the order of $10^{-4} - 10^{-3}$. In order to overcome this insufficiency, it is assumed that the distribution function of the largest value of an arbitrary storm exceeding the selected threshold level, Y, converges to an asymptotic form when considered conditionally upon the most probable largest storm response, $\tilde{y}$. A probabilistic model, $f_{\tilde{Y}}(\tilde{y})$, is fitted to the sample of most probable storm extremes, $\tilde{y}_1, \tilde{y}_2, \cdots, \tilde{y}_{k_0}$, and the distribution function of the extreme value of an arbitrary storm reads:

$$F_Y(y) = \int_{\tilde{y}} F_{Y|\tilde{Y}}(y|\tilde{y}) f_{\tilde{Y}}(\tilde{y}) \tag{5.1}$$

5.2.1 Generic Response Problem

$F_{Y|\tilde{Y}}(y|\tilde{y})$ represents the generic response problem. It is a function calculated from significant wave height H_s and spectral peak period T_p in this case. X_{3h}, the 3h maximum response, is modelled by the Gumbel distribution:

$$F_{X_{3h}|H_s,T_p}(x|h,t) = exp\{-exp\{-\frac{x-\alpha(h,t)}{\beta(h,t)}\}\} \tag{5.2}$$

The Gumbel parameters can be calculated from the significant wave height and spectral peak period for each 3-hour step. Then the largest value of $\alpha(h,t)$ for a storm is taken as the largest most probable maximum response:

$$\tilde{y}_k = max_{storm\ nok}(\alpha(h,t)) \tag{5.3}$$

If one perform this process for all storms, one can decide $\tilde{y}_k,\ k = 1, 2, \cdots,\ M$ for each storm.

It should be noticed that this is an approximate method to calculate y_k. By definition of the largest most probable response, y_k is calculated by solving:

$$F_{\overline{x}_s|storm\ k}(x|k) = \prod_{i=1}^{n} F_{\overline{X}_{3h}|H_{s,i},T_{p,i}}(x|h_{s,i}, t_{p,i}) = 0.37 \tag{5.4}$$

Or by solving,

$$\frac{d^2[F_{\overline{x}_s|storm\ k}(x|k)]}{dx^2} = 0 \tag{5.5}$$

But here, the approximate method is used to simplify calculation. The most probable storm maxima, $\tilde{y}_k$, $\tilde{y}_k,\ k = 1, 2, \cdots,\ M$, reflects the long term variability of the storm severity as felt by the response quantity. By ranking $\tilde{Y}$, one finds that there are 1299 $\tilde{Y}$ in total, with the smallest value 11.61, the largest value 32.61.

5.2.2 Distribution of Largest Most Probable Storm Maximum

The largest most probable storm maximum as a random variable, $\tilde{Y}$, is considered to be a 3-parameter Weibull disttribution:

$$F_Y(y) = 1 - exp\{-(-\frac{\tilde{y} - \tilde{y}_0}{\varepsilon})^\gamma\} \tag{5.6}$$

Basically, there are two methods to decide $\tilde{y}_0$, ε and γ. One is method of linear fitting, one is the method of moment. Firstly, the method of linear fitting on Weibull probability paper is utilized here. Method of moment is studied for comparison and verification in Section 5.3.1.

By doing a transformation of Eq. (5.6), it can be shown:

$$ln{-}ln[1 - F_{\tilde{Y}}(\tilde{y})] = \gamma ln(\tilde{y} - \tilde{y}_0) - \gamma ln(\varepsilon) \tag{5.7}$$

It shows that term $ln{-}ln[1 - F_{\tilde{Y}}(\tilde{y})]$ and $ln(\tilde{y} - \tilde{y}_0)$ has a linear relationship. By doing a linear fitting, the three parameters can be decided. The final parameters are decided as:

$$\tilde{y}_0 = 11.70; \tag{5.8}$$

$$\varepsilon = 3.4447; \tag{5.9}$$

$$\gamma = 1.1190; \tag{5.10}$$

Then the 3-parameter Weibull distribution is plotted on the probability paper in Fig. (5.1).

The relation between $F_Y(y)$ and $\tilde{y}$ is plotted in Fig. (5.2).

It can be found that the 3-parameter Weibull model gives a good description for the $\tilde{y}$, and the method of linear fitting seems to be a reasonable way to determine the distribution function.

5.2.3 Distribution of Storm Maximum Response given Largest Most Probable Storm Maximum

(1) Introduction of the Method

Monte Carlo simulation is utilized for deciding the storm maximum realization. For step no.m of storm no.k, a random number, $u_{m,k}$ between 0 and 1 is generated. After replacing $F_{X_{3h}|H_sT_p}(xh, t)$ in Eq(5.2) with $u_{m,k}$, a possible realization of X_{3h} is given by:

$$x_{m,k} = \alpha_{m,k} - \beta_{m,k} ln(-ln(u_{m,k})) \tag{5.11}$$

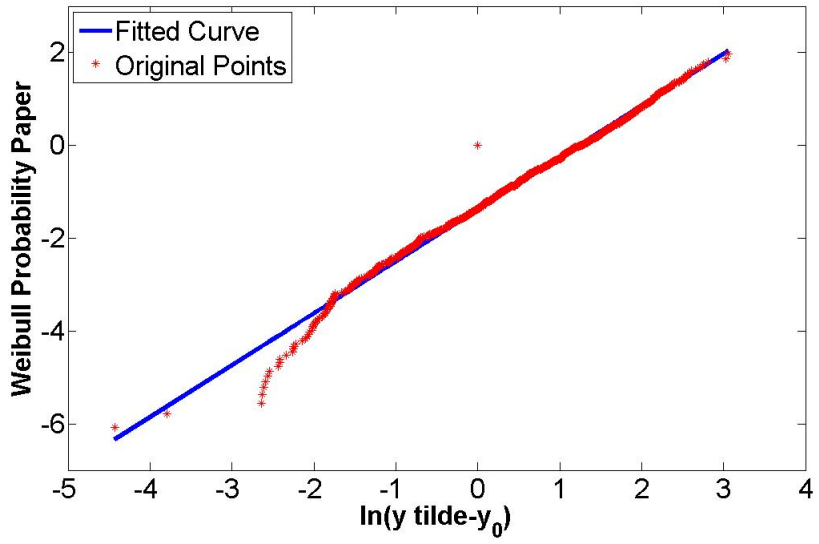

Figure 5.1: Linear Fitting plotted on Weibull Probability Paper

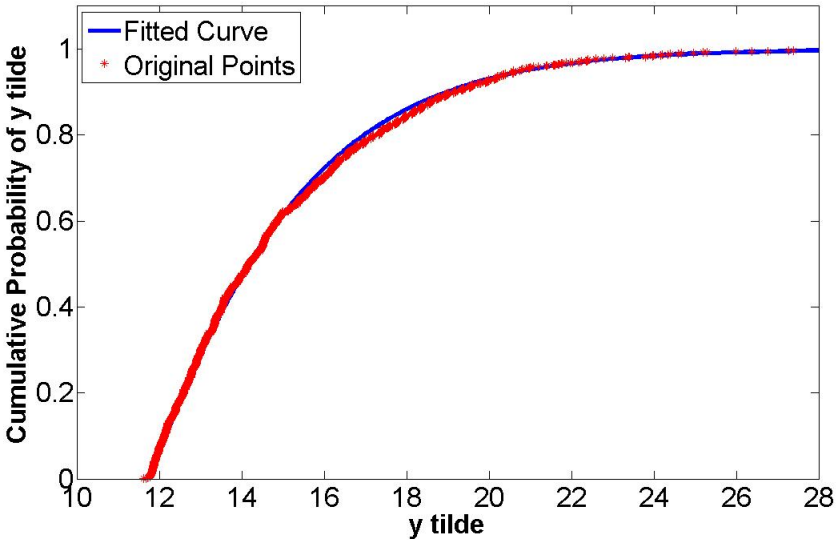

Figure 5.2: Cumulative Probability of the Most Probable Storm Maxima $\tilde{y}$

Storm maximum response for storm no.k is given by:

$$y_k = max_m(x_{m,k}) \tag{5.12}$$

The result of such a process is illustrated for one hurricane in Fig. (5.3). It is seen that the largest most probable storm maximum is usually found at the storm peak $\alpha(k, max)$. The 3-hour maxima y_k fluctuates around the 3-hour most probable maxima $\alpha(k, max)$.

If the variability of the 3-hour maximum around the most probable largest maximum can be neglected, one could estimate the q-probability response from Eq. (5.12). However, for a general case it is important to account for this variability (reflected by the green curve versus the magenta curve in Fig. (5.3)).

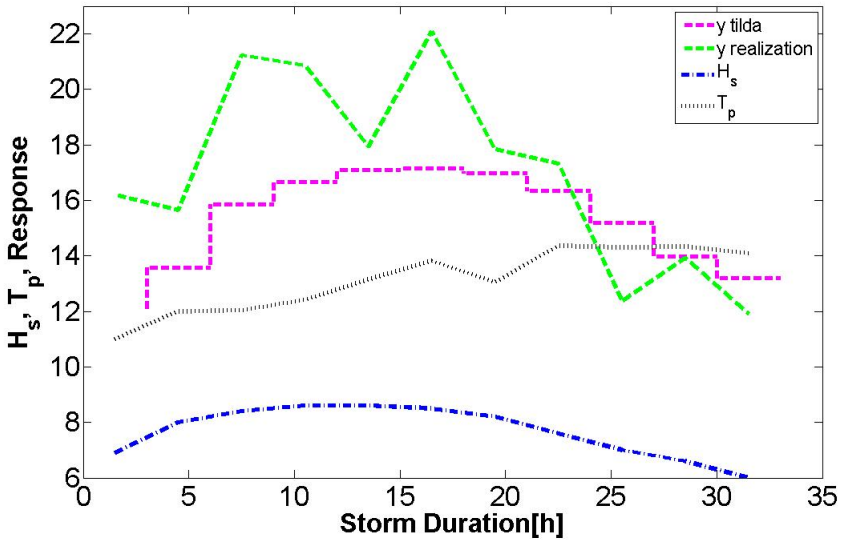

Figure 5.3: Storm Histories h_s,t_p,$\alpha(h_s, t_p)$ and Simulated Maxima for X_{3h} for a Particular Hurricane

The ratio $v_i = \frac{y_i}{\tilde{y}_i}$ is assumed to be a realization of a Gumbel distribution. v_i is assumed to be identically distributed for all hurricanes:

$$F_V(v) = exp\{-exp\{-\frac{v - \alpha_v}{\beta_v}\} \tag{5.13}$$

By calculating the ratio for all k_0 storms, v_1, v_2, $\cdots$,v_{k_0} , the mean $\overline{v}$ and the standard deviation, s_V, can be calculated. Applying the method of moments, the Gumbel parameters can be estimated by:

$$\hat{\beta}_v = 0.7797 s_v \tag{5.14}$$

$$\hat{\alpha}_v = \overline{v} - 0.57722\hat{\beta}_v \tag{5.15}$$

In this case, the value for α_v and β_v reads:

$$\hat{\alpha}_v = 1.0832 \tag{5.16}$$

$$\hat{\beta}_v = 0.1039 \tag{5.17}$$

The Gumbel distribution for v is plotted on a probability paper in Fig. (5.4).

The relation between $F_v(v)$ and v is plotted in Fig. (5.5).

using that,

$$F_{Y|\tilde{Y}}(y|\tilde{y}) = P[Y \leq y|\tilde{Y} \leq \tilde{y}] = P[V \leq \frac{y}{\tilde{y}}] \tag{5.18}$$

then,

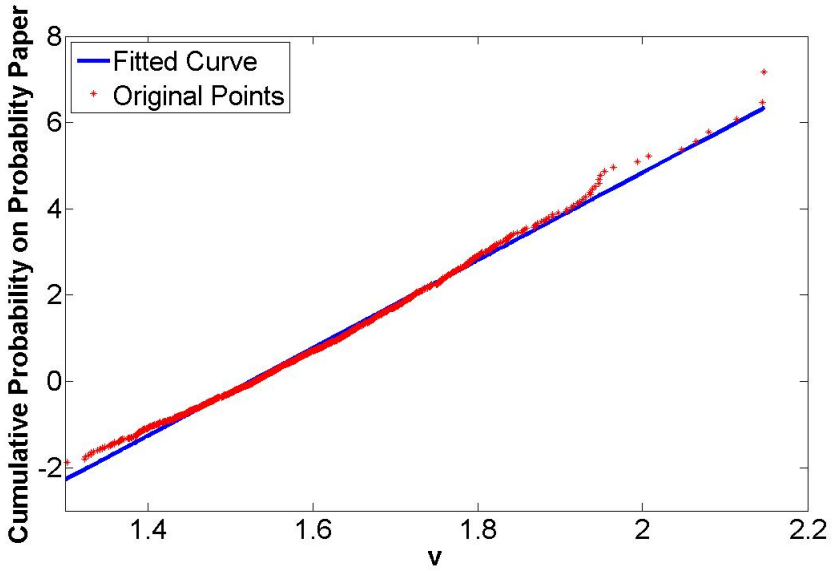

Figure 5.4: Cumulative Probability of v plotted on Gumbel Probability Paper

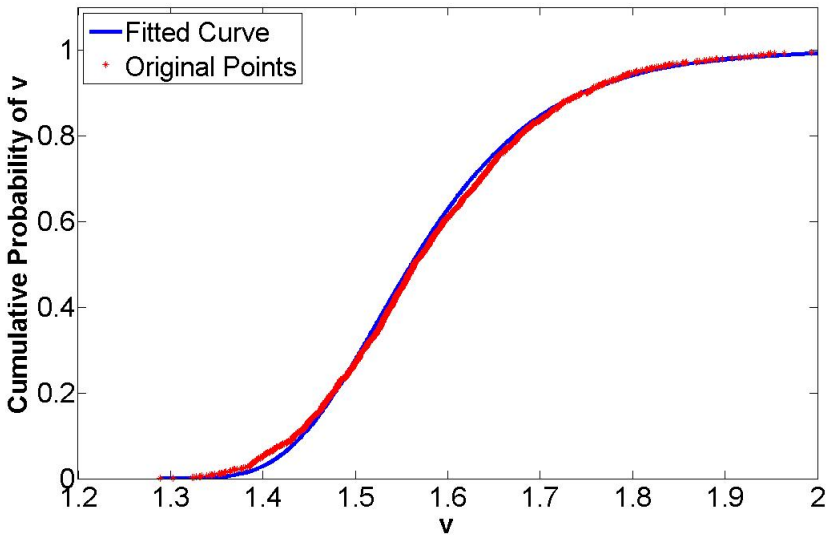

Figure 5.5: Cumulative Probability of v

$$F_{Y|\tilde{Y}}(y|\tilde{y}) = exp\{-exp\{-\frac{y-\alpha_v\tilde{y}}{\beta_v\tilde{y}}\} \tag{5.19}$$

It should be noticed that, as a consequence of the approximation of largest most probable 3-hour maximum response, the location parameter α_v is slightly larger than 1, and thus $\alpha_v\tilde{y}$ is slightly larger than $\tilde{y}$.

(2) Discussion of the Method

It is assumed here that if the storm extreme is normalized by $\tilde{y}$, the distribution of the normalized value is the same for all storms. This can be verified by comparing 3 storms of different severity.

For example, one storm with four 3-hour steps is chosen as the least severe storm.

Since there is only one storm, the largest significant wave height $h_s = 7.3m$, corresponding spectral peak period $t_p = 12.4s$ is chosen to calculate the most probable largest storm maxima $\tilde{y}$.

By performing Monte Carlo simulation, many realizations of storm response can be calculated. Then one can plot the distribution of the ratio $v_i = y_i/\tilde{y}$ on Gumbel Probability Paper. By comparing it with the result from all storms, one can see the uncertainties in this method.

The medium severe storm has with 16 3-hour steps, and the largest significant wave height $h_s = 10.1m$, corresponding spectral peak period $t_p = 13.5s$. The most severe storm has with 9 3-hour steps, and the largest significant wave height $h_s = 16.6m$, corresponding spectral peak period $t_p = 18.1s$.

The results are shown in Fig. (5.6).

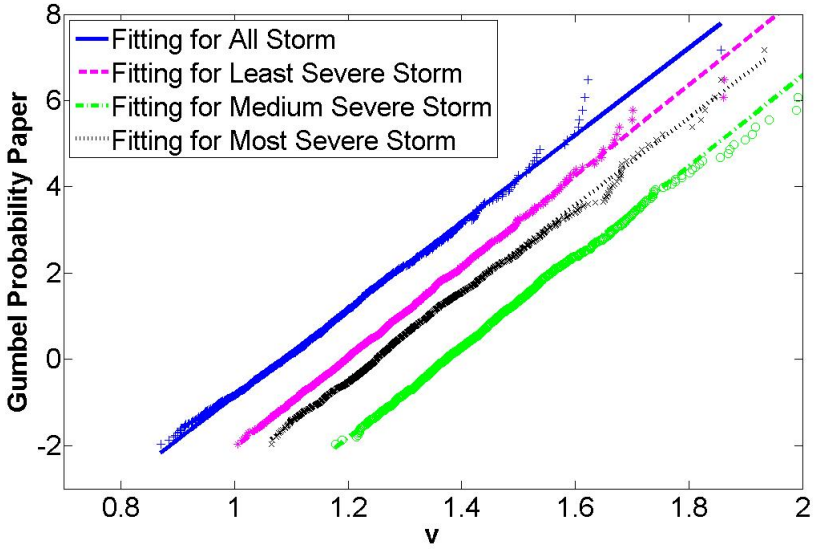

Figure 5.6: Fitting v for Storms with Different Severity

It can be seen from Fig. (5.6) that fitting for different storms are deviated from the fitting for all the storms. Before analyzing the reason for this behavior, one should firstly focus on the uncertainties regarding the approach.

a. Uncertainties in Number of Realizations for Each Storm Step

When using Monte Carlo simulation to generate realizations, the number of realizations from each storm step has a big effect on the result, shown as in Fig. (5.7).

The least severe storm is taken as an example:

Cases for medium severe storm and most severe storm are shown in Appendix, Figs. (A.16 to A.17).

In Fig. (5.7), blue solid line is the case where there are 20 realizations for each step of storm, the magenta dashed line is the case where there are only 1 realization for each step of storm. It can be seen that with the increasing realizations, the expected mean of sample v has an obvious increase.

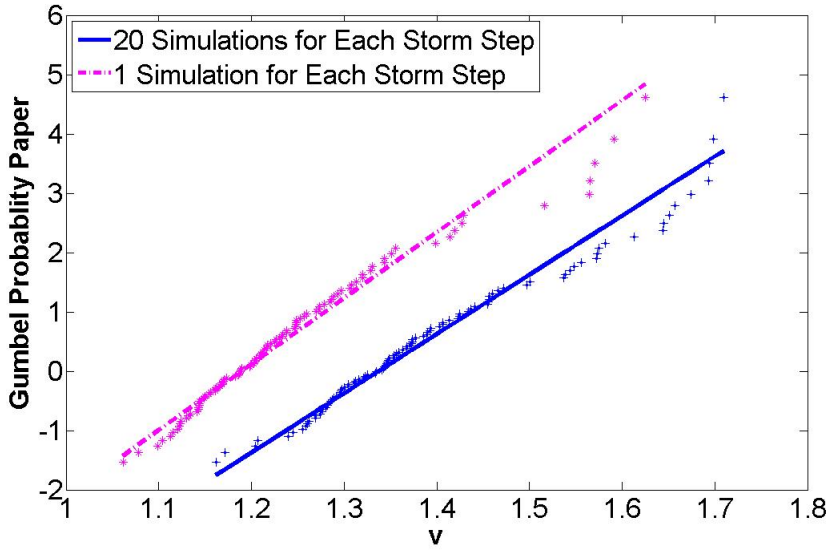

Figure 5.7: Effect of Realizations for Each Step on v for Least Severe Storm

Thus the uncertainties lie in number of realizations for each storm step. With the same most probable value, more realizations will give larger realization, thus a larger ratio, and then a more conservative estimation of response. In the following studies, the number of realization for each step is set to be 1, in order to compare with the one for all storms. However, the proper number of realizations remains to be discussed.

b. Uncertainties in Number of Repeated Storms for Each Case

Since for each case, only one storm is selected, and the identical distribution of the normalized value is assumed to be the same for all storms, thus a number of repetitions have to be done to generate a sample, which is large enough to overcome the uncertainties. In this case, a comparison between 100 repetitions and 1299 repetitions are shown in Fig. (5.8).

The least severe storm is taken as an example,

Cases for medium severe storm and most severe storm are shown in Appendix, Figs. (A.18 to A.20).

The figures show that the effect of number of reperitions is not quite obvious. However, in order to ensure the accuracy, number of repetitions is set to be 1299.

c. Discussion of Fitting v for Different Severity Storm

Firstly, the three fitted line lies to be right to the one for all storms. This may due to a poorly selected example for least severe storm. According to results, there are 685 storms with most probable largest significant wave height smaller than 7.3m. And there are 1206 storms with most probable largest significant wave height smaller than 10.1m.

It can be found from Eq. (5.11) that a smaller most probable largest value $\alpha_{m,k}$ will lead to a smaller realization $x_{m,k}$, if the uncertainties from the random number $u_{m,k}$ is neglected. By transforming Eq. (5.11), one can get:

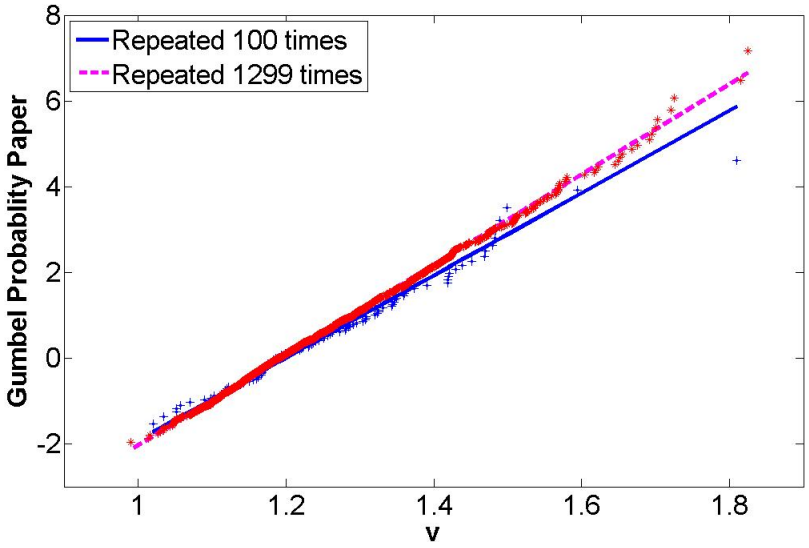

Figure 5.8: Effect of Repeated Storms on v for Least Severe Storm

$$v_i = \frac{y_i}{\alpha_k} = 1 - \frac{\beta_k ln(-ln(u))}{\alpha_k} \tag{5.20}$$

With a smaller $\alpha_{m,k}$, the ratio v_i will be smaller. This is the reason why the line for all storms appears to the left of the other three lines.

Secondly, fitted line for medium severe storm lies to the right of line for least and most severe storm. This is because there are 4 steps for the least severe storm, 9 steps for the most severe storm, but 16 steps for the medium severe storm.

This is related to Monte Carlo simulation. More steps mean more random number $u_{m,k}$ and more realizations for each storm. Thus the largest realization is more probable to be larger than the one with fewer realizations. Especially in this case, 16 realizations for the medium storm were generated, while only generate 9 realizations for the most severe storm and 4 for the least severe storm, thus the ratio for the medium storm will be larger. This is the reason why the line appears outside of the least severe and most severe line range.

5.2.4 Extreme Response Prediction

Eq. (5.19) is the POT analogy to the short term distribution of the all sea state approach. The long term distribution of storm maximum response reads:

$$F_Y(y) = \int_{\tilde{y}} F_{Y|\tilde{Y}}(y|\tilde{y}) f_{\tilde{Y}}(\tilde{y}) d\tilde{y} \tag{5.21}$$

Integration for Eq. (5.21) can be done in Matlab, the result is plotted in Fig. (5.9). In order to estimate extreme value with 100-year or 10000-year return period, the cumulative probability for response is plotted on a Gumbel probability paper against response value, shown in Fig. (5.10).

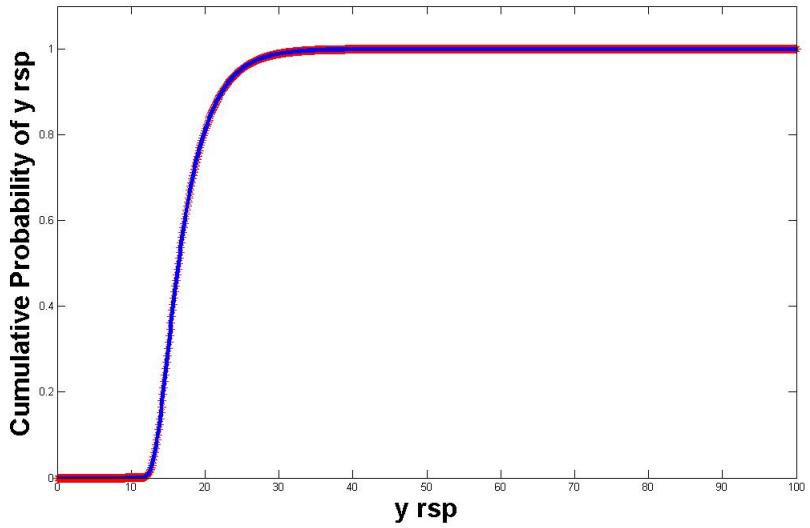

Figure 5.9: Cumulative Probability of Response

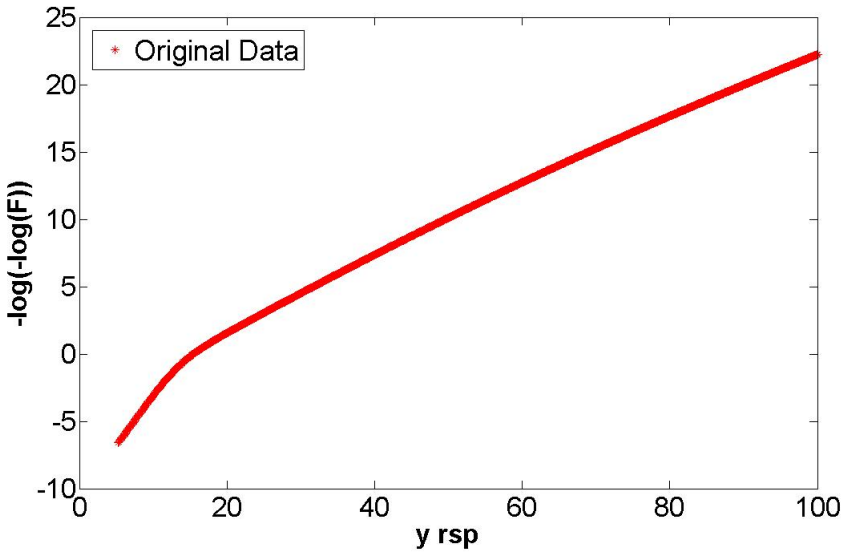

Figure 5.10: Cumulative Probability of Response plotted on Gumbel Probability Paper

It can be seen that the line does not necessarily behave linearly as a whole, but regarding the large response value, it has good linear characteristic, and reasonable value can be estimated by reading directly from the original data.

The q-probability response values are found by solving:

$$1 - F_Y(y_q) = \frac{q}{n_1} \tag{5.22}$$

n_1 is the expected number of hurricanes per year. In this case, there are 1299 storms in 56 years, thus the expected number of hurricanes per year:

$$n_1 = \frac{1299}{56} \tag{5.23}$$

Result for the POT analysis can be shown in Tab. (5.1).

Table 5.1: Extreme Response from POT Method

	$-ln\{-ln[F_Y(y_q)]\}$	y
q=0.1	5.444	33.1
q=0.01	7.749	41.1
q=0.0001	12.3543	58.0

5.3 Discussion of POT Method

In order to study the uncertainties of the POT method, different response cases are performed in this section. The results are given in Tab. (5.2).

Table 5.2: Comparison of Extreme Response from All Sea State Approach and POT Method

$c_2 = 1$	X_{10}		X_{100}		X_{10000}	
	NPS	PS	NPS	PS	NPS	PS
All Sea State Analysis	30.0	26.2	36.0	30.9	48.1	40.5
POT Method	33.1	40.9	41.1	54.4	58.0	76.6
$c_2 = 2$	X_{10}		X_{100}		X_{10000}	
	NPS	PS	NPS	PS	NPS	PS
All Sea State Analysis	397.9	336.7	625.2	482.4	1073.6	733.7
POT Method	493.3	482.1	708.5	742.5	1221.2	1380

It can be seen that for all the cases, results from the POT approach are much higher than the one from all sea state approach, especially for period sensitive cases. Based on the verification study of different approaches in Section 5.4, it is believed that all sea state approach gives more accurate results. Thus uncertainties from POT approach are studied here.

From Eq. (5.20), it is assumed that there are two sources of uncertainties, one is from $F_{Y|\tilde{Y}}(y|\tilde{y})$, and the other is from $f_{\tilde{Y}}(\tilde{y})d\tilde{y}$.

5.3.1 Uncertainties from Linear Fitting for $\tilde{y}$

(1) Data Study

The data studied in this thesis has its own characteristic. It is shown obviously in Fig. (5.11). This is an example from period sensitive and quadratic response case.

It can be seen that on the left side of the figure, the original points have quite strange behavior. It suggests that the first several $\tilde{y}$ is quite close to y_0.

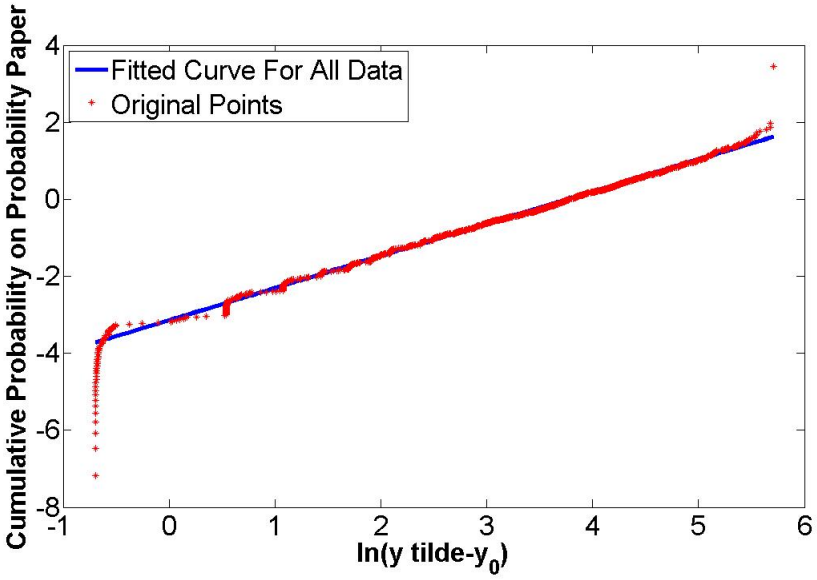

Figure 5.11: Weibull Probability Paper for all $\tilde{y}$

The author finds that from all 1299 storms, there are 72 of them which only have one 3-hour with the largest significant wave height $h_s = 6m$. The most probable response for these storms $\tilde{y}$ is very close to 36, while the y_0 in this case is 35.5. $ln(\tilde{y} - y_0) = -0.6931$, which corresponds to the coordinates of the first several original points.

These points are useless for long term response prediction, thus in the following study, only storms with at least two 3-hour steps are considered. The author suggests that in the POT method, there should be limitations on the minimum number of steps in each storm.

(2) Uncertainty Study

By the least square method, parameters for the 3-parameter Weibull Distribution are decided. Cumulative probability for $\tilde{y}$ is plotted in Weibull probability paper for different cases in Fig. (5.12), as the same as in Fig. (5.1). Non-period sensitive and linear case is taken as an example.

Cases for different linearity and period sensitivity are shown in Appendix, Figs. (A.21 to A.23).

By comparing the results, it is assumed that there are mainly three sources of uncertainties:

a. Entire Range Fitting and Important Region Fitting

In order to study the effect of different fitting range, period sensitive and linear case is selected as an example. It can be seen from Fig. (A.9) that the important contribution area to response regarding significant wave height h_s is from 9m to 17m. By doing a transformation to the x-axis on Weibull probability paper, the corresponding important range is 1.13 - 2.4. In Fig(5.13), fitting for all data and fitting only for important range is presented.

In Fig. (5.13), the green line gives good description for the upper region, but it does not describe all the data very well. Results from two fitting are given in Tab.

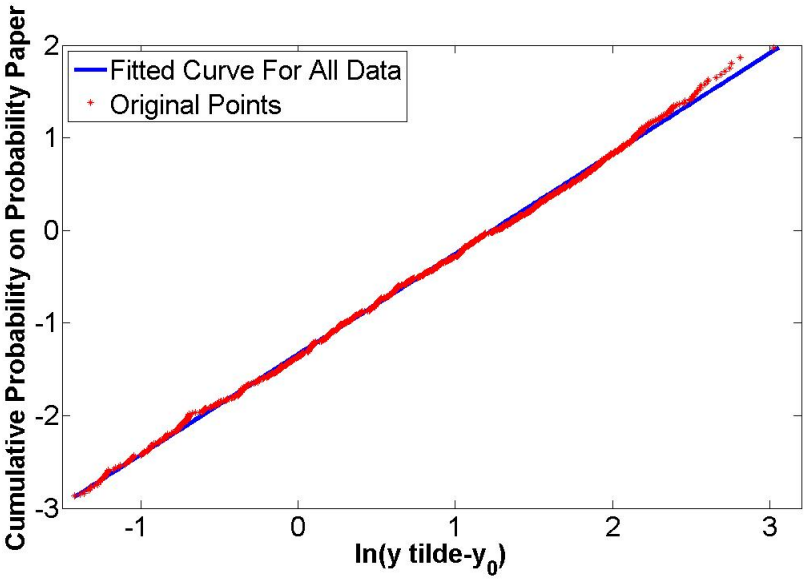

Figure 5.12: Cumulative Probability plotted on Weibull Probability Paper for Non-period Sensitive Case

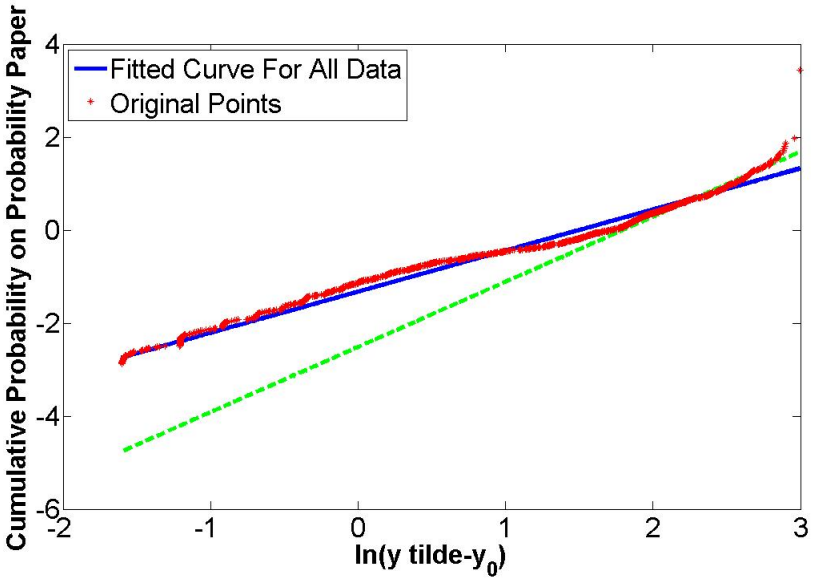

Figure 5.13: Comparison of Linear Fitting for All Data and Important Region on Weibull Probability Paper

(5.3).

Table 5.3: Extreme Response from Different Fitting Region

	X_{10}	X_{100}	X_{10000}
Fitting for All Data	40.9	54.4	76.6
Fitting for Upper Region	30.6	38.8	56.2

It can be seen that different choices of fitting region have substantial effect on the final result. And the unreasonable big results in Tab. (5.2) may due to a poor modelling in the important contribution region. Therefore, a compromise between

important contribution region fitting and whole range fitting should be reached to give trustworthy results.

It is found that different choices of location parameter y_0 will give different fitting and extreme response values. Thus the author believes that least square method can only give suggestions to choice of y_0, but the best y_0 should be chosen according to ones focus on different behavior of the fitted curve.

b. Least Square Method and Method of Moment

In order to see the uncertainties of using least square method, method of moment is performed.

The relationship between parameters of Weibull distribution and mean μ and variance σ^2 of sample reads: (Moan(2010))

$$\mu = \lambda\Gamma(1 + \frac{1}{k}) \tag{5.24}$$

$$\sigma^2 = \lambda^2\{\Gamma(1 + \frac{2}{k}) - [\Gamma(1 + \frac{1}{k})]^2\} \tag{5.25}$$

μ and σ^2 can be calculated from a sample of $\tilde{y}$. By solving Eq. (5.24) and Eq. (5.25) the parameters for Weibull distribution can be calcualted.

Non-period sensitive and linear case is taken as an example.

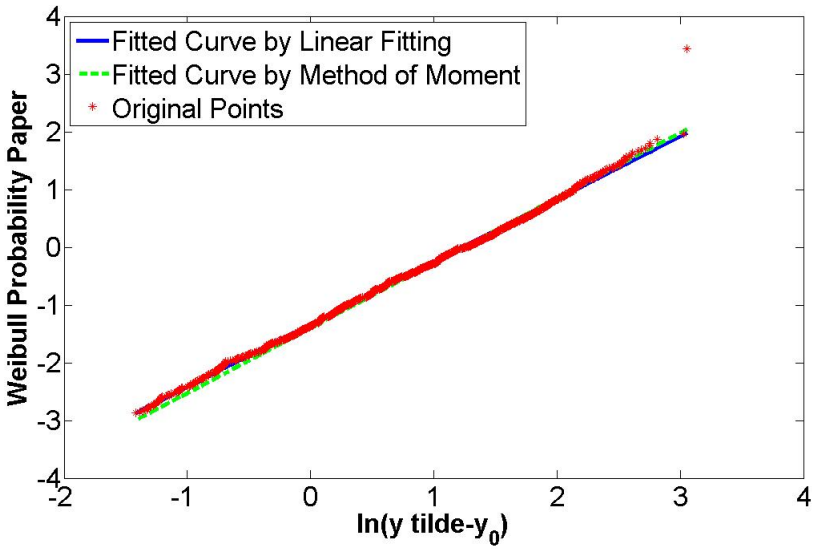

Figure 5.14: Comparison of Method of Moment and Linear Fitting for Non-period and Linear Case

Cases for different linearity and period sensitivity are shown in Appendix, Figs. (A.24 to A.26).

It can be seen that for the non-period sensitive cases fitted line by method of moment and linear fitting almost coincide with each other. The parameters for the curve and results are given in Tab. (5.4).

Table 5.4: Parameters for Fitted Line and Extreme Results

	k	λ	X_{10}	X_{100}	X_{10000}
Method of Moment	1.127	3.4776	33.1	41.2	58.0
Method of Linear Fitting	1.119	3.4447	33.1	41.1	58.0

It can be seen from Tab. (5.4) that in non-period sensitive case, the method of moment gives slightly smaller result. This is even more obvious for the period sensitive case.

Comparisons for results of different cases are shown in Tab. (5.5).

Table 5.5: Extreme Values and Target Percentile for Linear and Non-period Sensitive Case

$\tilde{y}$	X_{10}		X_{100}		X_{10000}	
	MoM	MoLF	MoM	MoLF	MoM	MoLF
NPS, $c_2 = 1$	33.1	33.1	41.1	41.8	58.0	58.0
NPS, $c_2 = 2$	497.0	493.9	708.5	723.2	1239.8	1221.2
PS, $c_2 = 1$	33.9	40.9	54.4	54.0	66.6	76.6
PS, $c_2 = 2$	441.2	482.1	742.5	734.4	1197.4	1380

In can be seen from Tab. (5.5) that generally speaking, the method of moment gives smaller results than method of linear fitting. It is believed that the method of moment is more accurate than method of linear fitting. Thus this might be one of the reasons that the POT method gives much higher results than all sea state long term approach in Tab. (5.2).

5.3.2 Uncertainties from Fitting for v

Similarly as in Section 3.1, Chapter 5, it is assumed that there are two sources of uncertainties regarding modelling of v. One is the adequacy of using method of moment to estimate parameters for Gumbel parameters. The other is the effect from upper tail region in the fitting process. They are studied separately as below:

a) Monte Carlo Simulation

v_i is the ratio between maximum response y_i and most probable largest response y_i. In order to find the maximum response y_i, a realization for response is generated by Monte Carlo Simulation, as in Eq. (5.11).

The author believes that Monte Carlo Simulation will introduce uncertainties in the extreme value prediction. In the following figures, Monte Carlo Simulation is performed several times for different response cases, and the results are plotted together with the most probable response y_i in Fig. (A.26).

The blue line in Fig. (5.15) is the most probable response curve, lines with other colors are results from Monte Carlo simulation. It can be seen that, different realizations will give very different largest response, thus result in very different v_i.

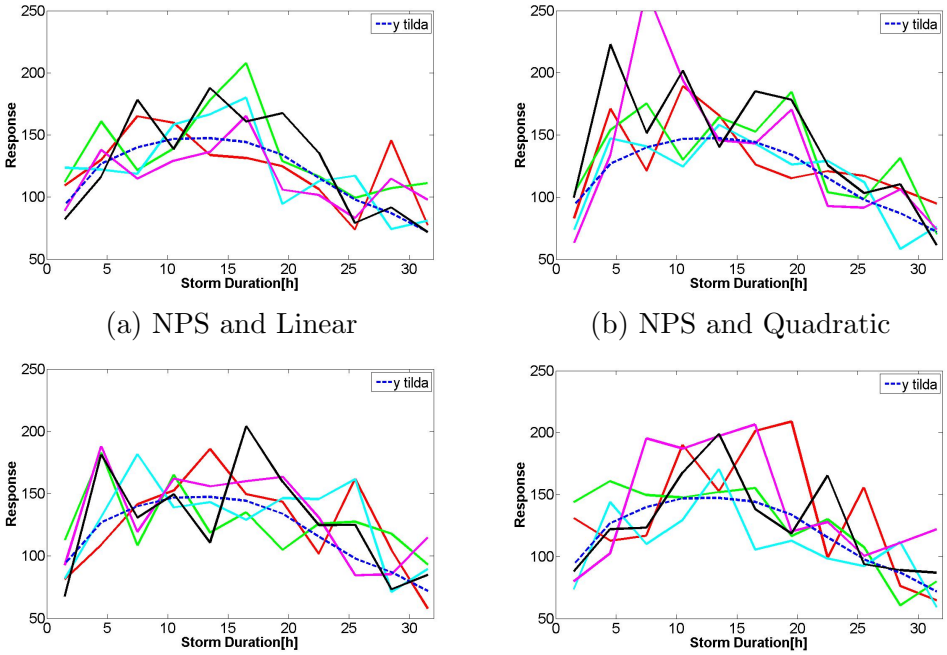

(a) NPS and Linear

(b) NPS and Quadratic

(c) PS and Linear

(d) PS and Quadratic

Figure 5.15: Monte Carlo Simulation plotted with Most Probable Response Curve

It can be observed in Fig. (5.10) that, the maximum realization is much higher than the most probable response, especially for non-period sensitive case. This will result in a larger v_i, and according to Eq. (5.14) and Eq. (5.15) a larger v_i will result in larger α_V. It suggests that the estimated most probable value is larger than the correct most probable value. Then according to Eq. (5.13), for same non-exceedance probability, the predicted extreme response will be larger than the true response. Thus the author believes that this is also one of the reasons that the POT method gives much higher results than all sea state long term approach.

b. Method of Moment and Method of Linear Fitting

In the previous study, method of moment is utilized to calculate the parameters in Eq. (5.13). Non-period sensitive and linear response case is taken as example. Linear fitting for $F_V(v)$ on Gumbel Probability paper is plotted in Fig. (5.11).

In Fig. (5.16), it can be seen that fitted line from two methods almost coincide with each other. Parameters for Gumbel distribution and response results are presented in Tab. (5.6).

Table 5.6: Parameters for Fitted Line and Extreme Results

	$\hat{\alpha}_V$	$\hat{\beta}_V$	X_{10}	X_{100}	X_{10000}
Method of Moment	1.0832	0.1039	33.1	41.1	58.0
Method of Linear Fitting	1.0808	0.1052	33.3	41.5	58.9

It can be seen from Tab. (5.6) that in non-period sensitive case, method of moment gives slightly smaller result. Comparisons for results of different cases are shown in Tab. (5.7).

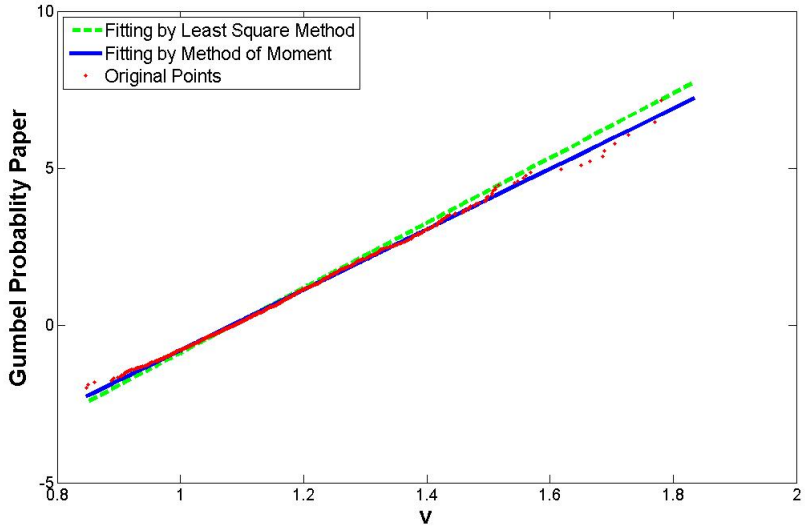

Figure 5.16: Comparison of Method of Moment and Linear Fitting

Table 5.7: Extreme Values and Target Percentile for Linear and Non-period Sensitive Case

v	X_{10}		X_{100}		X_{10000}	
	MoM	MoLF	MoM	MoLF	MoM	MoLF
NPS, $c_2 = 1$	33.1	33.1	41.1	41.2	58.0	58.2
NPS, $c_2 = 2$	493.3	498.8	708.5	718.5	1221.2	1243.5
PS, $c_2 = 1$	40.9	40.9	54.4	54.4	76.6	76.9
PS, $c_2 = 2$	482.1	481.0	742.5	740.0	1380	1378.5

It can be seen from Tab. (5.7) that method of moment gives very close result to method of linear fitting.

c. Effect from Upper Tail Region

It can also be seen from Fig. (5.16) that both methods gives poor description for the upper tail region of v.

In order to study the effect from upper tail region, similar steps are performed in Section 3.1 Chapter 4.

In Fig. (5.17), green line is fitted only to upper region data and blue line is fitted to all data. The predicted extreme values are shown in Tab. (5.8).

Table 5.8: Parameters for Fitted Line and Extreme Results

	$\hat{\alpha}_V$	$\hat{\beta}_V$	X_{10}	X_{100}	X_{10000}
Method of Moment	1.0832	0.1039	33.1	41.1	58.0
Fitting to All Data	1.0808	0.1052	33.1	41.2	58.2
Fitting to Upper Region	1.0127	0.1207	32.5	41.0	59.5

It is found that three methods give similar response results. This is mainly due to two reasons. One is that it is the conditional probability $F_{Y|\tilde{Y}}(y|\tilde{y})$ in Eq. (5.1)

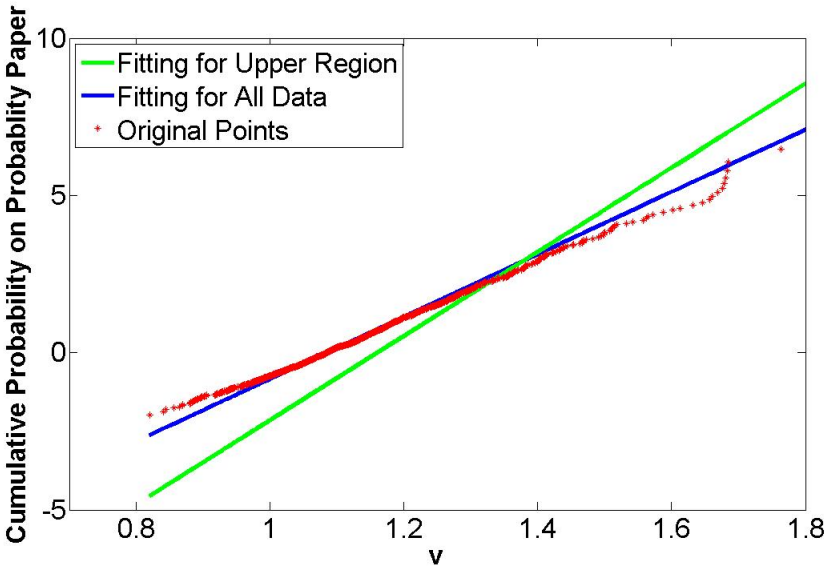

Figure 5.17: Comparison of Linear Fitting for All Data and Upper Region

which is calculated here, thus inaccuracies may be eliminated by $f_{\tilde{Y}}(\tilde{y})$. The other one is that the cumulative probability of v on Gumbel probability paper shows good linearity, thus no matter which method one is using, it should not have an obvious effect on the final results.

5.3.3 Effect from Threshold for Storm

In the previous study, $h_{th} = 6m$ is chosen as the threshold for storm. In this section, different thresholds are used to study the effect. The results are shown in Tab. (5.9).

Table 5.9: Parameters for Fitted Line and Extreme Results

	X_{10}				
	$h_{th} = 5m$	5.5m	6m	6.5m	7m
NPS, $c_2 = 1$	33.8	34.4	33.1	36.9	35.2
NPS, $c_2 = 2$	488.9	530.6	493.3	523.0	533.7
PS, $c_2 = 1$	48.8	37.6	40.9	42.7	42.3
PS, $c_2 = 2$	418.6	462.8	482.1	537.8	558.7
	X_{100}				
NPS, $c_2 = 1$	44	44.2	41.1	47.1	43.4
NPS, $c_2 = 2$	745.0	798	708.5	753.0	749.6
PS, $c_2 = 1$	61.3	51.3	54.4	55.6	54.3
PS, $c_2 = 2$	672.8	728.8	742.5	830.0	836.1

From Tab. (5.9), there is no obvious pattern for results with increasing threshold. Number of storm above each threshold is shown in Tab. (5.10).

It can be seen that the most influential variable when changing threshold is the size of sample. Number of storms with $h_{th} = 5m$ is almost three times to the one

Table 5.10: Number of Storms for Different Threshold

Threshold for Storm	$h_{th} = 5m$	5.5m	6m	6.5m	7m
Number of Storm	2053	1619	1299	1027	786

with $h_{th} = 7m$. Generally speaking, large sample will give more accurate result. However, POT method is mostly used for sea area where extreme response is basically governed by the occurrences of some few extreme hurricanes, for example the Gulf of Mexico. While NORA10 is hindcast data from North Sea area, which is known for its consistently severe weather characteristics. Thus the threshold for storm may only has a big effect regarding this specific hindcast data.

This suggests that POT method may not be a good approach to estimate long term extreme response in North Sea area. POT method should only be used as a verification method when all sea state long term approach is available.

5.4 Summary

In this chapter, the author gives a brief introduction of the POT method, and calculates the long term response based on the method. By discussing the uncertainties in different steps, the author gives explanation to the fact that POT method gives higher estimation than the all sea state long term approach.

For fitting for the most probable response for all storms: it is found that fitting for different range of data will give very different results. If one focus on a good fitting for the overall data set, one may get poor results when calculating the extreme value prediction. While if one focus on an accurate fitting for the long term extreme response, the result will be inaccurate in other part of the distribution. This is one of the major uncertainties in extreme value prediction.

For fitting for the ratio between largest realization and the largest most probable value, Monte Carlo simulation is the biggest source of uncertainty. Too many realizations for each step will generate an overestimation of ratio, while too few realizations will not give a reliable result. Further work should be done regarding the proper number of realization for each step. Besides the two major uncertainties above, method of linear fitting compared with method of moment, different choices of threshold, and limitations on minimum storm steps are sources of uncertainties.

In conclusion, compared with all sea state long term approach, there are too many uncertainties in POT approach. And according to the result, POT method does give overestimation for extreme response. Thus the author suggests that POT method should be carefully used, especially in North Sea condition. POT method can be used as verification when all sea state long term approach is available.

Chapter 6

Verification Study

In order to verify the method and result for all sea state approach and POT approach, several verification studies are performed.

6.1 Calculation of Response with All Sea State Time Domain Approach

6.1.1 Introduction of Method

In this approach, the environmental characteristic, H_s and T_p are taken directly from hindcast data, thus response is calculated for each 3-hour sea state, i.e. 163520 3-hour events.

The integration is:

$$\hat{F}_{X_{3h}}(x) = \sum_{j=1}^{J} F_{X_{3h}|E_j}(x|E_j) \cdot P(E_j) \tag{6.1}$$

with $\alpha(h,t)$ and $\beta(h,t)$ calculated directly from hindcast data.

The probability for choosing each sea state from the hindcast data is the same, thus:

$$P(E_j) = \frac{1}{56 \cdot 2920} \tag{6.2}$$

The q-probability response values are found by solving:

$$1 - F_X(x) = \frac{q}{2920} \tag{6.3}$$

6.1.2 Modification to Hindcast Data

In time domain approach, the weather characteristics are taken directly from hindcast data, thus single sea state will have relatively larger effect on final result.

According to the hindcast data, the largest significant wave height is 16.6m, while the second largest significant wave height is only 14.7m. The largest significant wave height may be related to freak wave, and should not be considered when estimating extreme value prediction in ULS and ALS cases.

Thus in order to avoid this uncertainty, the storm with the largest significant wave height is taken away from the original data. Difference in results are shown in Tab. (6.1).

Table 6.1: Effect of Largest Storm on Result for Time Domain Method

	x_{10}	x_{100}	x_{10000}
All Sea State Time Domain(without the largest storm)	30.4	35.8	46.5
All Sea State Time Domain(with the largest storm)	30.5	36.4	47.5

It can be seen that, the effect of the largest storm is quite significant, especially for 100-year and 10000-year cases. For the rest of thesis, as long as time domain approach is utilized, one only uses the data without the largest storm.

6.1.3 Discussion of Results

The integration in Eq. (6.1) is calculated within Matlab. The result is plotted on the Gumbel probability paper in Fig. (6.1). Results are shown in Tab. (6.2).

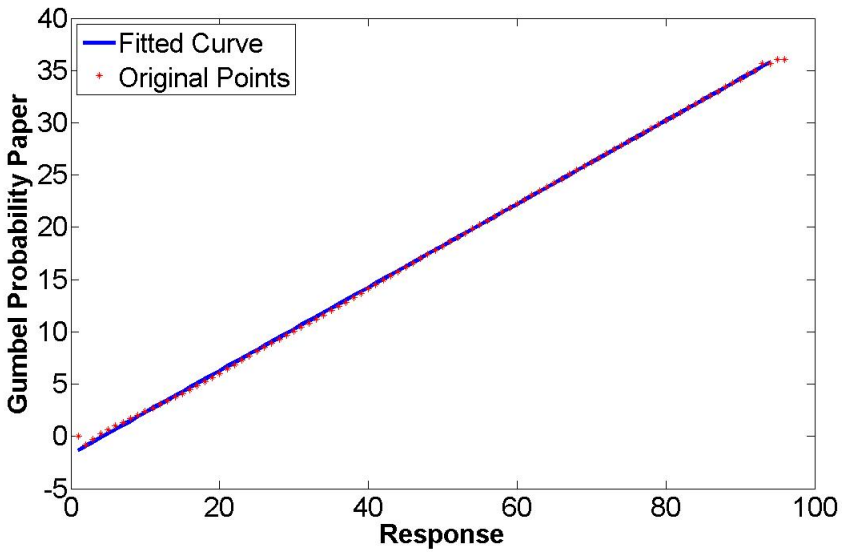

Figure 6.1: Study of Original Data

Table 6.2: Parameters for Fitted Line and Extreme Results

	$-ln\{-ln[F_X(x)]\}$	X
q=0.1	10.3	30.4
q=0.01	12.6	35.8
q=0.000	17.2	46.5

Response for all sea state analysis, all sea state time domain approach and peak over threshold approach are shown in Tab. (6.3).

Table 6.3: Summary of Results from Three Different Approaches

	X_{10}	X_{100}	X_{10000}
All Sea State Analysis	30.0	36.0	48.1
All Sea State Time Domain	30.4	35.8	46.5
POT Method	30.6	38.8	56.2

Since in all sea state time domain approach, the environmental characteristics are taken from hindcast data, therefore there will some unobserved sea states. Thus the response result gives smaller value than the all sea state approach.

However, according to experience, the result from POT method should give a smaller value than all sea state analysis, which is not the case here.

Due to this discrepancy, further study on verification of two methodologies is performed. In this verification study, instead of finding response value, wave crest height is studied. This is due to that there are already some previous work done in this part and the result is comparable.

6.2 Calculation of Wave Crest Height with All Sea State Time Domain Approach

6.2.1 Introduction of Method

The conditional distribution of 3-hour crest height given h_s and t_p is denoted as:

$$F_{C_{3h}|H_sT_p}(c|h,t) = [F_{C|H_sT_p}(c|h,t)]^{n(h,t)} \tag{6.4}$$

with,

$$n = \frac{10800}{t_z} \tag{6.5}$$

t_z is the zero crossing frequency, t_z is determined by $t_z = 0.77 \cdot t_p$.

The sea surface is Gaussian process. For each time step, the distribution of wave crest is assumed to be Rayleigh distributed. Further details can be found in Myhaug(2005).

$$F_C(c) = 1 - exp\{-\frac{1}{2}(\frac{c}{\sigma_E})^2\} \tag{6.6}$$

σ_E can be expressed as:

$$\sigma_E = \frac{h_s}{4} \tag{6.7}$$

Then the Rayleigh distribution function can be written as:

$$F_C(c) = 1 - exp\{-8(\frac{c}{h_s})^2\} \tag{6.8}$$

then,

$$F_{C_{3h}|H_sT_p}(c|h,t) = [1 - exp\{-8(\frac{c}{h_s})^2\}]^{n(h,t)} \tag{6.9}$$

The long term distribution of 3-hour maximum crest height can be written as:

$$F_{C_{3h}}(c) = \sum_{j=1}^{J} F_{C_{3h}|E_j}(c|E_j)P(E_j) = \sum_{j=1}^{J}(1 - exp\{-8(\frac{c}{h_s})^2\})^{\frac{10800}{t_z}} P(E_j) \tag{6.10}$$

6.2.2 Discussion of Results

By solving the integration in Eq. (6.10), cumulative probability for wave crest height can be calculated. Plot this relationship on a Gumbel probability paper, shown in Fig. (6.2).

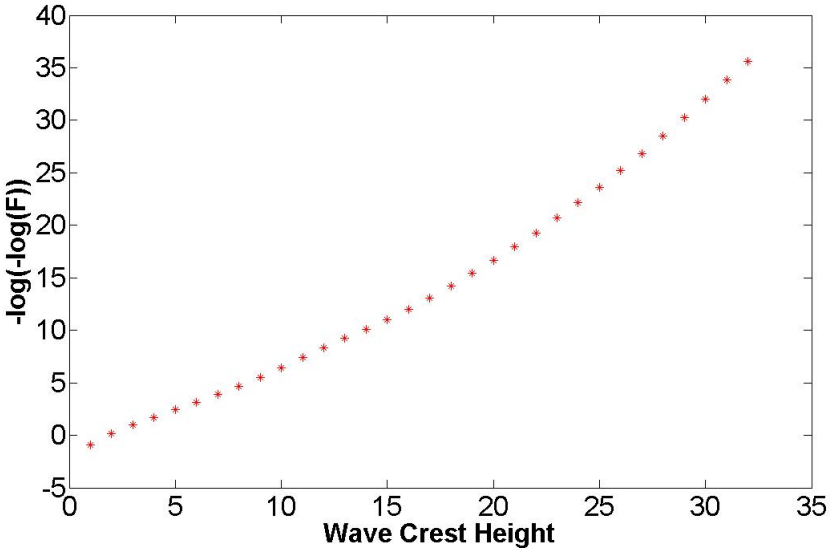

Figure 6.2: Gumbel Probability Paper for All Sea State Time Domain Approach

The non-exceedance probability for q-probability wave crest height is found by solving:

$$1 - F_{C_{3h}}(c) = \frac{q}{2920} \tag{6.11}$$

The result for wave crest height is shown in Tab. (6.4).

Discussion and comparison with other cases will be referred to Section 6.6, Chapter 6.

Table 6.4: Extreme Crest Height from All Sea State Time Domain Approach

	$-ln\{-ln[F_C(c)]\}$	c
q=0.1	10.2819	14.2
q=0.01	12.5845	16.5
q=0.0001	17.1897	21.0

6.3 Calculation of Wave Crest Height with All Sea State Long Term Analysis Approach

6.3.1 Introduction of Method

The only difference from the previous method is the calculation of $P(E_j)$. The probability for each h_s and t_p interval is taken from the probability scatter diagram mentioned in Section 3.1.4, Chapter 3, which is similar to all sea state approach for the response calculation.

6.3.2 Discussion of Results

By solving the integration Eq. (6.10), cumulative probability for increasing wave crest height can be calculated. Plot this relationship on a Gumbel probability paper, shown in Fig. (6.3).

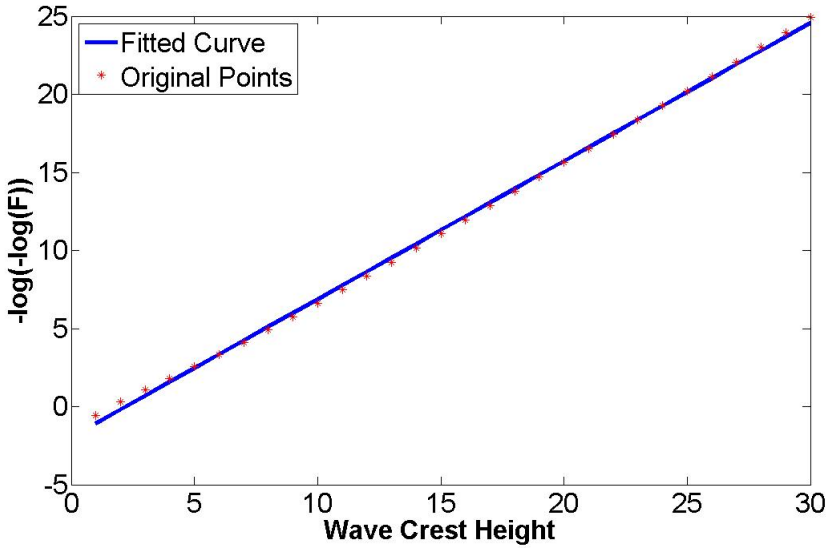

Figure 6.3: Gumbel Probability Paper for All Sea State Long Term Analysis Approach

Results are shown in Tab. (6.5).

Discussion and comparison with other cases will be referred to Section 6.6, Chapter 6.

Table 6.5: Extreme Crest Height from All Sea State Time Domain Approach

	$-ln\{-ln[F_C(c)]\}$	c
q=0.1	10.2819	14.1
q=0.01	12.5845	16.7
q=0.0001	17.1897	21.6

6.4 Calculation of Wave Crest Height with All Sea State Long Term Analysis Approach considering Weighting Factor

6.4.1 Introduction of Method

In this verification study, the weighting factor is considered in the integration:

$$F_{C_{3h}}(c) = \frac{1}{\widehat{v^+}} = \int_h \int_t v^+ F_{C_{3h}|H_sT_p}(ch,t) f_{H_sT_p}(h,t) dtdh \tag{6.12}$$

with,

$$\widehat{v^+} = \int_h \int_t v^+_{\Gamma,0}(h,t) f_{H_sT_p}(h,t) dtdh \tag{6.13}$$

Assuming that individual response maxima are statistically independent, the value corresponding to a return period of L-year is solved by:

$$1 - F_C(c^{(L)}) = \frac{q}{n^{(L)}} \tag{6.14}$$

with,

$$n^{(L)} = L \cdot 365 \cdot 24 \cdot 3600 \cdot \overline{v^+_{\Gamma,0}} \tag{6.15}$$

Where v^+ is the zero-crossing frequency, $v^+ = \frac{1}{t_z}$, $t_z = 0.77t_p$

By solving the integration Eq. (6.13), cumulative probability for increasing wave crest height can be calculated. Plot this relationship on a Gumbel probability paper, shown in Fig. (6.4). Results are shown in Tab. (6.6).

Table 6.6: Extreme Crest Height from All Sea State Long Term Analysis Approach considering Weighting Factor

	$-ln\{-ln[F_C(c)]\}$	c
q=0.1	17.5877	14.5
q=0.01	19.8903	16.9
q=0.0001	24.4955	21.8

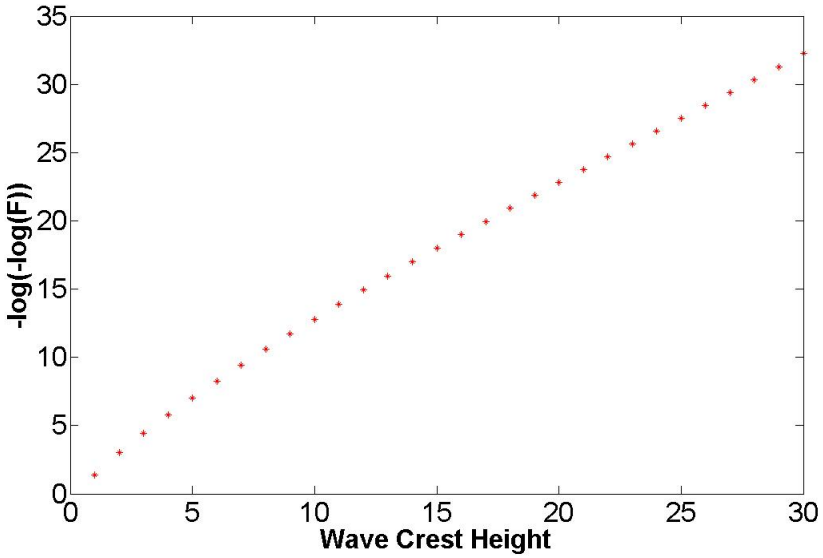

Figure 6.4: Gumbel Probability Paper for All Sea State Long Term Analysis with Weighting Factor

6.5 Calculation of Wave Crest Height with POT Method

6.5.1 Introduction of Method

The theory behind the POT method for calculating the crest height is the same with the POT method for response. The long term distribution of crest height is denoted as:

$$F_C(c) = \int_{\tilde{c}} F_{C|\tilde{C}}(c|\tilde{c}) f_{\tilde{C}}(\tilde{c}) d\tilde{c} \tag{6.16}$$

$F_{C|\tilde{C}}(c|\tilde{c})$ is Rayleigh distribution function for crest height given h_s, the distribution function is denoted as:

$$F_{C|\tilde{C}}(c|\tilde{c}) = [1 - exp{-}8(\frac{c}{h_s})^2]^m \tag{6.17}$$

Monte Carlo simulation is used to generate a realization for wave crest height:

$$c_{rlz,ij} = h_s[-\frac{1}{8} ln(1 - (u_j)^{\frac{1}{m_j}})]^{\frac{1}{2}} \tag{6.18}$$

u_j is a random number between 0 and 1.

The largest realization for each storm is by:

$$c_{rlz,i} = max_j(c_{rlz,ij}) \tag{6.19}$$

There are two ways to calculate the most probable crest height under a given sea state.

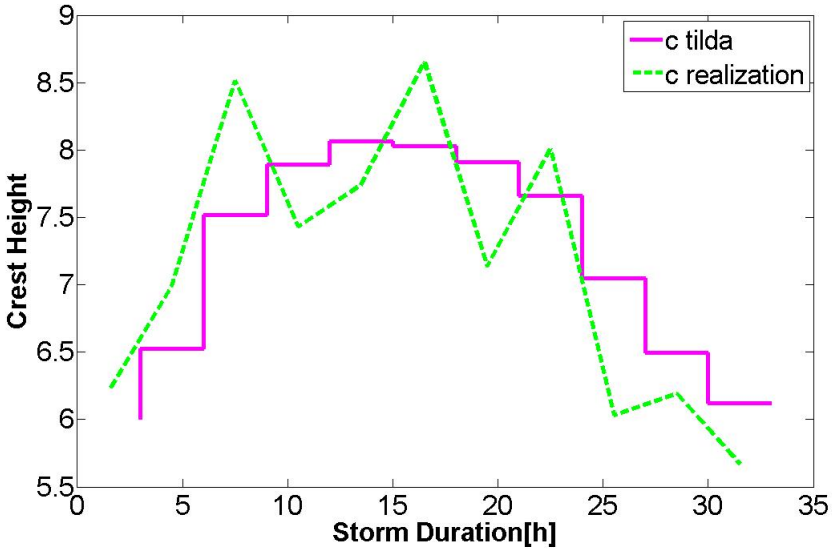

Figure 6.5: Storm Histories of Most Probable and Simulated Maxima Crest Height for a Particular Hurricane

(1) The most probable crest height can be decided as:

$$exp\{-8(\frac{c_{mpm,ij}}{h_s})^2\} = \frac{1}{m_j} \tag{6.20}$$

then,

$$c_{mpm,ij} = h_s\sqrt{\frac{1}{8}ln(m_j)} \tag{6.21}$$

with,

$$m_j = \frac{3 \cdot 3600}{0.77 \cdot t_p} \tag{6.22}$$

(2) According to experience, the most probable crest height occurs when the Rayleigh distribution for wave crest height $1 - F_{C|\tilde{C}}(c|\tilde{c})$ is equal to 0.37:

$$[1 - exp{-}8(\frac{c_{mpm,ij}}{h_s})^2]^{m_j} = 0.37 \tag{6.23}$$

then,

$$c_{mpm,ij} = h_s[\frac{1}{8}ln(1 - (o.37)^{\frac{1}{m_j}})]^{1/2} \tag{6.24}$$

The result for these two methods are quite close to each other. In Fig. (6.6), the wave crest height from the first method is taken as x-axis, the result from the second method is taken as y-axis.

The linear relationship suggests that two methods give very close results, thus either method can be used for further calculation.

Now the most probable wave crest height for each step is decided. Then for each storm, the most probable largest wave crest is found by:

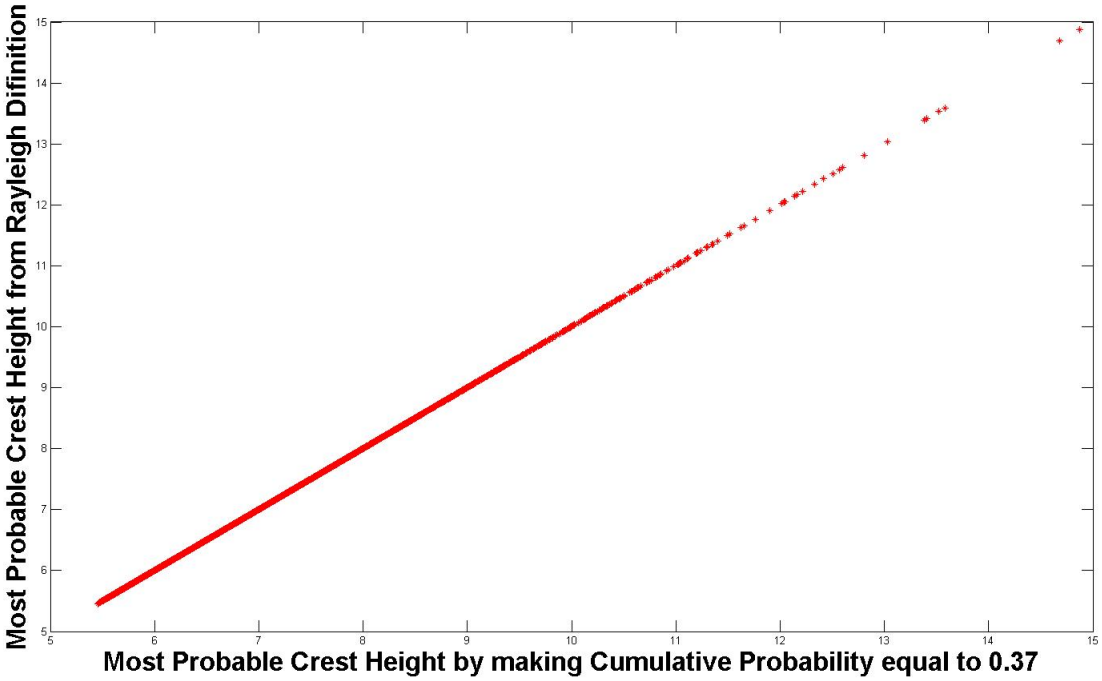

Figure 6.6: Comparison between Two Methods of Calculating the Most Probable Crest Height

$$c_{mpm,i} = max_j(c_{mpm,ij}) \tag{6.25}$$

The ratio between largest realization and largest most probable wave crest height for each storm no.i is decided as:

$$v_{ratio,i} = \frac{c_{rlz,i}}{c_{mpm,i}} \tag{6.26}$$

$v_{ratio,i}$ is assumed to be Gumbel distributed:

$$F_V(v) = exp\{-exp\{-\frac{v - \alpha_v}{\beta_v}\} \tag{6.27}$$

The parameters for the Gumbel distribution are decided as:

$$\beta_V = 0.7797 \cdot s_v \tag{6.28}$$

$$\alpha_V = \overline{v} - 0.57722 \cdot \beta_v \tag{6.29}$$

Further explanation can be found in Haver(2011). In this case, the value for α_v and β_v are:

$$\alpha_v = 1.0479 \tag{6.30}$$

$$\beta_v = 0.0628 \tag{6.31}$$

The distribution for v is plotted on Gumbel probability paper in Fig. (6.7).

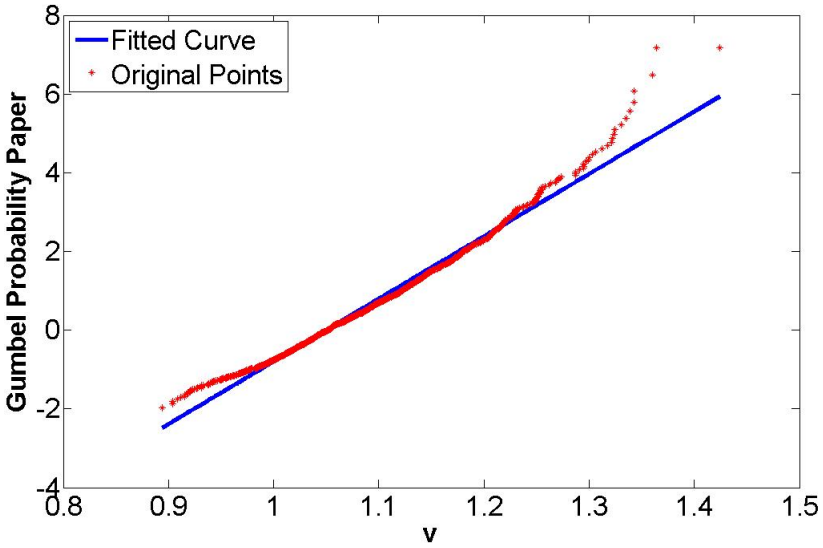

Figure 6.7: Cumulative Probability of v plotted on Gumbel Probability Paper

$\tilde{c}$ is assumed to be 3-parameter Weibull distributed:

$$F_{C|\tilde{C}}(c|\tilde{c}) = 1 - exp\{-(\frac{\tilde{c} - \tilde{c}_0}{\varepsilon})^{\gamma}\} \tag{6.32}$$

By method of linear fitting and least square method, the parameters for the Weibull distribution function are decided as:

$$\tilde{c}_0 = 5.54 \tag{6.33}$$

$$\gamma = 1.1649 \tag{6.34}$$

$$\varepsilon = 1.5782 \tag{6.35}$$

Then the cumulative probability for $\tilde{c}$ is plotted on the Weibull probability paper in Fig. (6.8).

Now since $F_{C|\tilde{C}}(c|\tilde{c})$ and $f_{\tilde{c}}(\tilde{c})$ have already been decided, the integration can be solved:

$$F_C(c) = \int_{\tilde{c}} F_{C|\tilde{C}}(c|\tilde{c}) f_{\tilde{c}}(\tilde{c}) d\tilde{c} \tag{6.36}$$

Plot the result on a Gumbel probability paper in Fig(6.9).

The q-probability wave crest height is found by solving:

$$1 - F_C(c_q) = \frac{q}{n_1} \tag{6.37}$$

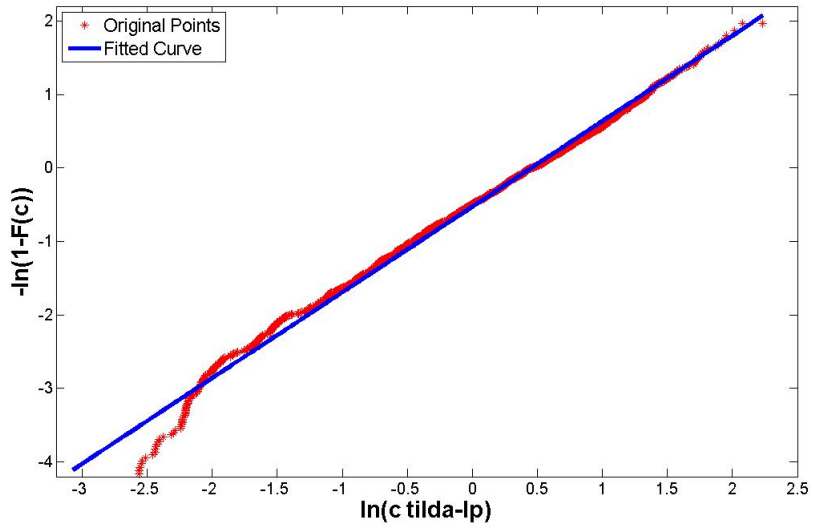

Figure 6.8: Linear Fitting for the Most Probable Crest Height plotted on Weibull Probability Paper

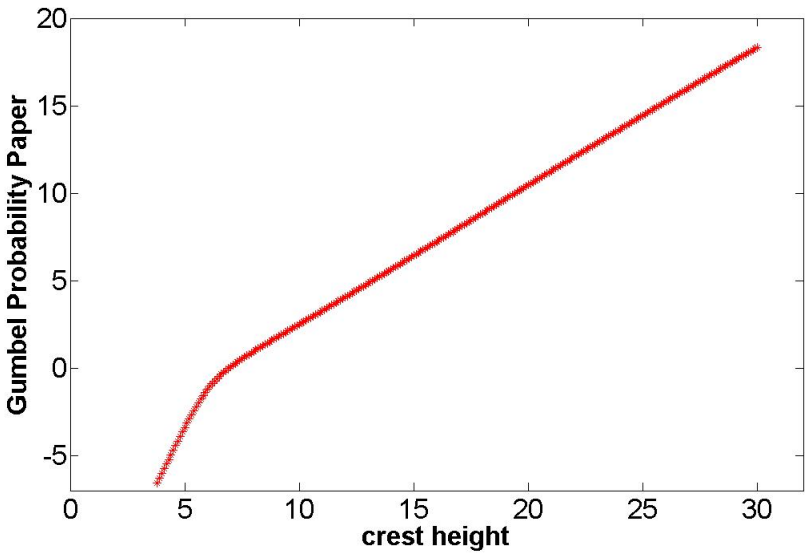

Figure 6.9: Cumulative Probability of Wave Crest Height plotted on Gumbel Probability Paper

n_1 is the expected number of hurricanes per year. In this case, there are 1299 storms in 56 years, thus the expected number of hurricanes per year:

$$n_1 = \frac{1299}{56} \tag{6.38}$$

6.5.2 Discussion of Results

Result for the POT analysis are shown in Tab. (6.7).

The Gumbel probability paper is used to plot the cumulative probability for c and

Table 6.7: Extreme Crest Height from All Sea State Time Domain Approach

	$-ln\{-ln[F_C(c)]\}$	c
q=0.1	5.444	13.7
q=0.01	7.749	16.6
q=0.0001	12.3543	22.3

$\tilde{c}$ in Fig. (6.10).

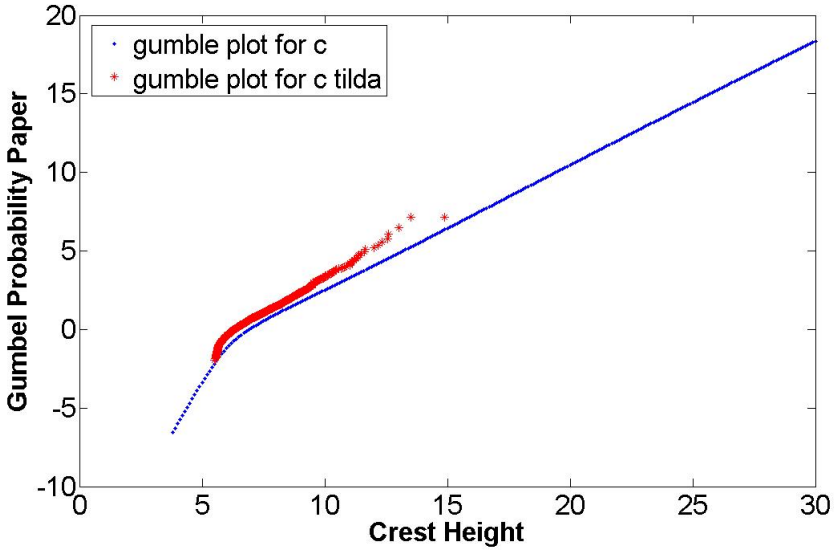

Figure 6.10: CDF of the most probable and the realization of crest height plotted on Gumbel Probability Paper

It can be seen from Fig. (6.10) that for same level of cumulative probability, the corresponding value for the $\tilde{c}$ is on the left side of c. Which satisfies the fact that the most probable largest value is smaller than the largest realization from Monte Carlo simulation.

6.5.3 Result Summary of Different Methods for Wave Crest Height Prediction

Table 6.8: Result Summary from Different Calculation Method

Response, NPS, $c_2 = 1$	q=0.1	q=0.01	q=0.0001
Significant wave height predicted from all sea state approach	14.2	16.5	21.0
Crest height from all sea state approach	14.1	16.7	21.6
Crest height from all sea state approach considering weight effect	14.5	16.9	21.8
Crest height predicted from all sea state time domain method	14.2	16.5	20.4
POT method	13.7	16.6	22.3

It can be seen from Tab. (6.3) and Tab. (6.8) that for time domain approach, i.e. as long as the weather characteristic is taken directly from the hindcast data, the

final result will be smaller than the one from fitted model. This is due to that since the hindcast data is measured for every 3 hours, there are some unobserved storms. One can overcome this shortage by fitting a long term distribution of weather characteristic, thus the result will be more accurate for this case.

It can be seen from Tab. (6.3) that for q=0.1 and q=0.01 case, POT method gives smaller result than all sea state approach, which is quite reasonable. While for q=0.0001 case, POT method gives slightly higher result than all sea state approach. This may due to the limited amount of data. One is trying to estimate the response with 10,000-year return period, but only data of 56 years is available. Thus a slightly higher value is still reasonable here, but it cannot be used for design purpose.

In conclusion, this chapter provides a good verification for two methods. All sea state long term approach gives more accurate estimation for extreme values, POT method is accurate for response with 10-year or 100-year return period, but is not accurate enough for 10,000-year return period.

Chapter 7

Verification Study

7.1 Conclusion

This master thesis has looked into uncertainties when predicting extreme wave induced platform response.

When estimating long term response from the all sea state approach and target percentile from the environmental contour line method, the major uncertainties come from the response function. Different choices of parameters of response function will result in different non-linearity to significant wave height, period sensitivity to wave period, and the final response will be quite different from each other. Thus a good modelling of response is the most important thing when using all sea state long term approach to estimate extreme response.

When performing the POT method. There are majorly two uncertainties. One is from finding a proper distribution for the largest most probable response for each storm. Different fitting range will result in quite different result. While the author suggests that one should focus more on the upper region, which corresponds to extreme value prediction. The other one is from Monte Carlo simulation: the random number generated each time leads to much variability. Other uncertainties such as method of linear fitting compared with method of moment, different choices of minimum threshold, and limitations on minimum storm steps, they also have effects on the final result.

Due to the uncertainties in the POT method, the author suggests that it should be carefully used in the North Sea condition. While it might give good estimation in sea area where the extreme response is governed by storms, such as the Gulf of Mexico.

7.2 Further Work

Further work is suggested based on the uncertainties from above.

The response function in this thesis is a generic function; it cannot describe complicated response problems very well. Thus the author suggests that further research

should be done to optimize the response function, in order to give more accurate description for the response problem.

One should also focus on application of Monte Carlo simulation in the POT method. Too few realizations might underestimate the response, while too many realizations will be an overestimation. Thus further work should be put on the proper number of realizations for each step in the POT method.

Further work should also be put on target percentile from the environmental contour line method. From Norsok-003, the recommendation percentile is between 85% to 95%. However, some of the target percentiles calculated in the thesis are well below this range, especially for period sensitive cases. Thus the author suggests that further work should be done regarding finding the correct target percentile for different response problems.

Appendix A

Appendix for Figure

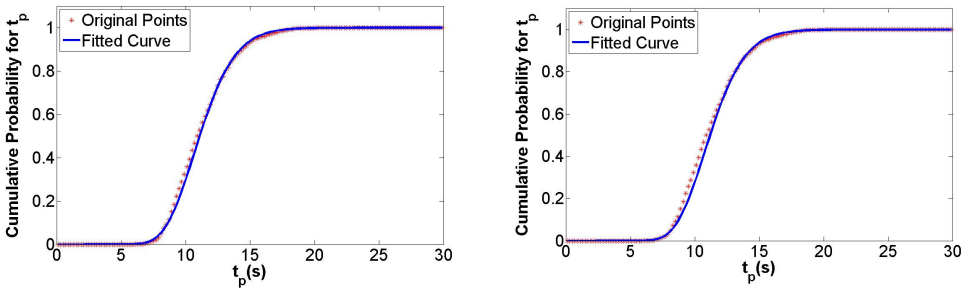

(a) Method of Moment (b) Method of Linear Fitting

Figure A.1: For $H_s = 3.9m$ (representing class [3.85m, 3.95m]):

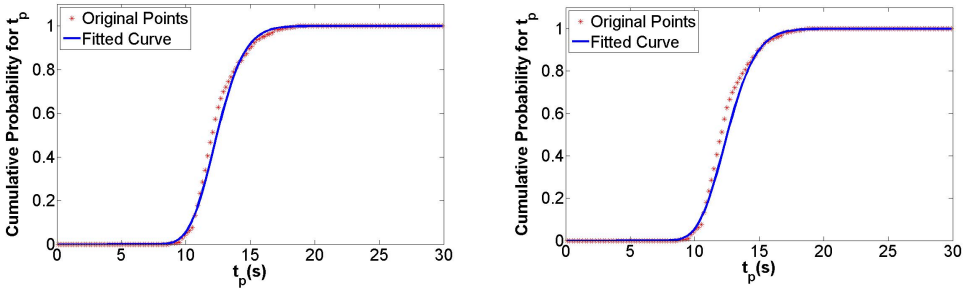

(a) Method of Moment (b) Method of Linear Fitting

Figure A.2: For $H_s = 5.9m$ (representing class [5.85m, 5.95m]):

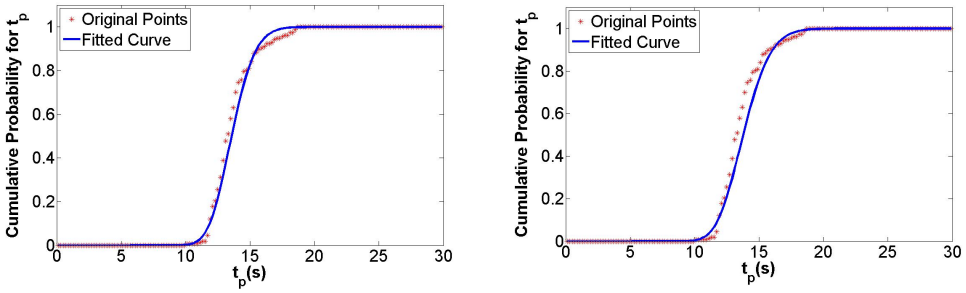

(a) Method of Moment (b) Method of Linear Fitting

Figure A.3: For $H_s = 7.9m$ (representing class [7.85m, 7.95m]):

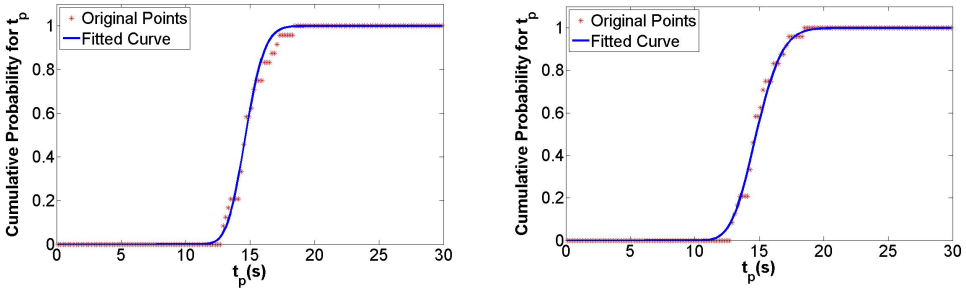

(a) Method of Moment (b) Method of Linear Fitting

Figure A.4: For $H_s = 9.9m$ (representing class [9.85m, 9.95m]):

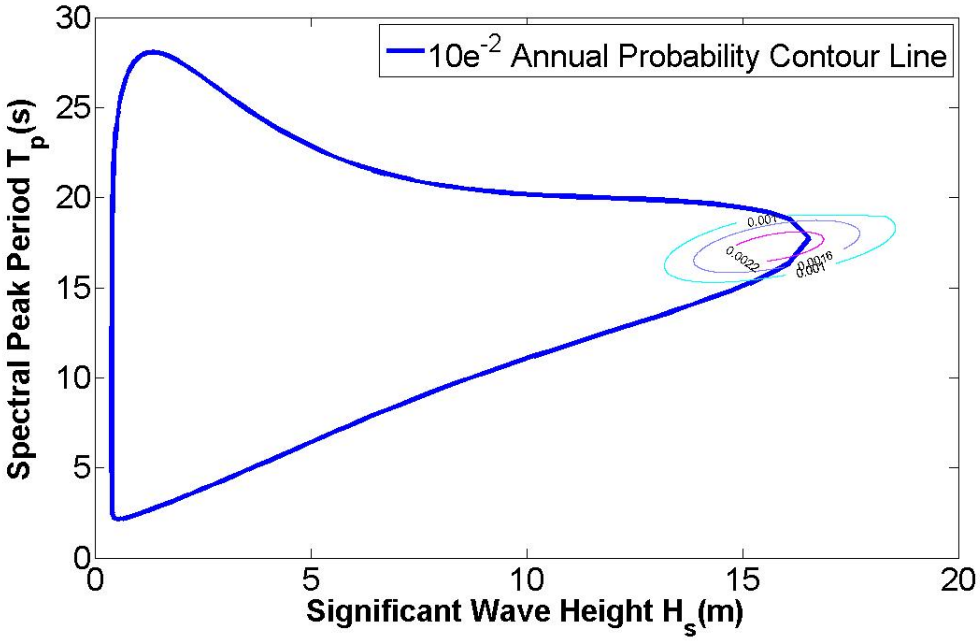

Figure A.5: Important Contribution Area for Non-period Sensitive Quadratic case with $b_1 = 0.005$

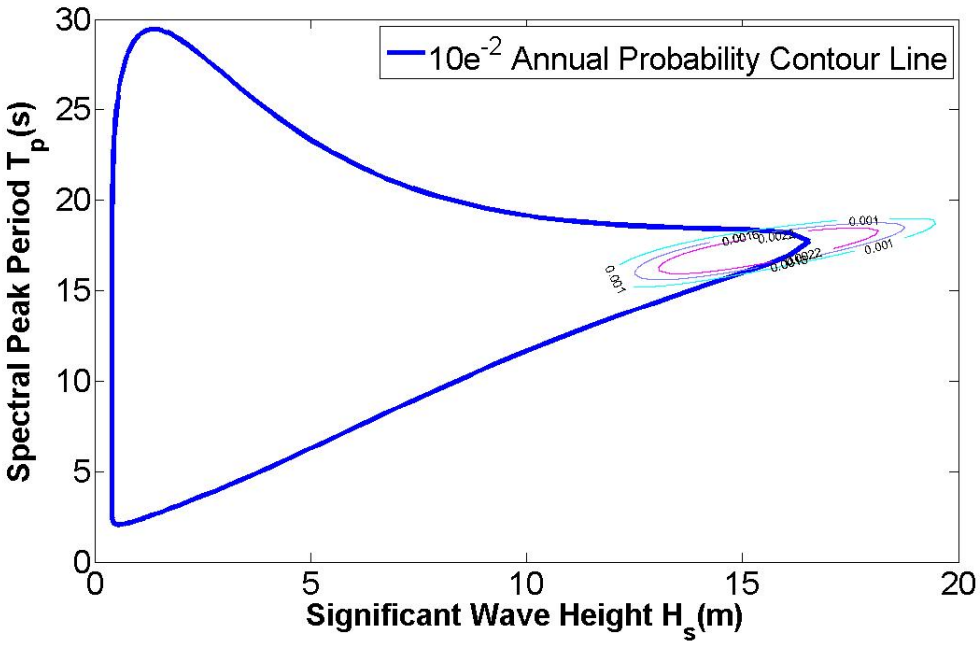

Figure A.6: Important Contribution Area for Non-period Sensitive Linear case with $b_1 = 0.00073$

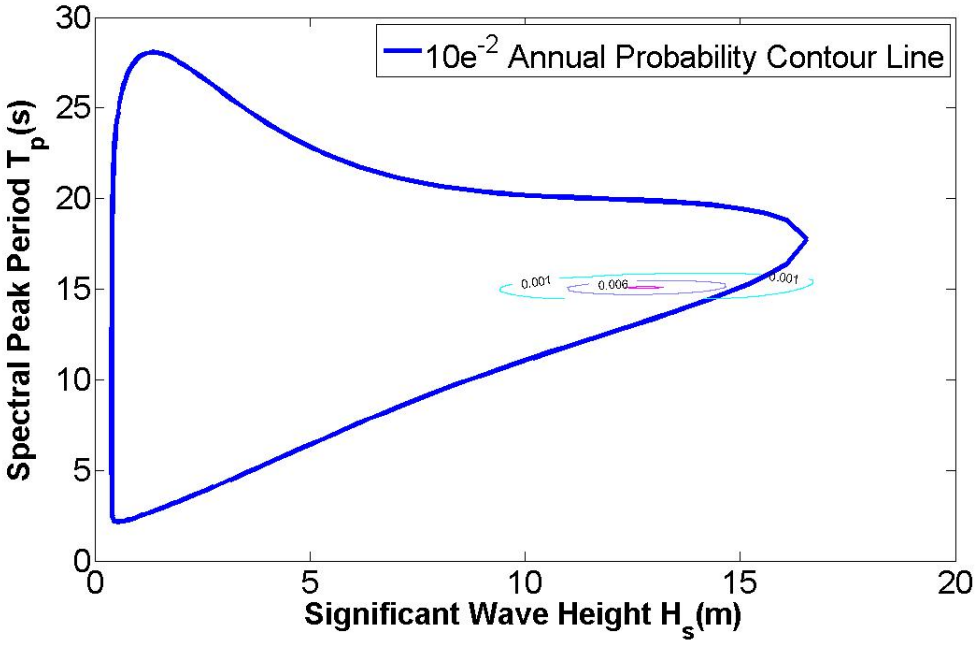

Figure A.7: Important Contribution Area for Period Sensitive Linear case with $b_1 = 0.005$

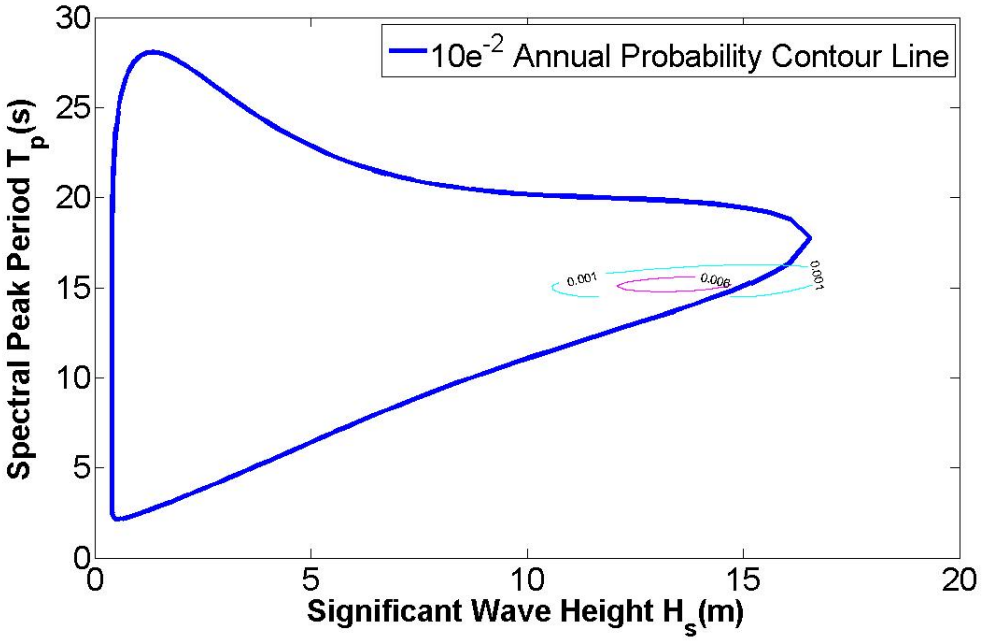

Figure A.8: Important Contribution Area for Period Sensitive Quadratic case with $b_1 = 0.005$

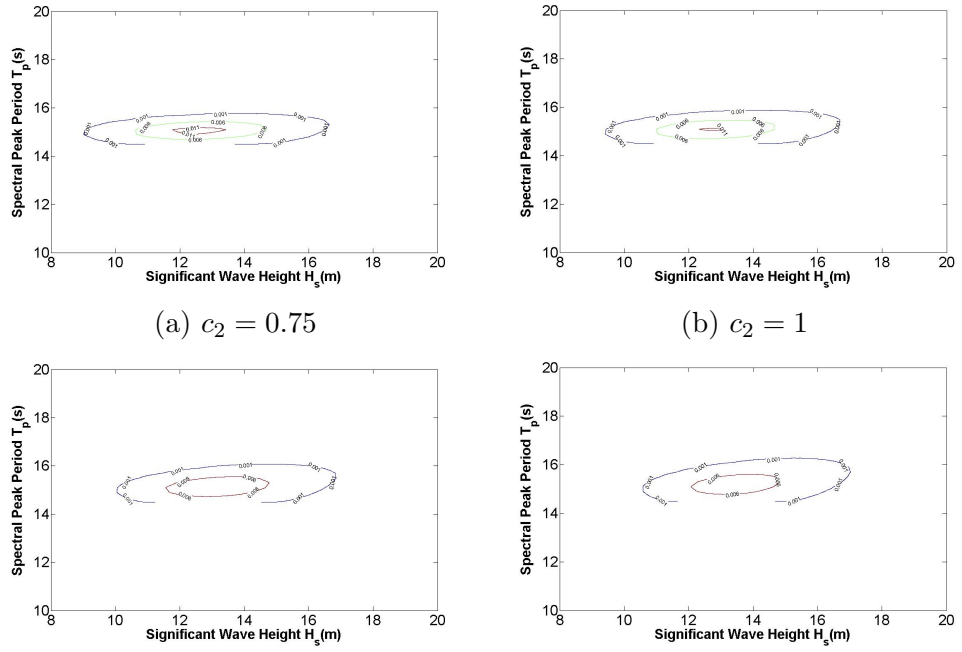

(a) $c_2 = 0.75$ (b) $c_2 = 1$

(c) $c_2 = 1.5$ (d) $c_2 = 2$

Figure A.9: Comparison between Different c_2 for Period Sensitive Case

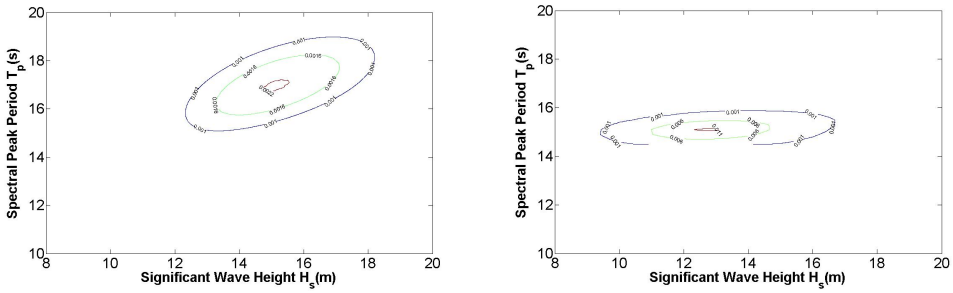

(a) Non-period Sensitive (b) Period Sensitive

Figure A.10: Comparison between Non-period Sensitive and Period Sensitive Case for $c_2 = 1$

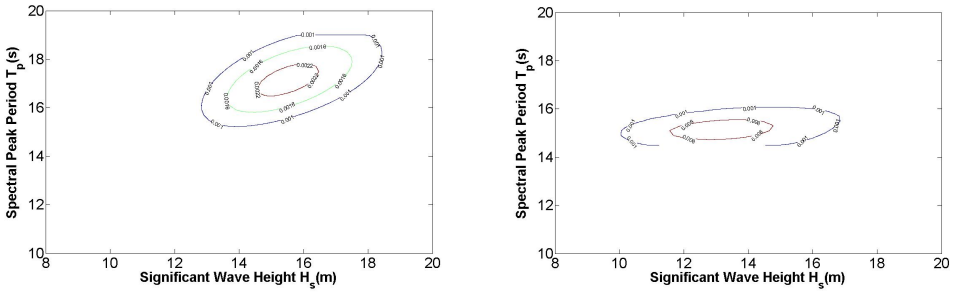

(a) Non-period Sensitive (b) Period Sensitive

Figure A.11: Comparison between Non-period Sensitive and Period Sensitive Case for $c_2 = 1.5$

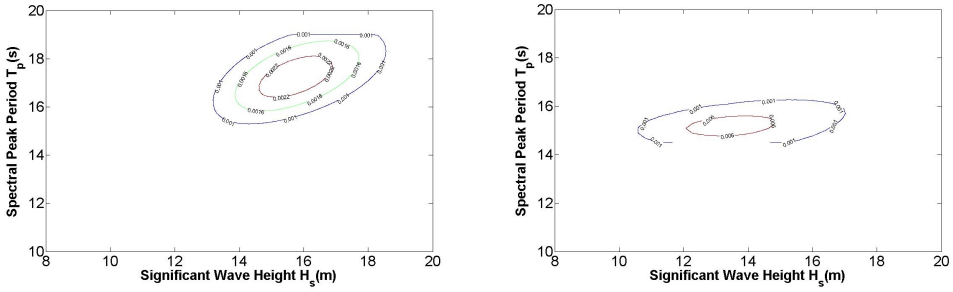

(a) Non-period Sensitive (b) Period Sensitive

Figure A.12: Comparison between Non-period Sensitive and Period Sensitive Case for $c_2 = 2$

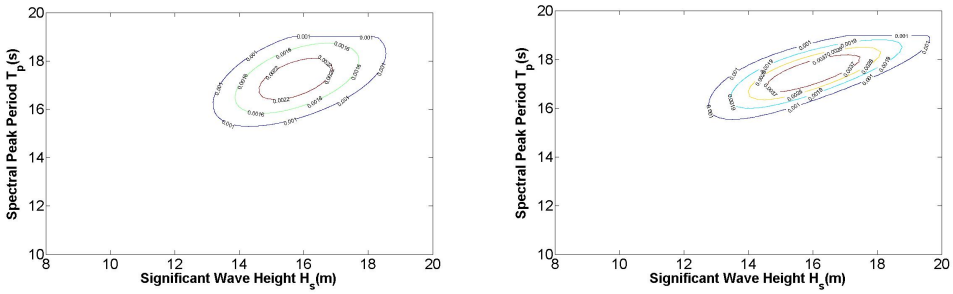

(a) $b_1 = 0.005$ (b) $b_1 = 0.00073$

Figure A.13: Comparison between Different b_1 in Quadratic and Non-Period Sensitive case

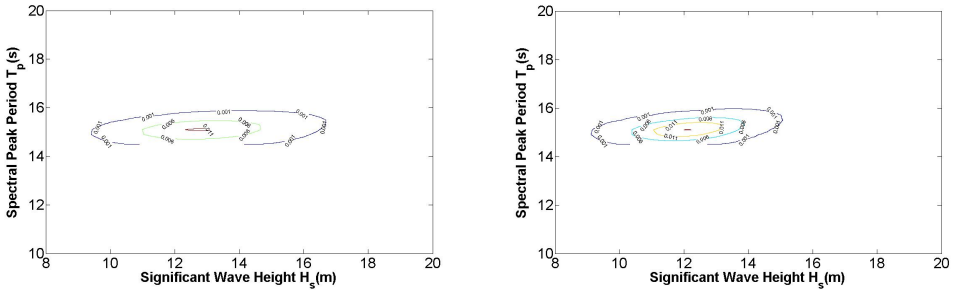

(a) $b_1 = 0.005$ (b) $b_1 = 0.00073$

Figure A.14: Comparison between Different b_1 in Linear and Period Sensitive case

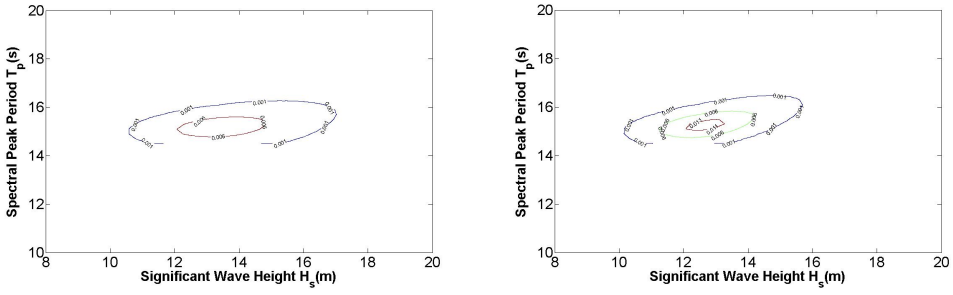

(a) $b_1 = 0.005$ (b) $b_1 = 0.00073$

Figure A.15: Comparison between Different b_1 in Quadratic and Period Sensitive case

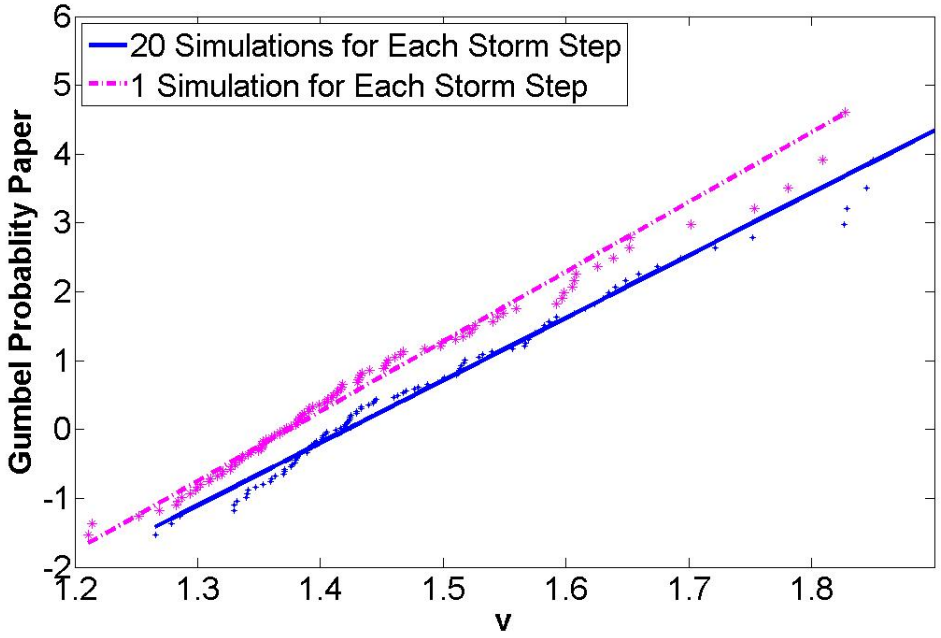

Figure A.16: Effect of Realizations for Each Step on v for Medium Severe Storm

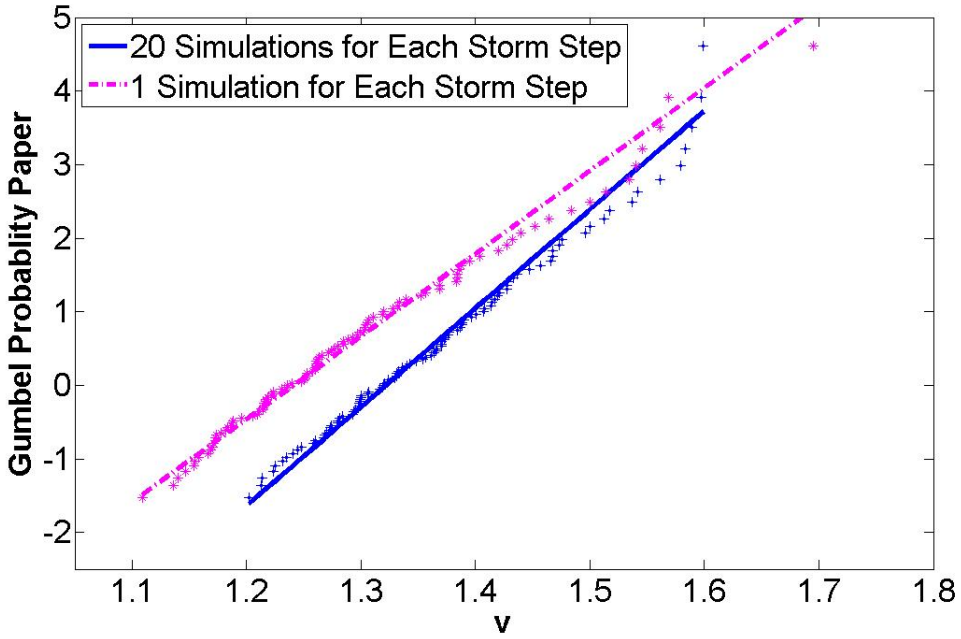

Figure A.17: Effect of Realizations for Each Step on v for Most Severe Storm

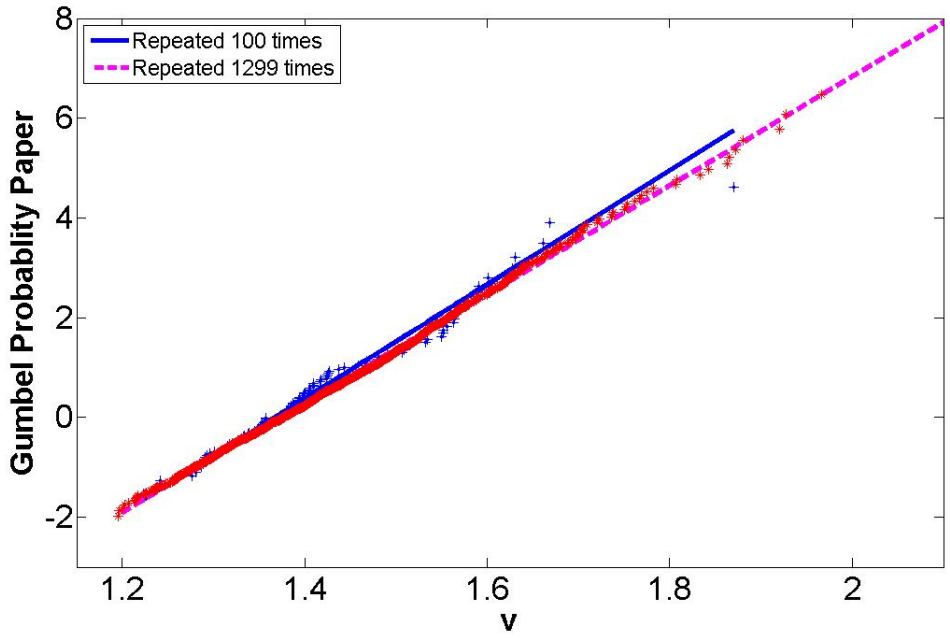

Figure A.18: Effect of Repeated Storms on v for Medium Severe Storm

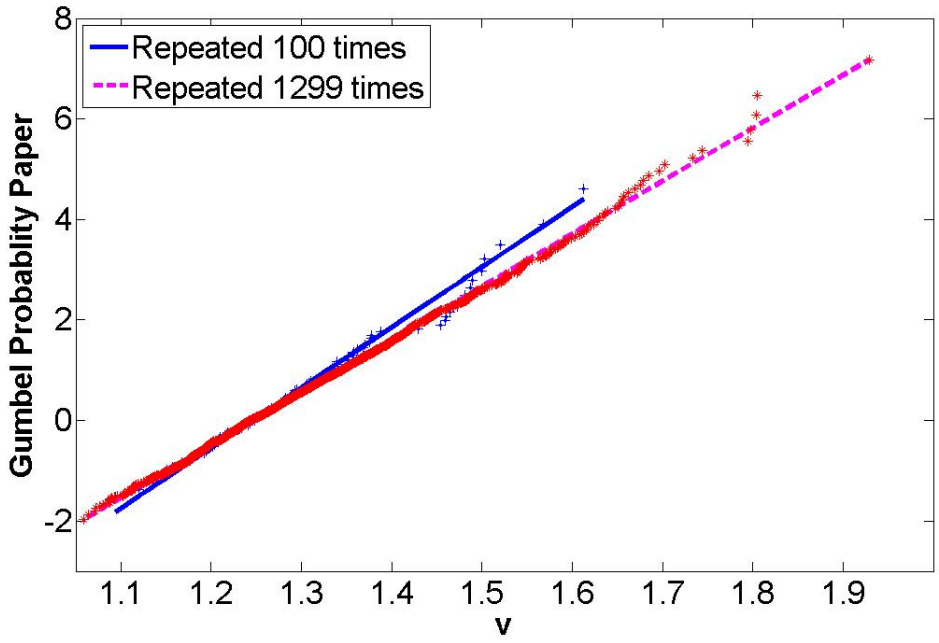

Figure A.19: Effect of v for Medium Severe Storm

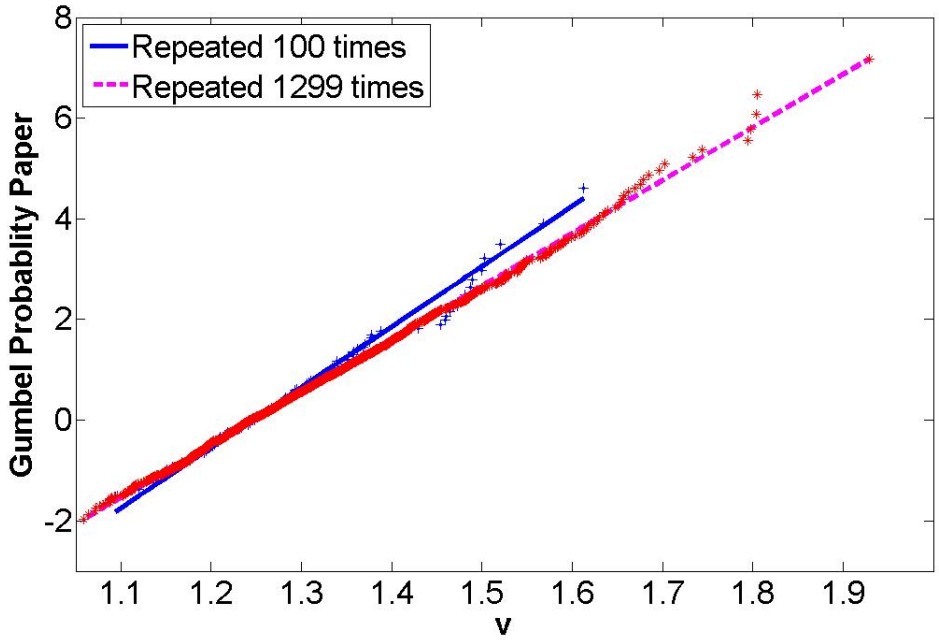

Figure A.20: Effect of Repeated Storms on v for Most Severe Storm

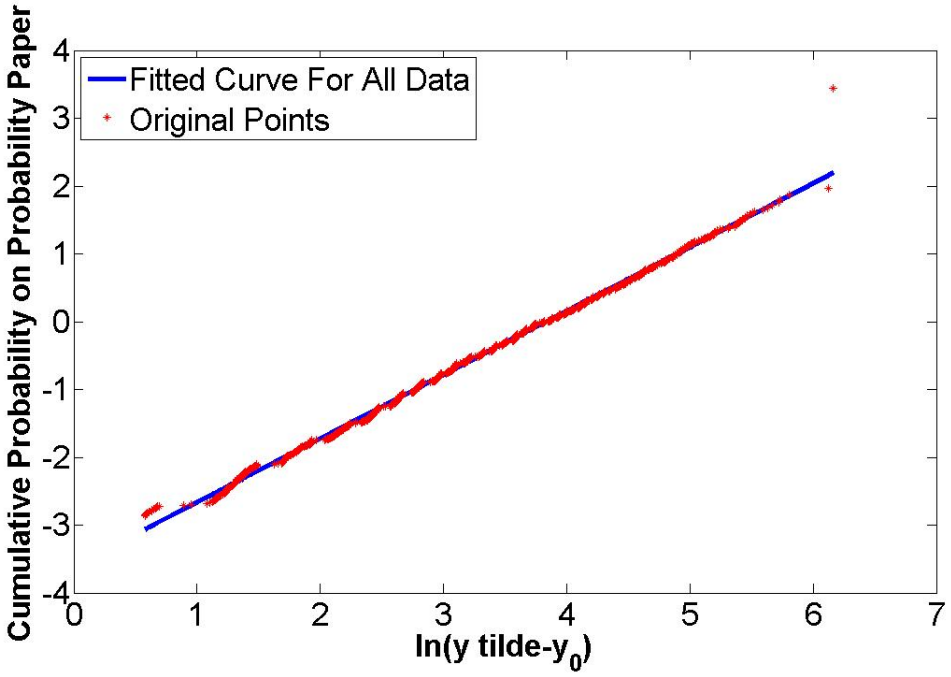

Figure A.21: Cumulative Probability plotted on Weibull Probability Paper for Non-period Sensitive and Quadratic Case

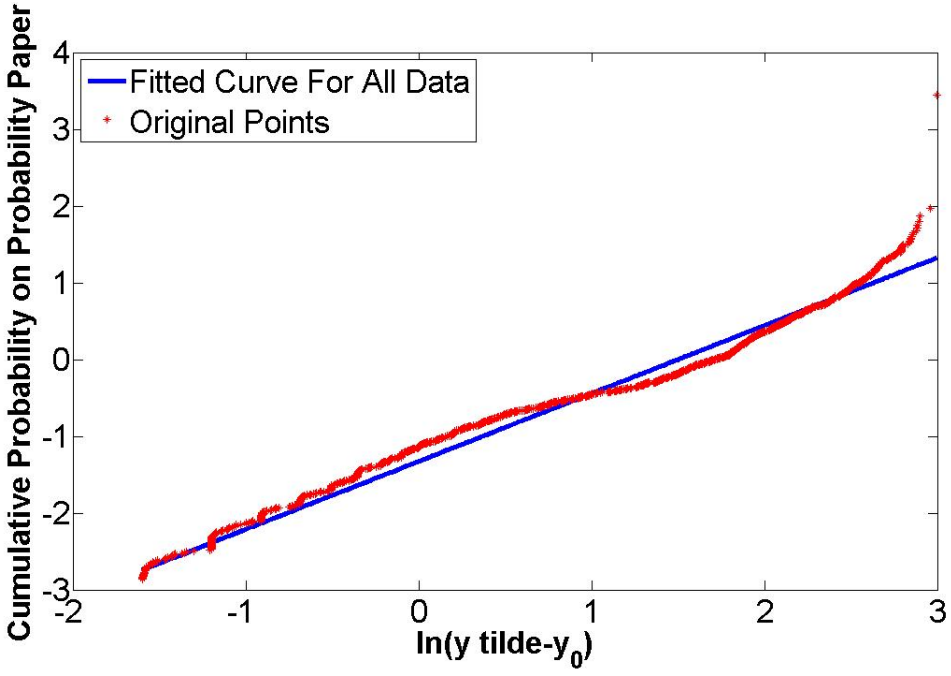

Figure A.22: Cumulative Probability plotted on Weibull Probability Paper for Period Sensitive and Linear Case

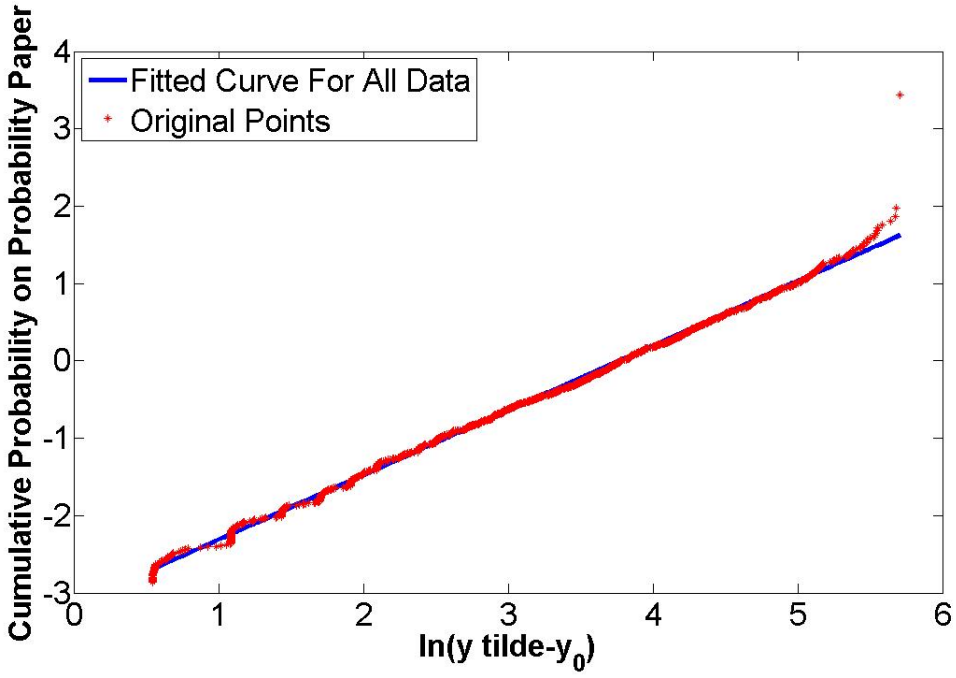

Figure A.23: Cumulative Probability plotted on Weibull Probability Paper for Period Sensitive and Quadratic Case

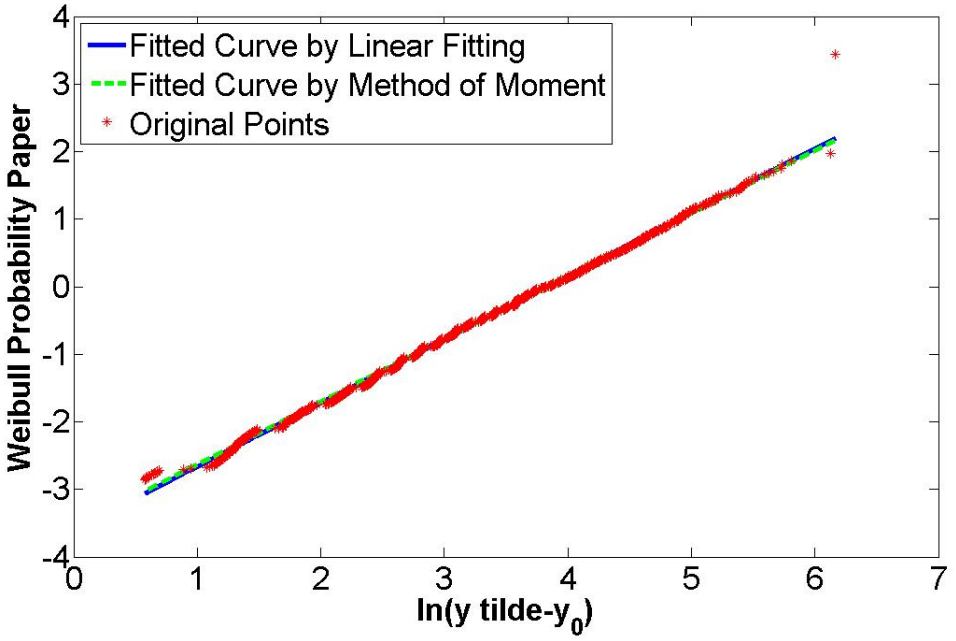

Figure A.24: Comparison of Method of Moment and Linear Fitting for Non-period and Quadraitc Case

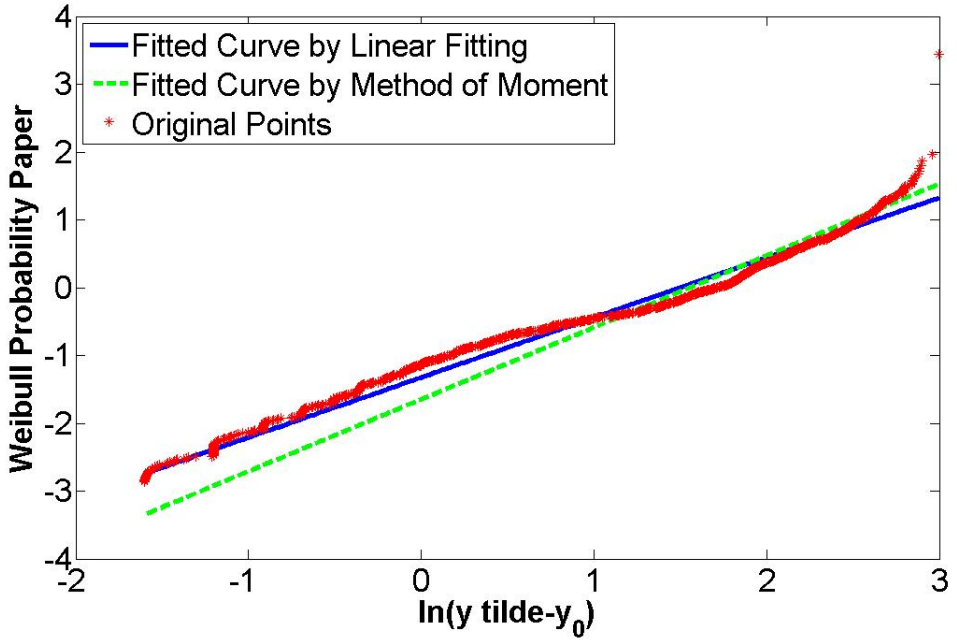

Figure A.25: Comparison of Method of Moment and Linear Fitting for Period and Linear Case

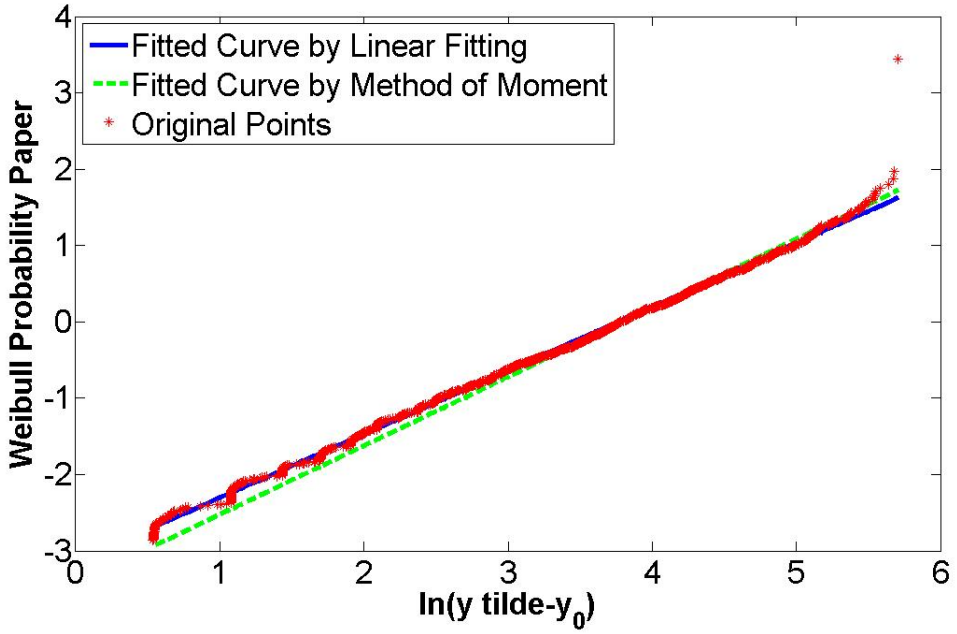

Figure A.26: Comparison of Method of Moment and Linear Fitting for Period and Quadraitc Case

Appendix B

Appendix for Table

Table B.1: Extreme Values and Target Percentile for Quadratic and Non-period Sensitive Case

	x(response)	α	β	P	$\frac{\alpha}{\beta}$
$q = 0.01$ per year	625.2	494.54	84.747	81.25%	0.17
$q = 0.0001$ per year	1073.6	787.29	134.91	89.76%	0.17

Table B.2: Extreme Values and Target Percentile for Linear and Period Sensitive Case

	x(response)	α	β	P	$\frac{\alpha}{\beta}$
$q = 0.01$ per year	30.9	28.32	2.32	71.90%	0.08
$q = 0.0001$ per year	40.5	33.47	2.73	92.67%	0.08

Table B.3: Extreme Values and Target Percentile for Quadratic and Period Sensitive Case

	x(response)	α	β	P	$\frac{\alpha}{\beta}$
$q = 0.01$ per year	482.4	410.05	70.27	69.95%	0.17
$q = 0.0001$ per year	773.7	573.39	98.26	87.79%	0.17

Reference

Baarholm G., Haver S., kland O. (2010). Combining Contours of Significant Wave Height and Peak Period with Platform Response Distribution for Predicting design Response. *Marine Structures-Desing, Construction and Safety*, 148-163.

Carl M. Larsen. (2012). Marine Dynamics. Trondheim: NTNU.

Dag Myrhaug. (2005). TMR4235 Stochastic Theory of Sea Loads. Trondheim: NTNU.

Haver S. (2012). Estimating Long Term Extremes for Linear and Non-linear Response Problems. *Compendium for TMR4195 Design of Offshore Structures.*

Haver S. (2011). Prediction of Characteristic Response for Design Purposes(Preliminary Version). Stavanger: Statoil ASA.

Haver S., Bergsvik J. (2010). Extreme Response in a Hurricane Governed Offshore Region: Uncertainties Related to Limited Amount of Data and Choice of Method of Prediction. Stavanger: Statoil ASA, 4Subsea AS.

Haver S., Bruserud K., Baarholm G. (2012). Environmental Contour Method: An Approximate Method for Obtaining Characteristic Response Extremes for Design Purposes. Stavanger: Statoil ASA, 4Subsea AS.

Haver S., Gro S. and Tone M., (1998). Long Term Response Analysis of Fixed and Floating Structures. *Ocean Wave Kinematics Dynamics and Loads on Structures*, 526, 240-247.

T. Moan, S. Haver, N. Spidse. (2010). *Analyse av Usikkerhet.*

Tianzuo Yao. (2013). Methods for Estimating Long Term Extremes of Structural Response. Trondheim: NTNU.